Scale-Up Aspects of PHA Production by Microbial Enrichment Cultures

Marang, Leonie

DOI
10.4233/uuid:1f3b0744-cc0a-44cb-95b1-d19354a0b157

Publication date
2017

Document Version
Final published version

Citation (APA)
Marang, L. (2017). *Scale-Up Aspects of PHA Production by Microbial Enrichment Cultures*. [Dissertation (TU Delft), Delft University of Technology]. https://doi.org/10.4233/uuid:1f3b0744-cc0a-44cb-95b1-d19354a0b157

SCALE-UP ASPECTS OF PHA PRODUCTION BY MICROBIAL ENRICHMENT CULTURES

Leonie MARANG

SCALE-UP ASPECTS OF PHA PRODUCTION BY MICROBIAL ENRICHMENT CULTURES

Proefschrift

ter verkrijging van de graad van doctor
aan de Technische Universiteit Delft,
op gezag van de Rector Magnificus prof. ir. K.C.A.M. Luyben,
voorzitter van het College voor Promoties,
in het openbaar te verdedigen op
donderdag 26 oktober 2017 om 15:00 uur

door

Leonie MARANG

ingenieur in Life Science and Technology,
Technische Universiteit Delft
geboren te Deventer, Nederland

Dit proefschrift is goedgekeurd door de

promotor: prof. dr. dr.h.c. ir. M.C.M. van Loosdrecht
copromotor: dr. ir. R. Kleerebezem

Samenstelling promotiecommissie:

Rector Magnificus	voorzitter
Prof. dr. dr.h.c. ir. M.C.M. van Loosdrecht	Technische Universiteit Delft
Dr. ir. R. Kleerebezem	Technische Universiteit Delft

Onafhankelijke leden:

Prof. dr. ir. J.J. Heijnen	Technische Universiteit Delft
Prof. dr. ir. J.B. van Lier	Technische Universiteit Delft
Prof. dr. G. Muyzer	Universiteit van Amsterdam
Dr. A.G. Werker	Promiko.se
Prof. dr. M.A.M. Reis	Universidade Nova de Lisboa
Prof. dr. I.W.C.E. Arends	Technische Universiteit Delft, reservelid

This research is supported by the Dutch Technology Foundation STW, which is part of the Netherlands Organisation for Scientific Research (NWO) and partly funded by the Ministry of Economic Affairs (project number 11605).

Keywords: feast-famine, microbial enrichment culture, *Plasticicumulans acidivorans*, polyhydroxyalkanoate (PHA), resource recovery

Printed by: Ipskamp Drukkers, Enschede

ISBN 978-94-028-0815-5

An electronic version of this dissertation is available at
http://repository.tudelft.nl/

CONTENTS

SUMMARY

Polyhydroxyalkanoates (PHAs) are microbial storage polymers accumulated by many different prokaryotes as an intracellular carbon and energy reserve. The properties of the polymer make PHA an interesting bioplastic that is fully biodegradable. Moreover, the monomers could serve as chiral building blocks for the production of biochemicals, or be esterified and used as a biofuel.

Currently, PHA is commercially produced using pure cultures and well-defined substrates. To reduce the cost of PHA production and allow broad application, microbial enrichment cultures could be used. This eliminates the need for axenic conditions and allows the use agro-industrial waste streams as substrate, contributing to the development of a circular economy. The process for waste-based PHA production by microbial enrichment cultures comprises four steps: (1) acidogenic fermentation of the waste stream, (2) enrichment of a PHA-producing culture, (3) production of the PHA, and (4) recovery of the product. The first step aims to convert the waste organic carbon, primarily carbohydrates, to more suitable substrates for PHA production, primarily volatile fatty acids (VFAs). In the second step, the microbial community is enriched in bacteria with a high PHA productivity. This step is generally performed in a sequencing batch reactor (SBR) operated under feast-famine conditions, as intermittent substrate availability creates a competitive advantage for bacteria that store substrate inside their cell. Once a stable culture is obtained, the SBR will operate as a biomass production step for step three: maximization of the culture's PHA content.

A strong selective pressure for PHA-producing bacteria can be established by operating the SBR at an SRT of 1 d, feast-famine cycles of 12 h, and a temperature of 30°C. Microbial enrichment cultures obtained under these conditions, fed with acetate or lactate, have been reported to accumulate more than 8 Cmol PHA per Cmol active biomass (>87 wt.%). These PHA contents are comparable to those obtained using pure cultures, and the kinetic properties of the enrichment cultures are better.

The aim of this thesis was to investigate scale-up aspects of the PHA production by microbial enrichment cultures. A translation of the laboratory process to industrial application raises new questions concerning the impact of (variable) wastewater composition and process design. **Chapter 2** and **3**, therefore, focus on the fate of different constituents of an acidified waste stream, and the second part (**Chapter 4-6**) of the thesis focusses on alternative process configurations. **Chapter 1** provides a general introduction to the topic and describes the research preceding this thesis.

Chapter 2 assesses the suitability of butyrate as substrate for poly(3-hydroxybutyrate) (PHB) production. Two SBRs were operated: one fed with butyrate, and another fed with a mixture of acetate and butyrate (1:1 Cmol). In both reactors *Plasticicumulans acidivorans* dominated the enrichment culture. The biomass-specific carbon uptake rate and PHB yield were significantly higher on butyrate than on acetate. Due to the reduced respiration requirements for butyrate, as much as 90% of the carbon was converted to PHB. This resulted in a doubling of the specific PHB production rate. When both substrates were available *P. acidivorans* strongly preferred the uptake of butyrate. Only after butyrate depletion acetate was taken up at a high rate. The molar substrate uptake rate remained the same, suggesting that uptake or activation of the substrate is the rate-limiting step. The results indicate that for optimized waste-based PHA production the pre-fermentation step should be directed towards the production of butyrate.

Acidified waste streams will also contain compounds that are not suitable for PHA production. The presence of these compounds leads to the co-enrichment of non-PHA-storing bacteria. Their impact on the overall PHA production process is investigated in **Chapter 3**, using a simple substrate mixture of acetate and methanol (1:1 Cmol). The enrichment culture was dominated by *P. acidivorans* (40%) and *Methylobacillus flagellatus*, an obligate methylotroph that cannot store PHA. The presence of the non-storing population reduced the maximum PHB content of the culture from more than 80 to 66 wt.% (>5 to 2.3 $Cmol_{PHB} \cdot Cmol_X^{-1}$). When ammonium was supplied during the accumulation step – to mimic a nitrogen-rich waste stream – *P. acidivorans* still accumulated large amounts of PHB, but unrestricted growth of the methylotrophic population further reduced the maximum PHB content. Other strategies than ammonium limitation should be developed to reduce the size and impact of non-storing populations. Upon acetate depletion, 80% of the dosed methanol remained in the reactor liquid. The inclusion of a solid-liquid separation step directly after depletion of the VFAs would allow the selective removal of substrates unsuitable for PHA production from the SBR.

Chapter 4 explores the feasibility of combining the enrichment and production step in a single reactor. Harvesting PHA-rich biomass directly from the SBR reduces capital cost, but may increase downstream-processing cost if the PHA content is significantly reduced. Operating the SBR at a volume exchange ratio of 0.75 (18 h cycles, 1 d SRT) allowed the production of biomass with 70 wt.% PHB (2.8 $Cmol_{PHB} \cdot Cmol_X^{-1}$) in a single-step process from acetate. By increasing the exchange ratio to 0.83 (20 h cycles), the PHB content of the harvested biomass increased to 75 wt.% (3.6 $Cmol_{PHB} \cdot Cmol_X^{-1}$), but the operational stability decreased. When operating the SBR at these high exchange ratios, bacteria have to increase their growth rate and external substrate is available for relatively long periods. This allows the establishment of larger flanking populations and negatively affected the kinetic properties of *P. acidivorans*. The PHA storage rate, yield, and capacity of the culture were compromised. Although maximizing the volume

exchange ratio is a suitable strategy to produce large amounts of PHA in the SBR, it does not ensure the enrichment of a culture with superior PHA productivity.

The feast-famine conditions of the SBR can also be established using two or more continuous stirred-tank reactors (CSTRs) in series, with partial biomass recirculation. The use of CSTRs offers several advantages, but will result in distributed residence times and a less strict separation between feast and famine conditions. **Chapter 5** describes a set of mathematical models, developed to predict the growth of *P. acidivorans* in competition with a non-storing heterotroph. The models were used to investigate the impact of various process and biomass-specific parameters on the enrichment of PHA-producing bacteria in feast-famine SBR and staged CSTR systems. Simulations showed that in the 2-stage CSTR system the selective pressure is significantly lower than in the SBR, and strongly dependent on the chosen feast-famine ratio. To study the effect of residence time distribution and the resulting distributed bacterial states, both a macroscopic model considering lumped biomass and an agent-based model considering individual cells were created. Although the macroscopic model overestimates the selective pressure in the 2-stage CSTR system, it provides a quick and fairly good impression of the reactor performance. To strengthen the competitive advantage of PHA-producing bacteria, the number of CSTRs in series should be increased.

The impact of continuous carbon supply, and thereby the continuous presence of residual substrate, on the enrichment of PHA-producing bacteria was investigated experimentally in **Chapter 6**. Two SBRs were operated. In the first reactor, the substrate (acetate) was dosed continuously and *Zoogloea* sp. was enriched. The culture accumulated PHB upon exposure to excess carbon, but the PHB production rate and storage capacity (53 wt.%, 1.3 $Cmol_{PHB} \cdot Cmol_X^{-1}$) were one-fifth of that observed for enrichment cultures in a standard, pulse-fed SBR dominated by P. *acidivorans*. In the second reactor, half the acetate was dosed at the beginning of the cycle and the other half continuously. Having a true feast phase, the enrichment of *P. acidivorans* was not impeded by the continuous supply of acetate, and the culture accumulated 85 wt.% PHB (6.6 $Cmol_{PHB} \cdot Cmol_X^{-1}$). This shows that for the enrichment of bacteria with a superior PHA-producing capacity periodic substrate excess – a true feast phase – is essential, while periodic substrate absence – a true famine phase – is not. The possibility to apply less strict famine conditions is a prerequisite for the use of a 2-stage CSTR system, but also has strong advantages for scale-up of the SBR process itself.

Chapter 7 summarizes and integrates the main findings. Although further optimization and fine-tuning of the process will be required, especially for the acidogenic fermentation step, the major obstacle for industrial implementation is currently the application development.

SAMENVATTING

Polyhydroxyalkanoaten (PHA's) zijn microbiële opslagpolymeren die door vele verschillende prokaryoten worden opgehoopt in de cel als koolstof- en energiereserve. De eigenschappen van de polymeer maken PHA interessant als, volledig biologisch afbreekbaar, bioplastic. Bovendien zouden de monomeren gebruikt kunnen worden als chirale bouwstenen voor de productie van chemicaliën, of worden veresterd en gebruikt als biobrandstof.

Momenteel wordt PHA commercieel geproduceerd met behulp van reinculturen en gedefinieerde substraten. Om de kosten voor PHA-productie omlaag te brengen en brede toepassing mogelijk te maken, zouden ook microbiële verrijkingsculturen gebruikt kunnen worden. Dit neemt de noodzaak voor steriele omstandigheden weg en maakt het gebruik van agro-industriële afvalstromen als substraat mogelijk, wat bijdraagt aan de totstandkoming van een circulaire economie. Het proces voor PHA-productie uit afvalstromen met behulp van microbiële verrijkingsculturen omvat vier stappen: (1) acidogene fermentatie van de afvalstroom, (2) verrijking van een PHA-producerende cultuur, (3) productie van de PHA, en (4) opwerking van het product. De eerste stap beoogt de organische koolstof in de afvalstroom, voornamelijk koolhydraten, om te zetten naar geschiktere substraten voor PHA-productie, voornamelijk korte vetzuren (VFA's). In de tweede stap wordt de microbiële populatie verrijkt in bacteriën met een hoge PHA-productiviteit. Deze stap wordt doorgaans uitgevoerd onder *feast-famine*-omstandigheden in een sequentiële batch reactor (SBR), aangezien de afwisselende aan- en afwezigheid van substraat een competitief voordeel biedt aan bacteriën die substraat opslaan binnen hun cel. Zodra een stabiele cultuur is verkregen, zal de SBR dienen voor de productie van biomassa voor stap drie: het maximaliseren van het PHA-gehalte van de cultuur.

Een sterke selectiedruk voor PHA-producerende bacteriën kan worden bereikt door de SBR te draaien bij een slibverblijftijd van 1 dag, *feast-famine*-cycli van 12 uur en een temperatuur van 30°C. Voor microbiële verrijkingsculturen verkregen onder deze omstandigheden, gevoed met azijn- of melkzuur, is gerapporteerd dat ze meer dan 8 Cmol PHA ophopen per Cmol actieve biomassa (>87 wt.%). Dergelijke PHA-gehalten zijn vergelijkbaar met die bereikt in reinculturen, en de kinetische eigenschappen van de verrijkingsculturen zijn beter.

Het doel van dit proefschrift was opschalingsaspecten van de PHA-productie door

microbiële verrijkingsculturen te onderzoeken. De vertaling van het lab-proces naar industriële toepassing doet nieuwe vragen rijzen met betrekking tot het effect van (variabele) afvalwatersamenstelling en procesontwerp. **Hoofdstuk 2** en **3** richten zich daarom op het lot van de verschillende bestanddelen van een verzuurde afvalstroom, en het tweede deel (**Hoofdstuk 4-6**) van het proefschrift richt zich op alternatieve procesconfiguraties. **Hoofdstuk 1** geeft een algemene introductie tot het onderwerp en beschrijft het onderzoek dat voorafging aan dit proefschrift.

Hoofdstuk 2 beoordeelt de geschiktheid van boterzuur als substraat voor de productie van poly(3-hydroxybutyraat) (PHB). Er zijn twee SBR's gedraaid: één gevoed met butyraat, en een ander gevoed met een mengsel van acetaat en butyraat (1:1 Cmol). In beide reactoren domineerde *Plasticicumulans acidivorans* de verrijkingscultuur. De biomassa-specifieke koolstofopnamesnelheid en PHB-opbrengst voor butyraat waren significant hoger dan voor acetaat. Door de lagere dissimilatiebehoefte voor butyraat werd maar liefst 90% van de koolstof omgezet in PHB. Dit resulteerde in een verdubbeling van de specifieke PHB-productiesnelheid. Wanneer beide substraten beschikbaar waren, verkoos *P. acidivorans* sterk de opname van butyraat. Pas nadat alle butyraat opgenomen was, werd ook acetaat op een hoge snelheid opgenomen. De molaire substraatopnamesnelheid bleef gelijk, wat suggereert dat de opname of activatie van het substraat de snelheidsbepalende stap is. De resultaten geven aan dat voor een optimale productie van PHA uit afvalstromen de pre-fermentatiestap gestuurd zou moeten worden naar de productie van boterzuur.

Verzuurde afvalstromen zullen ook verbindingen bevatten die niet geschikt zijn voor PHA-productie. De aanwezigheid van deze verbindingen leidt tot de co-verrijking van bacteriën die geen PHA ophopen. Hun invloed op het algehele PHA-productieproces is onderzocht in **Hoofdstuk 3**, met behulp van een eenvoudig substraatmengsel van acetaat en methanol (1:1 Cmol). De verrijkingscultuur werd gedomineerd door *P. acidivorans* (40%) en *Methylobacillus flagellatus*, een obligate methylotroof die geen PHA kan opslaan. De aanwezigheid van de niet-accumulerende populatie verlaagde het maximale PHB-gehalte van de cultuur van meer dan 80 naar 66 wt.% (>5 naar 2.3 $Cmol_{PHB} \cdot Cmol_X^{-1}$). Wanneer tijdens de accumulatiestap ammonium werd gedoseerd – om een stikstofrijke afvalstroom na te bootsen – hoopte *P. acidivorans* nog steeds grote hoeveelheden PHB op, maar onbeperkte groei van de methylotrofe populatie deed het maximale PHB-gehalte verder dalen. Andere strategieën dan het beperken van ammonium zouden moeten worden ontwikkeld om de grootte en invloed van niet-accumulerende populaties te beperken. Op het moment dat alle acetaat opgenomen was, resteerde in de reactorvloeistof nog 80% van de gedoseerde methanol. Het invoegen van een scheidingsstap (vloeistof - vaste stof) direct nadat de VFA's zijn opgenomen, zou het mogelijk maken om substraten die niet geschikt zijn voor PHA-productie selectief uit de SBR te verwijderen.

Hoofdstuk 4 verkent de haalbaarheid van het combineren van de verrijkings- en productiestap in één enkele reactor. Het oogsten van PHA-rijke biomassa direct uit de SBR verlaagt de kapitaalkosten, maar zou tot hogere opwerkingskosten kunnen leiden indien het PHA-gehalte significant lager wordt. Door de SBR te draaien bij een uitwisselingsvolume van 75% (18-uurs cycli, 1 dag slibverblijftijd) was het mogelijk om biomassa met 70 wt.% PHB (2.8 $Cmol_{PHB} \cdot Cmol_X^{-1}$) te produceren in één enkele processtap vanaf acetaat. Door het uitwisselingsvolume te verhogen naar 83% (20-uurs cycli), nam het PHB-gehalte van de geoogste biomassa toe tot 75 wt.% (3.6 $Cmol_{PHB} \cdot Cmol_X^{-1}$), maar daalde de operationele stabiliteit. Wanneer de SBR draait bij zulke grote relatieve uitwisselingsvolumes, moeten bacteriën hun groeisnelheid verhogen en is het externe substraat beschikbaar over relatief lange periodes. Dit laat de vorming van grotere zijpopulaties toe en had een negatief effect op de kinetische eigenschappen van *P. acidivorans*. De PHA-opslagsnelheid, -opbrengst en -opslagcapaciteit van de cultuur daalden. Hoewel het maximaliseren van het relatieve uitwisselingsvolume een geschikte strategie is om grote hoeveelheden PHA te produceren in de SBR, zorgt het niet voor de verrijking van een cultuur met superieure PHA-productiviteit.

De *feast-famine*-omstandigheden van de SBR kunnen ook bereikt worden met twee of meer continue geroerde tankreactoren (CSTR's) in serie, met gedeeltelijke recirculatie van de biomassa. Het gebruik van CSTR's biedt meerdere voordelen, maar zal ook resulteren in verblijftijdspreiding en een minder strikte scheiding tussen *feast*- en *famine*-omstandigheden. **Hoofdstuk 5** beschrijft een set rekenkundige modellen, ontwikkeld om de groei van *P. acidivorans* in concurrentie met een niet-accumulerende heterotroof te voorspellen. De modellen zijn gebruikt om het effect van diverse proces- en biomassaspecifieke parameters op de verrijking van PHA-producerende bacteriën te bestuderen. De simulaties lieten zien dat in het tweetraps CSTR-systeem de selectiedruk significant lager is dan in de SBR en sterk afhankelijk is van de gekozen *feast-famine*-verhouding. Om het effect van verblijftijdspreiding en de resulterende spreiding in de toestand van individuele bacteriën te bestuderen, is zowel een macroscopisch model gemaakt, dat de biomassa als geheel beschouwt, als een agent-baseerd model, dat individuele cellen beschouwt. Alhoewel het macroscopische model de selectiedruk in het tweetraps CSTR-system overschat, geeft het een snelle en redelijk goede indruk van de reactorprestaties. Om het competitieve voordeel van PHA-producerende bacteriën te versterken, zou het aantal CSTR's in serie verhoogd moeten worden.

Het effect van continue koolstofdosering, en daarmee de continue aanwezigheid van residueel substraat, op de verrijking van PHA-producerende bacteriën is experimenteel onderzocht in **Hoofdstuk 6**. Er zijn twee SBR's gedraaid. In de eerste reactor, werd het substraat (acetaat) continu gedoseerd en werd *Zoogloea* sp. verrijkt. De cultuur hoopte PHB op bij blootstelling aan een overmaat koolstof, maar de PHB-productiesnelheid en -opslagcapaciteit (53 wt.%, 1.3 $Cmol_{PHB} \cdot Cmol_X^{-1}$) waren éénvijfde van dat waarge-

nomen voor verrijkingsculturen in een gewone, puls-gevoede SBR gedomineerd door *P. acidivorans*. In de tweede reactor werd de helft van de acetaat gedoseerd aan het begin van de cyclus en de andere helft continu. Met het hebben van een echte *feast*-periode, werd de verrijking van *P. acidivorans* niet gehinderd door de continue toevoer van acetaat, en de cultuur hoopte 85 wt.% PHB (6.6 $Cmol_{PHB} \cdot Cmol_X^{-1}$) op. Dit laat zien dat voor het verrijken van bacteriën met een superieure PHA-productiecapaciteit de periodieke overmaat aan substraat – een werkelijke *feast*-periode – essentieel is, terwijl de periodieke afwezigheid van substraat – een werkelijke *famine*-periode – dat niet is. De mogelijkheid om minder strikte *famine*-omstandigheden toe te passen, is een vereiste voor het gebruik van het tweetraps CSTR-system, maar heeft ook belangrijke voordelen voor het opschalen van het SBR-proces zelf.

Hoofdstuk 7 recapituleert en integreert de belangrijkste bevindingen. Hoewel verdere optimalisatie en afstemming van het proces nodig zal zijn, met name voor de acidogene fermentatiestap, is de ontwikkeling van toepassingen momenteel het belangrijkste obstakel voor industriële implementatie.

1

INTRODUCTION

Parts of this chapter have been published as: L. Marang, Y. Jiang, J. Tamis, H. Moralejo-Gárate, M.C.M. van Loosdrecht, and R. Kleerebezem. 2012. Microbial community engineering: Producing bioplastic from waste. Bioplastics Magazine 7, 22-24.

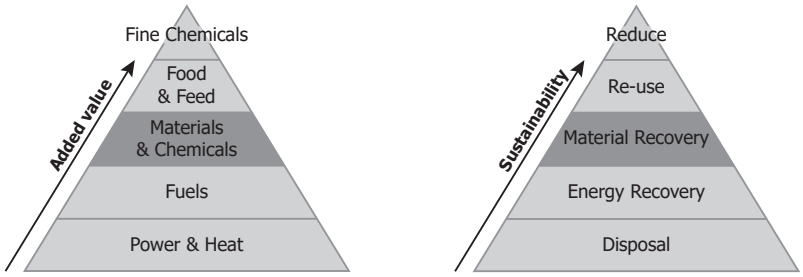

Figure 1.1: Pyramids depicting the added value of biobased products and the waste hierarchy.

1.1. RESOURCE RECOVERY

Production of waste is a sign of inefficiency. The amounts of waste generated in our agro-industrial production chains are nevertheless enormous. Effective reclamation and valorization of these organic residues is one of the main challenges towards the establishment of a sustainable society. Many organic waste streams are variable in composition and strength, too heterogeneous to allow the direct recovery of valuable compounds, and too wet to allow efficient thermochemical processing by combustion, gasification, or pyrolysis (Pham et al., 2015). Microorganisms possess the ability, though, to convert the multitude of (complex) molecules in these residues to products that are easier to recover.

In the naturally-occurring anaerobic digestion process, microbial communities hydrolyze organic matter to the monomeric building blocks, then convert these to organic acids and alcohols, and, ultimately, to biogas – a mixture of methane and carbon dioxide (Agler et al., 2011; Kleerebezem et al., 2015). Anaerobic digestion is widely applied – at domestic as well as industrial scale – to recover energy (heat and/or power) from manure, sewage sludge, the organic fraction of municipal solid waste, or wastewater, for example (Kleerebezem et al., 2015). However, the economic value of biogas is low.

The organic acids and alcohols, produced as intermediate products of the anaerobic digestion process, could also be used for the production of higher added value products, such as polyhydroxyalkanoates (PHA) or medium-chain fatty acids (Agler et al., 2011; Kleerebezem et al., 2015). Depending on the nature of the waste stream – the size and fraction of readily fermentable organic matter, for example – the recovery of these materials and chemicals is to be preferred over the recovery of energy, from an economic as well as a sustainability perspective (Figure 1.1).

The research program “Waste to Resource” (W2R) of the Dutch Technology Foundation STW aimed to develop biotechnological processes for the conversion of organic waste to renewable resources. The research described in this thesis was part of this program and aimed to further develop the production of PHA from acidified, agro-industrial waste streams.

1.2. POLYHYDROXYALKANOATES

PHAs are microbial storage polymers. They are accumulated by many different prokaryotes as a carbon and energy reserve, and can be stored in large amounts (up to 90% of the cell dry weight) in granules inside the cell (Figure 1.2) (Anderson and Dawes, 1990; Steinbüchel, 1991; Tan et al., 2014). PHA is synthesized when excess carbon is present during intermittent substrate feeding, or when microorganisms are exposed to a nutrient or oxygen limitation (Reis et al., 2003; Steinbüchel, 1991).

Chemically, PHA is a polyester of hydroxy fatty acids and over 90 different hydroxyalkanoate monomer units have been identified (Steinbüchel and Valentin, 1995). The type of monomer formed depends on the available substrate and the type of PHA synthase the microorganism possesses. Based on the substrate specificity of the different PHA synthases, PHAs are divided in two classes: PHAs comprising monomers of 3-5 carbon atoms are called short-chain-length (scl) PHAs, and PHAs with monomers of 6-14 carbon atoms are called medium-chain-length (mcl) PHAs (Anderson and Dawes, 1990; Lee, 1996). The common structure of all these PHAs is shown in Figure 1.3a.

The most abundant PHA is poly(3-hydroxybutyrate) (PHB) (Figure 1.3b). PHB was firstly isolated and characterized by the French microbiologist Maurice Lemoigne in 1926 (Lemoigne, 1926). Its material properties are similar to those of polypropylene (PP, Figure 1.3d): both polymers have a compact helical structure, a glass-transition temperature (T_g) around 0°C, and a melting temperature (T_m) between 170 and 180°C (Anderson and Dawes, 1990; Lee, 1996). PHB has a better UV resistance than polypropylene, but is highly crystalline (60-80%) and therefore relatively stiff (Anderson and Dawes, 1990; Lee, 1996). The most important drawbacks of PHB are, however, its brittleness and poor melt stability – PHB decomposes at approximately 200°C (Lee, 1996).

The polymer properties can be improved by the inclusion of other monomer units, such as 3-hydroxyvalerate (HV, Figure 1.3c) (Anderson and Dawes, 1990). HV is synthesized when the substrate contains volatile fatty acids (VFAs) with an odd number of carbon atoms – i.e., propionate or valerate. The random copolymer of 70 mol% 3-hydroxybutyrate (HB) and 30 mol% 3-hydroxyvalerate (HV) has a lower crystallinity (30-40%) and lower melting temperature (143°C) than the homopolymer PHB (Anderson and Dawes, 1990; Lee, 1996). This yields a less stiff, more tough polymer.

The described properties make PHA an interesting bioplastic that – besides being produced from renewable resources – is fully biodegradable and the only bioplastic completely synthesized by microorganisms (Chen, 2009). PHAs are applied for packaging and for disposable or compostable items such as razors, cups, and bags (Chen, 2009; Lee, 1996). Furthermore, they are used in the medical field as drug delivery carriers or medical implants such as sutures, cardiovascular patches, stents, or orthopedic pins (Chen, 2009; Lee, 1996; Luef et al., 2015). As HB monomers and oligomers naturally occur in human blood and tissue, PHB is considered biocompatible (Anderson and Dawes,

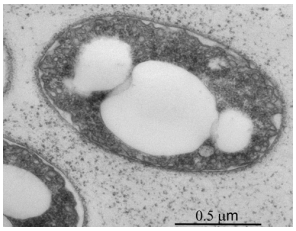

Figure 1.2: Electron microscopy image of a bacterial cell with PHA granules.

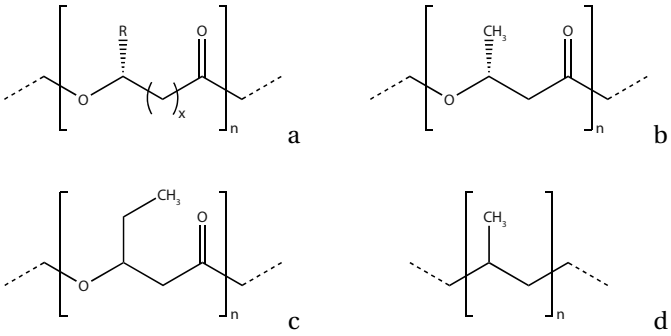

Figure 1.3: (a) General structural formula of PHA. The number of monomers in the polymer (n) ranges from 100–30,000 (Steinbüchel, 1991). (b) Structural formula of poly(3-hydroxybutyrate) (PHB), where x = 1 and R = CH_3. (c) Structural formula of poly(3-hydroxyvalerate) (PHV), where x = 1 and R = C_2H_5. (d) Structural formula of polypropylene (PP).

1990; Lee, 1996). PHB and other PHAs are even investigated as a feed supplement for (aquatic) animals (Defoirdt et al., 2009).

The interest for PHA is broader than just the use of the polymer though. Due to the stereospecificity of the PHA synthases all monomers of the PHA polymer are in the R-configuration (Anderson and Dawes, 1990; Lee, 1996). The enantiomerically pure hydroxyl fatty acid monomers could, therefore, serve as chiral building blocks for the production of various fine chemicals (Chen, 2009). PHB can be converted – via crotonic acid – to *n*-butanol (Schweitzer et al., 2015) or acrylic acid and propylene (Spekreijse et al., 2015), for example. Moreover, the PHA monomers could be esterified with methanol to hydroxy fatty acid methyl esters and used as a biofuel (Chen, 2009; Zhang et al., 2009).

1.3. CONVENTIONAL PHA PRODUCTION

At this moment, PHA is commercially produced by a handful of companies, located mainly in China (e.g., Ecomann Biotechnology, TianAn Biologic Materials, and Tianjin GreenBio Materials) and the USA (e.g., Metabolix and MHG) (Chanprateep, 2010; Chen, 2009). The PHA is produced using pure cultures of, generally, wild type *Cupriavidus*

necator – formerly *Ralstonia eutropha* (Vandamme and Coenye, 2004) – or recombinant *Escherichia coli* (Chen, 2009; Choi and Lee, 1999). These microorganisms are grown on well-defined substrates such as glucose and propionic acid, and accumulate large amounts of PHA (75-90 wt.%) (Chen, 2009; Choi and Lee, 1999).

The use of expensive, pure substrates and the need for sterile operation result in a high price for PHA. PHA is currently still 2-5 times more expensive than comparable petroleum-based plastics (Chanprateep, 2010; Choi and Lee, 1999; Jacquel et al., 2008; Reis et al., 2003). For specific applications – e.g., in the medical field – the superior biocompatibility and biodegradability of PHA justify the higher price (Luef et al., 2015). In many other cases, the high price hampers broad application (Choi and Lee, 1999; Reis et al., 2003). Moreover, the use of pure glucose for large-scale bioplastic and/or biofuel production competes with food and feed production (Chanprateep, 2010).

1.4. MICROBIAL COMMUNITY ENGINEERING

Many researchers have investigated the use of cheap substrates, such as organic waste, as a way to reduce the cost of PHA (Chanprateep, 2010; Khosravi-Darani et al., 2013; Koller et al., 2010). Conventional pure culture processes require sterilization of the reactor and liquid streams entering the process, and are therefore not suitable for waste-based PHA production. To eliminate the need for axenic conditions, the natural function of PHA as storage polymer can be exploited to enrich open microbial communities in bacteria that have a high PHA storage capacity. By creating a selective environment in which PHA-producing bacteria thrive, an inherently stable culture can be obtained. Such a culture can be cultivated on agro-industrial waste streams, in a simple, non-sterile reactor (Figure 1.4) (Reis et al., 2003). This reduces the raw material cost, equipment cost, and energy cost for PHA production – making PHA a more economical and sustainable bioplastic.

One example of a selective environment in which PHA-producing bacteria have a competitive advantage is found in the enhanced biological phosphorus removal (EBPR) process, with its alternating anaerobic and aerobic periods (van Loosdrecht et al., 1997; Reis et al., 2003; Serafim et al., 2008). As substrate is fed during the anaerobic period, the availability of electron donor and (external) electron acceptor is separated. Biomass growth during the anaerobic period is thus prevented, but specific groups of bacteria – the phosphate-accumulating organisms (PAOs) and glycogen-accumulating organisms (GAOs) – are able to secure the supplied substrate inside their cell by storing it as PHA (Reis et al., 2003; Serafim et al., 2008). The energy (ATP) required for this is provided by the hydrolysis of previously stored polyphosphate – for the PAOs – or glycogen – for the GAOs (Reis et al., 2003; Serafim et al., 2008). When the aerobic period commences, the external carbon has been depleted. Only bacteria that stored substrate inside their cell can use this for growth, maintenance, and replenishment of their polyphosphate

and glycogen pools. PHA-producing bacteria will thus outcompete bacteria that did not store substrate during the anaerobic period.

The amount of PHA that PAOs and GAOs can accumulate anaerobically depends on the amount of polyphosphate or glycogen that they stored during the preceding aerobic period and is generally less than 40 wt.% (Reis et al., 2003; Serafim et al., 2008). The use of microaerophilic instead of strictly anaerobic conditions may increase the maximum PHA content, but this requires very strict oxygen control (Satoh et al., 1998). Another way to reach higher PHA contents is to include an accumulation step under aerobic, nutrient-limited conditions (Bengtsson, 2009; Serafim et al., 2008). Bengtsson (2009) reported the accumulation of 60 wt.% PHA when applying this strategy to a GAO-dominated culture. A maximum PHA content of 60 wt.% is, however, still low compared to the PHA contents reached in pure cultures and will give rise to high downstream-processing cost (Chen, 2009; Choi and Lee, 1999). Moreover, part of the substrate will always be used for the synthesis of glycogen rather than PHA, which reduces the product yield (Reis et al., 2003).

The research described in this thesis follows a more promising approach, which is based on the observed accumulation of PHA in aerobic wastewater treatment plants (van Loosdrecht et al., 1997; Reis et al., 2003; Serafim et al., 2008). In these systems, intermittent substrate availability – having alternating periods of substrate presence (feast) and absence (famine) – creates a competitive advantage for PHA-producing bacteria (Reis et al., 2003; Serafim et al., 2008). During the feast phase, when excess substrate is present, bacteria can use the substrate either for growth or storage. The storage of (volatile) fatty acids as PHA is fast and involves only a few enzymatic steps (Figure 1.5) (Lee, 1996; Reis et al., 2003; Serafim et al., 2008). Bacteria can therefore use PHA storage to quickly adjust their substrate uptake capacity to the increased carbon availability, before, or without, enlarging their growth machinery (van Loosdrecht et al., 1997; Reis et al., 2003). During the subsequent famine phase no external carbon source is available, but bacteria that stored PHA can continue their growth (Figure 1.6). Bacteria that quickly store substrate as soon as it becomes available can thus balance their growth rate over the cycle, and have a competitive advantage over bacteria that grow merely during the – relatively short – feast phase (van Loosdrecht et al., 1997; Reis et al., 2003; Serafim et al., 2008).

Various researchers investigated the use of a feast-famine regime, or aerobic dynamic feeding (ADF), as enrichment strategy for the production of PHA from fermented waste streams of the paper and food industry (Albuquerque et al., 2010b; Bengtsson et al., 2008b; Coats et al., 2007; Dionisi et al., 2005a; Jiang et al., 2012; Tamis et al., 2014a). For several of these microbial enrichment cultures, maximum PHA contents between 70 and 80 wt.% have been reported (Albuquerque et al., 2010b; Jiang et al., 2012; Tamis et al., 2014a). These values are comparable to those obtained using pure cultures, while they are obtained using waste rather than a well-defined substrate (Figure 1.4) (Chen, 2009). Moreover, the kinetic properties of the enrichment cultures – the biomass-specific PHA

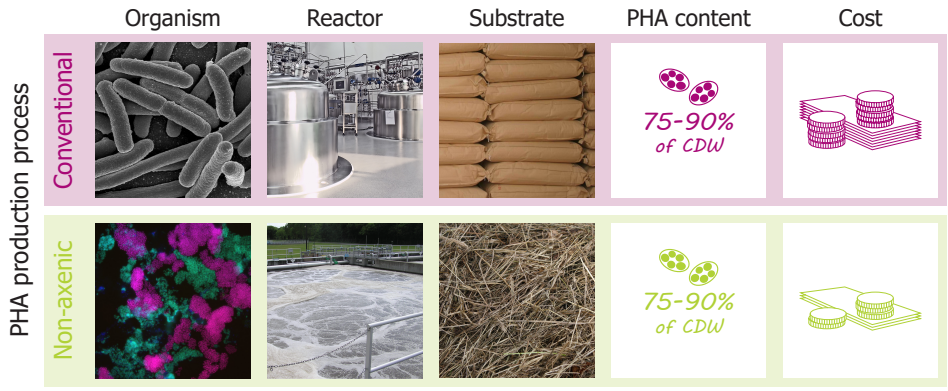

Figure 1.4: Comparison of the conventional process for PHA production (using pure culture biotechnology) and the studied, non-axenic process for PHA production (using microbial enrichment cultures).

production rates, for example – are better than those of the pure cultures (Reis et al., 2003).

1.5. PHA PRODUCTION BY MICROBIAL ENRICHMENTS

The overall process for non-axenic PHA production from organic waste comprises four steps (Figure 1.7): (1) acidogenic fermentation of the waste stream, (2) enrichment of a PHA-producing culture, (3) production of the PHA, and (4) recovery of the product (Dionisi et al., 2004; Serafim et al., 2008). The first or acidogenic fermentation step (Bengtsson et al., 2008a; Temudo et al., 2007) aims to convert the waste organic carbon, primarily carbohydrates, to a mixture of volatile fatty acids (VFAs). These acids are more suitable substrates for PHA production than the original carbohydrates (Bengtsson et al., 2008a; Reis et al., 2003) and will be used as such in the following two steps.

In the second step, an open microbial community is enriched in bacteria with a high PHA storage capacity. This enrichment step is performed in a sequencing batch reactor (SBR) operated under the feast-famine regime described in the previous section (Dionisi et al., 2004; Reis et al., 2003). At the start of each cycle, substrate is fed to the reactor (Figure 1.6). The bacteria compete for this substrate based on their maximum biomass-specific substrate uptake rate and use the substrate for growth and/or PHA storage (Reis et al., 2003). After substrate depletion – i.e., during the famine phase – bacteria may use their stored PHA for growth and maintenance (Figure 1.6). Before new substrate is fed to the reactor and another feast phase starts, part of the bacteria is removed from the SBR. In this way, the biomass concentration in the reactor is controlled and it is assured that only bacteria that grow fast enough can survive in the system (Dionisi et al., 2004). By repeating this feast-famine cycle, the microbial community is gradually enriched in PHA-producing bacteria, whereas non-PHA producers are washed out.

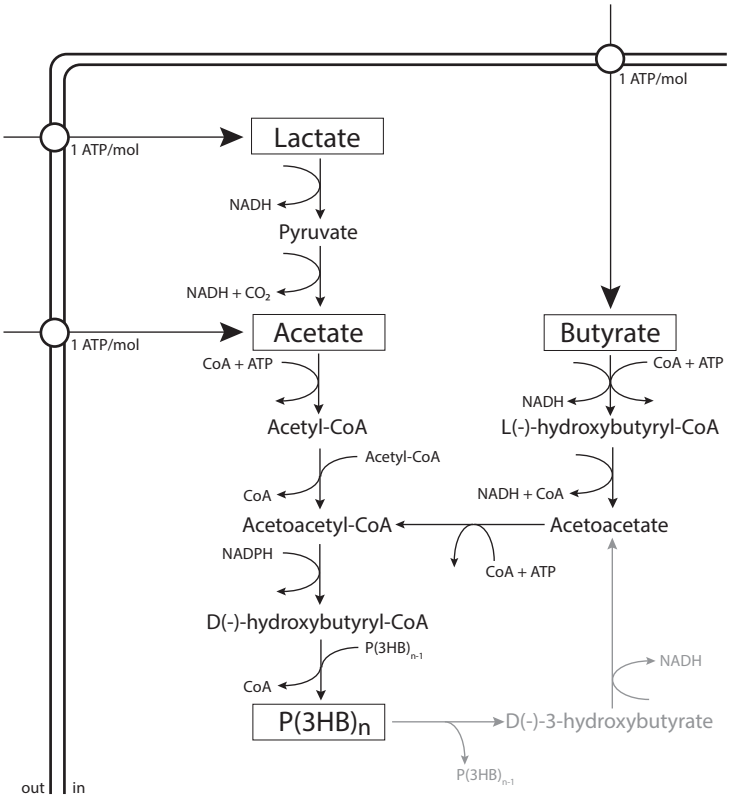

Figure 1.5: Metabolic pathway for the synthesis and degradation of PHB from acetate, butyrate, and/or lactate. Adapted from Reis et al. (2003).

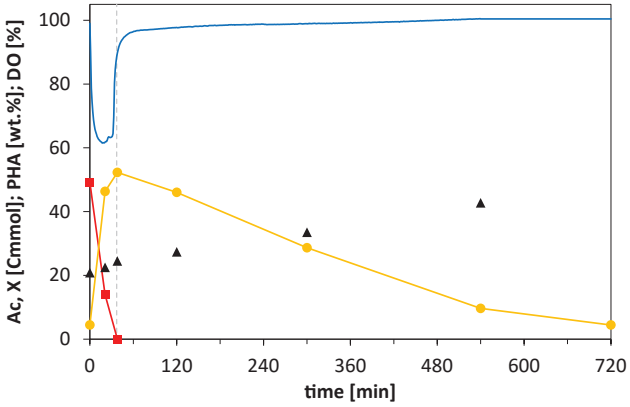

Figure 1.6: Typical SBR cycle of a PHA-producing microbial enrichment culture on acetate. The acetate present in the reactor (Cmmol) is represented by red squares, active biomass (Cmmol) by black triangles, and PHA (wt.%) by yellow circles. The blue line displays the dissolved oxygen level (%) in the reactor liquid. Adapted from Jiang et al. (2011c).

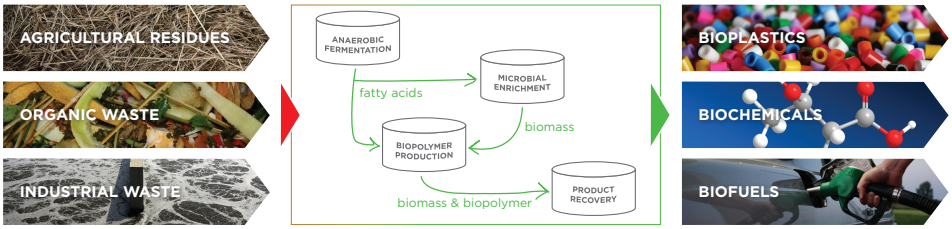

Figure 1.7: Schematic overview of the process for PHA production by microbial enrichment cultures.

Once a stable culture is obtained, the SBR will be operated as a biomass production step and the excess sludge – removed at the end of each cycle – used in step three: maximization of the PHA content of the biomass in a (nitrogen-limited) fed-batch reactor (Dionisi et al., 2004; Johnson et al., 2009a). Under growth-limiting conditions and the continuous supply of carbon the bacteria will saturate their storage capacity and produce up to nine times their own dry weight of PHA (Jiang et al., 2011c; Johnson et al., 2009a).

The produced PHA is extracted from the cells and further purified in the fourth and final step of the process. The extraction methods can roughly be divided in two categories: either the PHA is solubilized (e.g., solvent extraction) or the non-PHA cell material is solubilized (e.g., digestion by surfactants) (Jacquel et al., 2008). The optimal isolation and purification method will have to be chosen in view of the envisioned application and corresponding product requirements with respect to purity and molecular weight.

1.6. PRIOR RESEARCH

The key to successful non-axenic PHA production is the enrichment of bacteria with a superior PHA productivity, i.e., a high PHA storage capacity and high PHA storage rate. In 2009, Johnson et al. (2009a) reported the enrichment of a microbial culture producing 89 wt.% PHB from acetate in 7.6 h. This was by far the highest PHA content reported for a microbial enrichment culture (Johnson et al., 2009a; Serafim et al., 2008) and an important breakthrough.

Two important differences between the enrichment strategy of Johnson et al. (2009a) and that of other researchers (e.g., Albuquerque et al., 2007; Bengtsson et al., 2008b; Serafim et al., 2004) are the applied solids retention time (SRT) and the temperature. As a shorter SRT should lead to higher conversion rates, higher yields, and less inert biomass, Johnson et al. (2009a) applied an SRT of 1 day rather than the more common activated sludge-based SRT of 7-10 days. The length of a feast-famine cycle was comparable (12 h), which means that the number of cycles per SRT was greatly reduced and bacteria had to double each cycle in order to stay in the system (Johnson et al., 2009a). This requires the storage of significant amounts of PHA (up to 56 wt.%) during each feast phase (Jiang

et al., 2011a; Johnson et al., 2009a). Also the higher temperature used by Johnson et al. (2009a) – 30°C instead of 20-25°C – contributed to a general increase of the conversion rates. However, it affected in particular the microbial species that was enriched. The culture was dominated by a novel bacterium, *Plasticicumulans acidivorans*, that was later shown to have an optimal growth temperature of 30°C (Jiang et al., 2011d). At a temperature of 20°C but otherwise identical operational conditions, *Zoogloea* sp. was enriched (Jiang et al., 2011a). This organism has a significantly lower PHA storage capacity (72 wt.%) and biomass-specific PHA production rate (Jiang et al., 2011a).

The enrichment strategy applied by Johnson et al. (2009a) – i.e. operating the SBR at a short SRT (1 d), feast-famine cycles of 12 h, and a temperature of 30°C – has been validated with a study on non-axenic PHA production from lactate (Jiang et al., 2011c). The use of a different substrate (lactate) had a direct impact on the microbial community structure, but did not affect the functionality of the enrichment culture. The culture accumulated more than 90 wt.% PHA in 6 h: the best result reported for a bacterial culture in terms of both final PHA content and biomass-specific PHA production rate (Jiang et al., 2011c). Also when using a mixture of acetate and lactate (Jiang et al., 2011c) or acetate and propionate (Jiang et al., 2011b), high PHA contents (>80 wt.%) were reached within several hours. Overall, the establishment of a general and strong selective pressure for bacteria with a high PHA productivity was confirmed. This opened the way for further development of the process for non-axenic PHA production from agro-industrial waste streams.

1.7. SCOPE AND OUTLINE OF THIS THESIS

The aim of this thesis was to investigate scale-up aspects of the PHA production by microbial enrichment cultures. A translation of the laboratory process – developed and studied by Johnson (2010) and Jiang (2011) – to industrial application raises new questions concerning the impact of (variable) wastewater composition and process design, for example.

The first part (Chapter 2-3) of this thesis focusses on the fate of the different constituents of an acidified, agro-industrial waste stream. Detailed knowledge on the impact of individual substrates, alone and in combination with others, on the microbial community structure and kinetics of PHA production enables the prediction of waste stream suitability and optimization of the PHA production process. Besides the acetate, propionate, and lactate already studied (Jiang et al., 2011b,c; Johnson et al., 2009a), butyrate can be a major product of acidogenic fermentation (Bengtsson et al., 2008a; Reis et al., 1991; Temudo et al., 2007). **Chapter 2** assesses the suitability of butyrate as substrate for PHA production. As butyrate has a 40% higher theoretical product yield and lower oxygen requirements than acetate (Shi et al., 1997), butyrate may be preferred over acetate as substrate.

Fermented organic waste streams typically also contain compounds that are less suitable for PHA production. The presence of these compounds leads to the co-enrichment of non-PHA-storing bacteria that will lower the overall PHA content of the culture (Albuquerque et al., 2007; Jiang et al., 2012; Morgan-Sagastume et al., 2010). In **Chapter 3** the impact of these non-PHA-storing bacteria on the overall PHA production process is investigated using a simple substrate mixture of acetate and methanol.

The second part (Chapter 4-6) of this thesis focusses on alternative process configurations. As described in section 1.5, the process for non-axenic PHA production generally comprises four steps: acidogenic fermentation of the waste stream, enrichment of a PHA-producing culture, production of the PHA, and recovery of the product. **Chapter 4** explores the feasibility of combining the enrichment and production step. Harvesting PHA-rich biomass directly from the reactor used for enrichment of the microbial culture reduces capital cost, but may increase downstream-processing cost if the PHA content is significantly reduced. By increasing the volume exchange ratio of the reactor, the PHA content at the end of the feast phase may reach sufficiently high levels (Jiang et al., 2011a).

Although the SBR commonly used for the enrichment of PHA-producing cultures is a highly convenient system at small scale, its discontinuous nature requires relatively large buffer volumes and pumping capacity. Furthermore, there is a large difference between the oxygen transfer rate required during the feast and famine phase of the SBR cycle. These issues inhibit an economic scale-up of the process, and could be addressed by establishing the feast-famine conditions in two or more continuous stirred-tank reactors (CSTRs) in series, with partial biomass recirculation. The use of such a staged CSTR system facilitates the inclusion of a solid-liquid separation step between the feast and famine reactor(s), and thus their independent design. It will also result in distributed residence times and a less strict separation between feast and famine conditions, though – two factors that may significantly affect the selective pressure for PHA-producing bacteria.

Chapter 5 describes a set of mathematical models, developed to predict the growth of *P. acidivorans* – as model PHA producer – in competition with a non-storing heterotroph. The models are used to investigate the impact of various process and biomass-specific parameters on the enrichment of PHA-producing bacteria in feast-famine SBR and staged CSTR systems. Both a macroscopic model considering lumped biomass and an agent-based model considering individual cells were created in order to study the effect of distributed residence times and the resulting distributed bacterial states.

In **Chapter 6** the impact of continuous carbon supply, and thereby the continuous presence of residual substrate, on the enrichment of PHA-producing bacteria is investigated experimentally. Two SBRs with an additional, continuous feed stream were operated. In the first, all substrate was dosed continuously to remove the selective pressure

for PHA-producing bacteria. In the second, the leaching of substrate – as it will occur in a staged CSTR system – was mimicked by dosing half of the substrate at the beginning of the cycle and the other half continuously.

Chapter 7 summarizes and integrates the main findings of the studies presented in Chapter 2-6. In addition, it discusses some remaining issues and provides recommendations for further research.

2

BUTYRATE AS PREFERRED SUBSTRATE FOR PHB PRODUCTION

In this study, the suitability of butyrate as substrate for polyhydroxyalkanoate (PHA) production by microbial enrichment cultures was assessed. Two sequencing batch reactors were operated under feast-famine conditions: one fed with butyrate, and another with mixed acetate and butyrate. The obtained results were compared to previous results with acetate as sole substrate. In all three reactors Plasticicumulans acidivorans *dominated the enrichment culture. The carbon uptake rate and PHA yield were significantly higher on butyrate than on acetate, resulting in a higher PHA production rate. When both substrates were available the bacteria strongly preferred the uptake of butyrate. Only after butyrate depletion acetate was taken up at a high rate. The molar substrate uptake rate remained the same, suggesting that substrate uptake is the rate-limiting step. The results show that for optimized waste-based PHA production the pre-fermentation process should be directed towards butyrate production.*

Published as: L. Marang, Y. Jiang, M.C.M. van Loosdrecht, and R. Kleerebezem. 2013. Butyrate as preferred substrate for polyhydroxybutyrate production. Bioresource Technology 142, 232-239.

2.1. INTRODUCTION

Polyhydroxyalkanoates (PHAs) are microbial storage polymers accumulated by many different groups of bacteria as an intracellular reserve of energy and carbon (Steinbüchel, 1991). The chemical properties of the polymer are similar to those of petrochemical plastics like polypropylene, and PHA is already commercially available as a fully biodegradable bioplastic. The interest for PHA is broader than just its use as a biopolymer though (Chen, 2009). The methyl esters of its monomers could be used as a biofuel. Moreover, since the polymer is enantiomerically pure, its hydroxy fatty acid monomers could serve as chiral building blocks for the production of all kinds of biochemicals (Chen, 2009).

The use of cheap substrates, such as organic waste, has been investigated by many researchers as a way to reduce the production cost of PHA (Khosravi-Darani et al., 2013; Koller et al., 2013). Pure culture processes require however sterilization of the reactor and liquid streams entering the process. To eliminate this need for axenic conditions – and lower the energy and equipment cost – microbial enrichment cultures can be used (Albuquerque et al., 2010b; Bengtsson et al., 2008b; Dionisi et al., 2005a; Jiang et al., 2012). These enrichments of natural bacteria are obtained from activated sludge by subjecting the microbial community to feast-famine conditions, thus generating a competitive advantage for bacteria that store substrate inside their cell as a reserve (Reis et al., 2003). In 2009, Johnson et al. (2009a) reported the enrichment of a culture producing 89 wt.% PHA from acetate in 7.6 h. This still is the highest PHA content reported for a microbial enrichment culture on volatile fatty acids (VFAs). The culture was dominated by *Plasticicumulans acidivorans* – a microorganism with high specific substrate uptake rates for a wide range of VFAs, including butyrate (Jiang et al., 2011d).

Butyrate is an interesting substrate for PHA production for two reasons. First, it has a high theoretical product yield. The stoichiometric yield of PHA on butyrate is 0.94 $Cmol \cdot Cmol^{-1}$, which is 40% higher than the yield on acetate (Shi et al., 1997). Second, and more important, butyrate is produced in large amounts during acidogenic fermentation of organic waste streams. The presence of butyrate in, e.g., fermented sugar cane molasses, olive oil mill effluents, paper mill wastewater, waste activated sludge, or food waste has been reported by various researchers (Albuquerque et al., 2007; Beccari et al., 2009; Bengtsson et al., 2008a,b, 2010; Dionisi et al., 2005a; Jiang et al., 2012; Morgan-Sagastume et al., 2010; Rhu et al., 2003). Nevertheless, PHA production from butyrate has hardly been studied. Long-term experiments on the production of PHA from butyrate are limited to microbial enrichments on fermented waste (Albuquerque et al., 2007, 2010b, 2013; Bengtsson et al., 2010; Jiang et al., 2012). Due to the complexity of the substrate and the resulting microbial community, these results are not conclusive. The two reports found on experiments with pure butyrate or defined VFA mixtures, Lemos et al. (2006) and Jiang et al. (2012), report the conversion by non-adapted communities only.

The aim of this study was to assess the suitability of butyrate as substrate for PHA production by microbial enrichment cultures. Detailed knowledge on the impact of butyrate on the composition of the microbial community and the kinetics of PHA production enables the prediction of waste stream suitability and optimization of the PHA production process. To study the production of PHA from butyrate two sequencing batch reactors (SBRs) were operated: one on sole butyrate and one on a 1:1 Cmol mixture of acetate and butyrate. These enrichment cultures were compared to a similar PHA-accumulating enrichment culture on acetate.

2.2. MATERIALS AND METHODS

2.2.1. SBR FOR ENRICHMENT OF A PHA-PRODUCING CULTURE

A double-jacket glass bioreactor with a working volume of 2 L (Applikon, Netherlands) was used to enrich and maintain the PHA-producing microbial community. The basic setup and operation of the reactor were the same as described by Johnson et al. (2009a). The reactor was operated as a non-sterile SBR with 12 h cycles, each consisting of a start phase (5 min), feeding phase (10 min), reaction phase (685 min), and effluent phase (20 min). Since there was no settling phase, the solids retention time (SRT) equaled the hydraulic retention time (HRT), and both were 1 day. The air flow rate to the reactor was set to 0.2 $L_N \cdot min^{-1}$ using a mass flow controller (Brooks Instrument, USA). The total gas flow rate through the reactor was increased to 1.4 $L_N \cdot min^{-1}$ by partial recirculation of the off-gas. The temperature in the reactor was controlled at 30±1°C, and the pH was maintained at 7.0±0.1 by the addition of 1 M HCl and 1 M NaOH. Controlling of the pumps, stirrer, airflow, temperature, and pH was done by a biocontroller (Biostat Bplus, Sartorius Stedim Biotech, Germany).

The culture previously enriched on acetate by Johnson et al. (2009a) had been maintained for comparison. Biomass from this enrichment culture, highly dominated by *P. acidivorans* (Figure 2.1), was used as inoculum for both SBRs operated in this study. Except for the carbon source, the medium composition was the same as described by Johnson et al. (2009a). During each cycle 1 L of fresh medium was dosed into the reactor. The carbon source herein was either sodium butyrate (9.5 mM) or a mixture of sodium acetate and butyrate (11 and 5.5 mM respectively). The other chemical compounds in the medium were: 6.74 mM NH_4Cl, 2.49 mM KH_2PO_4, 0.55 mM $MgSO_4 \cdot 7H_2O$, 0.72 mM KCl, 1.5 $mL \cdot L^{-1}$ trace elements solution according to Vishniac and Santer (1957), and 5 $mg \cdot L^{-1}$ allylthiourea (to prevent nitrification).

The enrichment cultures were considered stable, or at stable operational performance, when the length of the feast phase and the ammonium concentration at the end of the cycle had become constant for at least 5 days. Once a stable culture was obtained cycle experiments were conducted to characterize the operational performance of the SBR and to generate the data required for process modeling. In addition, biomass from the

SBR was collected for accumulation experiments and analysis of the microbial community structure.

2.2.2. FED-BATCH REACTOR FOR PHA ACCUMULATION

To evaluate the PHA storage capacity of the obtained enrichment culture, accumulation experiments were performed in another double-jacket glass bioreactor (Applikon, Netherlands) operated as a non-sterile fed-batch reactor. The reactor, with a working volume of 2 L, was operated at the same aeration rate, pH, and temperature as the SBR. At the beginning of each experiment the reactor was filled with 1 L biomass from the enrichment SBR, and 1 L of carbon- and ammonium-free medium (otherwise the same composition). In this way growth in the fed-batch reactor was limited by the amount of ammonium remaining from the preceding SBR cycle. The production of PHA was initiated by feeding a pulse of 60 mmol of the substrate (mixture) on which the culture had been enriched. Further carbon source was continuously supplied to the reactor via pH control, using a 1.5 M solution of the substrate's acid (i.e., butyric acid or a 1:1 Cmol mixture of acetic and butyric acid) instead of the 1 M HCl solution used in the SBR (Johnson et al., 2009a). When necessary a few drops of antifoam B (Sigma-Aldrich) were added. After 10 h the experiments were stopped.

2.2.3. ANALYTICAL METHODS

During the cycle and accumulation experiments the reactor was monitored closely by both online (dissolved oxygen, temperature, pH, acid and base dosage, off-gas O_2 and CO_2) and offline (substrate, ammonium, TSS, PHA) measurements.

Samples taken to determine the substrate and ammonium concentration in the reactor were immediately filtered with a 0.45 µm pore size filter (PVDF membrane, Millipore, Ireland) to remove the biomass. The ammonium concentration in the supernatant was determined spectrophotometrically using a commercial cuvette test kit (Hach Lange, Germany). The organic acid concentrations in the supernatant were analyzed using a high-performance liquid chromatograph (HPLC) with a BioRad Aminex HPX-87H column and a UV detector (Waters 484, 210 nm). The mobile phase, 1.5 mM H_3PO_4 in Milli-Q water, had a flow rate of 0.6 mL·min^{-1} and a temperature of 59°C.

The biomass concentration in the reactor was measured as total suspended solids (TSS). The samples were collected in 15 mL tubes with five drops of formaldehyde (37%) to stop all biological activity and centrifuged at 4500 rpm (3850*g*) for 10 min. After removing the supernatant and pre-freezing the samples (-20°C) the samples were freeze-dried overnight (-40°C, 10^{-1} atm). Subsequently, the PHA content of the freeze-dried biomass was determined using a gas chromatograph (Agilent 6890N, USA) equipped with a flame ionization detector (FID) and a HP-INNOWax column. A detailed description of the procedure can be found elsewhere (Johnson et al., 2009a). The PHA content of

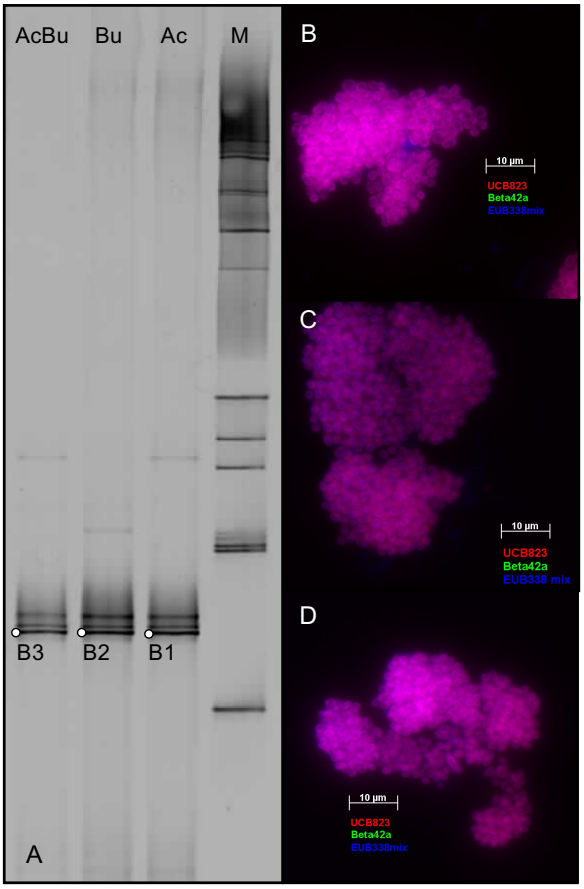

Figure 2.1: DGGE gel and FISH microscopic photographs. (A) DGGE gel of PCR-amplified 16S rRNA gene fragments from the enrichment cultures on acetate (lane labeled Ac), butyrate (Bu) and mixed acetate and butyrate (AcBu). SmartLadder (Eurogentec) was loaded in the lane labeled with M. The bands labeled with B1-3 were excised and re-amplified for microbial identification. Previous analyses have shown that the bands just above B1-3 also belong to *P. acidivorans* (Jiang et al., 2011a). (B, C, D) Fluorescence microscopy images of the enrichment cultures on acetate, butyrate, and mixed acetate and butyrate, respectively. The general probe mixture EUB338I-III (Cy5) was used to indicate all bacterial species. The probes BET42a (FLUOS) and UCB823 (Cy3) were used to indicate the presence of, respectively, betaproteobacteria and *P. acidivorans*. In order to minimize erroneous hybridizations the unlabeled probe GAM42a was used to compete with the BET42a probe.

Table 2.1: Oligonucleotide probes for FISH analysis and primers for PCR-DGGE analysis used in this study.

Code	Function	Sequence (5'-3')	Specificity	Reference
EUB338 I	Probe	gct gcc tcc cgt agg agt	Bacteria	Amann et al. (1990)
EUB338 II	Probe	gca gcc acc cgt agg tgt	Bacteria	Daims et al. (1999)
EUB338 III	Probe	gct gcc acc cgt agg tgt	Bacteria	Daims et al. (1999)
BET42a	Probe	gcc ttc cca ctt cgt tt	Betaproteobacteria	Manz et al. (1992)
GAM42a	Probe	gcc ttc cca cat cgt tt	Gammaproteobacteria	Manz et al. (1992)
UCB823	Probe	cct ccc cac cgt cca gtt	*P. acidivorans*	Johnson et al. (2009a)
341F-GC	Primer	cct acg gga ggc agc ag*	Bacteria	Schäfer and Muyzer (2001)
907R	Primer	ccg tca att cmt ttg agt tt	Bacteria	Schäfer and Muyzer (2001)

* Contains GC-clamp (5'-cgcccgccgcgccccgcgcccgtcccgccgcccccgcccg-3') at the 5' end of the primer.

the cells, expressed as the weight percentage PHA of TSS, was calculated using pure PHB (Sigma-Aldrich, CAS 26063-00-3) as standard, and benzoic acid as internal standard. The determined PHA content was subtracted from the TSS to obtain the concentration of active biomass in the reactor. The biomass composition was assumed to be $CH_{1.8}O_{0.5}N_{0.2}$ and its molecular weight 25.1 g·Cmol^{-1} (including ash).

2.2.4. MICROBIAL COMMUNITY ANALYSIS

In order to analyze the microbial composition of the enrichment cultures by DGGE, biomass samples were collected from the SBR and washed with TE buffer. The genomic DNA was extracted using the Ultra Clean Soil DNA extraction kit (MoBio Laboratories, USA) and subsequently used as template DNA in the PCR. 16S rRNA gene fragments of the different community constituents were obtained using a "touchdown" PCR program with the primers 341F-GC and 907R (Table 2.1) (Schäfer and Muyzer, 2001). The 16S rRNA gene amplicons were loaded onto 8% polyacrylamide gels with a denaturing gradient from 20% to 70% DNA denaturants (100% denaturants is a mixture of 5.6 M urea and 32% formamide) (Schäfer and Muyzer, 2001). The DNA was visualized by UV illumination after staining with SYBR® Safe, and photographed with a digital camera. Individual bands were excised from the gel with a sterile razor blade and incubated overnight in 50 µL water at 4°C. Re-amplification was performed using the same primer pair (Table 2.1) and the PCR products were sequenced by a commercial company (Macrogen, South Korea). The sequences have been stored in GenBank under accession numbers: KC311782–KC311784.

In addition to the DGGE analysis, FISH was performed on biomass samples from the SBR. A detailed description of the procedure can be found in Johnson et al. (2009a). The probes used in this study are listed in Table 2.1. They were all commercially synthesized and 5' labeled with either FLUOS or one of the sulfoindocyanine dyes Cy3 and Cy5 (Thermo Hybaid interactive, Germany).

2.2.5. DATA TREATMENT AND MODELING

The online and offline data collected during the cycle and accumulation experiments were corrected for effects of sampling, the addition of liquids, and inorganic carbon dissolution, according to the approach proposed by Johnson et al. (2009b). After correcting the data using Microsoft Excel, carbon and electron balances were setup to assess the accuracy of the measurements.

The corrected measurement data were evaluated using a metabolic model to determine the biomass-specific reaction rates ($q_{S,max}$, μ_{max}, $q_{PHB,max}$, m_{ATP}) and other kinetic parameters (α, k, f_{Bu}). A model published by Jiang et al. (2011b) – describing the production of PHA from mixtures of acetate and propionate – was adjusted to describe the PHA production from mixtures of acetate and butyrate in different ratios. Using these substrates the homopolymer polyhydroxybutyrate (PHB) is produced. Table 2.2 summarizes the reactions that were considered in the model. Balances of the conserved moieties (NADH, ATP, AcCoA) in these reactions were used to derive the maximum stoichiometric yields (Table 2.3). The yields are expressed as functions of the efficiency of the oxidative phosphorylation (δ) and the fraction of butyrate in the total substrate uptake (f_{Bu} in Cmol·Cmol^{-1}). The efficiency of the oxidative phosphorylation was assumed to be 2.0 mol ATP/mol NADH for all enrichments in this study.

The kinetic equations in the metabolic model are the same as those described by Jiang et al. (2011b). A minor difference is the maximum specific substrate uptake rate ($q_{S,max}$), which is now expressed in mol·Cmol^{-1}·h^{-1}. The maximum specific substrate uptake rate in Cmol·Cmol^{-1}·h^{-1} can be calculated from the actual f_{Bu} using Eq. 2.1.

$$q_{S,max}^{Cmol} = (4 \times q_{S,max})/(2 - f_{Bu}) \tag{2.1}$$

The metabolic model was written in Matlab™ (Mathworks, USA), where the built-in function *ode113* was used to solve the differential equations and *fmincon* was used to minimize the sum of the squared relative error (SSqRE) between the measured and modeled data. For each of the compounds (acetate, butyrate, biomass, PHB, NH_4^+, CO_2, and O_2) the SSqRE was calculated according to Eq. 2.2. These squared relative errors were subsequently multiplied by their weight factor, and summated to yield the overall error. The weight factor was set to one for all compounds except for the substrate, and in the cycle experiments also for the ammonium, which had a weight factor of ten to reflect the reliability of the measurements.

$$SSqRE_i = \sum_0^t \left(\frac{c_i^{measure}(t) - c_i^{model}(t)}{c_i^{measure}(t)} \right)^2 \tag{2.2}$$

During the experiments the enrichment cultures showed a stable operational performance. This implies that the net amount of biomass and PHB formed during each

Table 2.2: Reactions considered in the metabolic model on a carbon-mole base (adapted from Johnson et al., 2009b). The efficiency of the oxidative phosphorylation (δ) was assumed to be 2.0 mol ATP/mol NADH for all enrichments in this study.

	Reaction	Stoichiometry
1.	Acetate uptake, activation	1 HAc + 1 ATP → 1 AcCoA
2.	Butyrate uptake, activation	1 HBu + 0.75 ATP → 1 AcCoA + 0.5 NADH
3.	Catabolism	1 AcCoA → 1 CO_2 + 2 NADH
4.	PHB production	1 AcCoA + 0.25 NADH → 1 PHB
5.	Anabolism	1.267 AcCoA + 0.2 NH_3 + 2.16 ATP → 1 $CH_{1.8}O_{0.5}N_{0.2}$ + 0.267 CO_2 + 0.434 NADH
6.	PHB consumption	1 PHB + 0.25 ATP → 1 AcCoA + 0.25 NADH
7.	Oxid. phosphorylation	1 NADH + 0.5 O_2 → δ ATP

cycle equals the amount of biomass and PHB removed at the end of the cycle. The final concentration of biomass and PHB in the reactor can therefore be calculated from the SRT, the cycle length, and the initial concentration (Jiang et al., 2011b). To ensure this stable performance when modeling the cycle experiments an additional error (Eq. 2.3) was defined and minimized, together with the squared relative errors, using *fmincon*.

$$\left(c_X^{model}(t_{end}) - 2 \times c_X^{model}(t_0)\right)^2 + \left(c_{PHB}^{model}(t_{end}) - 2 \times c_{PHB}^{model}(t_0)\right)^2 \tag{2.3}$$

2.3. RESULTS AND DISCUSSION

2.3.1. CULTURE ENRICHMENT AND MICROBIAL CHARACTERIZATION

Two SBRs were operated in this study. The first (SBR 1) was fed with sodium butyrate as sole carbon source, and the second (SBR 2) with a 1:1 Cmol mixture of sodium acetate and butyrate. After reaching stable operational performance the length of the feast phase was in both reactors shorter than in the acetate-fed reactor: 20 min in SBR 1 and 25 min in SBR 2 versus 38 min in the acetate-fed SBR (Table 2.4).

The same microorganism was enriched using respectively acetate, butyrate, and their mixture as substrate. Both DGGE analysis of PCR-amplified 16S rRNA gene fragments and FISH microscopic images confirmed the predominance of *P. acidivorans* (Figure 2.1). Band B2 and B3 were excised, re-amplified, sequenced, and compared to the sequences stored in GenBank (NCBI) using the nBLAST algorithm. Both derived sequences showed 100% similarity to that of *P. acidivorans*.

2.3.2. SBR PERFORMANCE ON BUTYRATE

To evaluate the performance of SBR 1 in detail and to determine the biomass-specific reaction rates, the dynamic change of several compounds was evaluated through multiple cycles. The results of one representative cycle measurement and the consecutive model-

Table 2.3: Stoichiometric yields derived from the metabolic reactions (Table 2.2) and balances for the conserved moieties (NADH, ATP, AcCoA), expressed as a function of the efficiency of the oxidative phosphorylation (δ) and the butyrate fraction in the total substrate uptake rate (f_{Bu} in Cmol·Cmol^{-1}).

Feast phase		
Growth	$Y_{CO2,X}^{feast,max} = \frac{\delta - 2.5\cdot f_{Bu} - 5\cdot\delta\cdot f_{Bu} + 31.6}{20\cdot\delta + 2.5\cdot f_{Bu} + 5\cdot\delta\cdot f_{Bu} - 10}$	$Y_{O2,X}^{feast,max} = -\frac{1.11\cdot f_{Bu} + 12.84}{8\cdot\delta + f_{Bu} + 2\cdot\delta\cdot f_{Bu} - 4}$
	$Y_{X,S}^{feast,max} = -\frac{20\cdot\delta + 2.5\cdot f_{Bu} + 5\cdot\delta\cdot f_{Bu} - 10}{21\cdot\delta + 21.6}$	$Y_{N,X}^{feast,max} = -0.2$
PHB production	$Y_{CO2,PHB}^{feast,max} = \frac{\delta - f_{Bu} - 2\cdot\delta\cdot f_{Bu} + 4}{8\cdot\delta + f_{Bu} + 2\cdot\delta\cdot f_{Bu} - 4}$	$Y_{O2,PHB}^{feast,max} = -\frac{36 - 9\cdot f_{Bu}}{64\cdot\delta + 8\cdot f_{Bu} + 16\cdot\delta\cdot f_{Bu} - 32}$
	$Y_{PHB,S}^{feast,max} = -\frac{8\cdot\delta + f_{Bu} + 2\cdot\delta\cdot f_{Bu} - 4}{9\cdot\delta}$	
Maintenance	$Y_{CO2,S}^{feast,max} = -1$	$Y_{O2,S}^{feast,max} = 0.25\cdot f_{Bu} + 1$
	$Y_{ATP,S}^{feast,max} = 2\cdot\delta + 0.25\cdot f_{Bu} + 0.5\cdot\delta\cdot f_{Bu} - 1$	
Famine phase		
Growth	$Y_{CO2,X}^{famine,max} = \frac{241 - 15\cdot\delta}{225\cdot\delta - 25}$	$Y_{O2,X}^{famine,max} = -\frac{10.77}{9\cdot\delta - 1}$
	$Y_{X,PHB}^{famine,max} = -\frac{225\cdot\delta - 25}{210\cdot\delta + 216}$	$Y_{N,X}^{famine,max} = -0.2$
Maintenance	$Y_{CO2,PHB}^{famine,max} = -1$	$Y_{O2,PHB}^{famine,max} = 1.125$
	$Y_{ATP,PHB}^{famine,max} = 0.25 - 2.25\cdot\delta$	

Table 2.4: Overview of observed variables, and model-derived yields and biomass-specific rates in the SBR and fed-batch reactor. The yields for the accumulation experiments were determined over the first 4.5 h only. For some parameters of SBR 2 two values are presented. In the cycle experiments the left value describes the first part of the feast phase (0-10 min) and the right value the second part of the feast phase (10-25 min). In the accumulation experiments the left value describes the first hour and the right value the following 3.5 h, when the butyrate consumption had become limited by its dosage.

		SBR 1	SBR 2	SBR 3
		Butyrate	**Acetate/Butyrate**	**Acetate**
		This study	*This study*	*Jiang et al. (2011c)*
SBR/cycle experiment				
Observed				
Length feast phase	[min]	20	25 (10/15)	38
PHB max. feast	[wt.%]	57	54	52
Model-derived				
$Y_{PHB,S}^{feast}$	[Cmol·Cmol^{-1}]	0.93	0.91 / 0.66	0.67
$Y_{X,S}^{feast}$	[Cmol·Cmol^{-1}]	0.01	0.00 / 0.00	0.00
$Y_{CO2,S}^{feast}$	[Cmol·Cmol^{-1}]	0.06	0.08 / 0.33	0.33
$Y_{O2,S}^{feast}$	[mol·Cmol^{-1}]	0.19	0.19 / 0.25	0.25
$Y_{X,PHB}^{famine}$	[Cmol·Cmol^{-1}]	0.67	0.67	0.67
$Y_{CO2,PHB}^{famine}$	[Cmol·Cmol^{-1}]	0.33	0.33	0.33
f_{Bu}	[Cmol·Cmol^{-1}]	1.00	0.90 / 0.00	0.00
$q_{S,max}$	[mol·Cmol^{-1}·h^{-1}]	1.67	1.84	2.19
$q_{S,max}$	[Cmol·Cmol^{-1}·h^{-1}]	6.66	6.70 / 3.68	4.38
μ_{max}	[Cmol·Cmol^{-1}·h^{-1}]	0.07	0.01	0.00
k	[Cmol$^{1/3}$·Cmol$^{-1/3}$·h^{-1}]	-0.18	-0.17	-0.16
m_{ATP}	[mol·Cmol^{-1}·h^{-1}]	0.00	0.00	0.00
Fed-batch/accumulation experiment				
Observed				
PHB max. acc	[wt.%]	88	88	88
Time PHB max.	[h]	8.9	9.0	9.2
Time PHB >80 wt.%	[h]	3.4	3.5	4.2
Model-derived				
$Y_{PHB,S}^{acc}$	[Cmol·Cmol^{-1}]	0.89	0.91 / 0.75	0.61
$Y_{X,S}^{acc}$	[Cmol·Cmol^{-1}]	0.04	0.02 / 0.03	0.04
$Y_{CO2,S}^{acc}$	[Cmol·Cmol^{-1}]	0.07	0.07 / 0.21	0.35
$Y_{O2,S}^{acc}$	[mol·Cmol^{-1}]	0.21	0.20 / 0.24	0.27
f_{Bu}	[Cmol·Cmol^{-1}]	1.00	0.97 / 0.48	0.00
$q_{PHB,max}$	[Cmol·Cmol^{-1}·h^{-1}]	3.64	3.72	1.74
μ_{max}	[Cmol·Cmol^{-1}·h^{-1}]	0.08	0.06	0.09
m_{ATP}	[mol·Cmol^{-1}·h^{-1}]	0.00	0.00	0.00
α	-	1.00	1.00	1.31

ing are shown in Figure 2.2b and Table 2.4. During the feast phase butyrate was taken up quickly: $q_{S,max}$ equaled 6.7 Cmol·Cmol^{-1}·h^{-1}. This is an increase of 50% compared to the maximum specific uptake rate previously reported for *P. acidivorans* on acetate (Jiang et al., 2011c). Virtually all of the consumed carbon was converted to PHB ($Y_{PHB,S}$ = 0.93 Cmol·Cmol^{-1}) and at the end of the feast phase the PHB content of the cells reached 57 wt.%. Only a minor fraction of the consumed substrate was used for growth ($Y_{X,S}$ = 0.01 Cmol·Cmol^{-1}) or respired to carbon dioxide ($Y_{CO2,S}$ = 0.06 Cmol·Cmol^{-1}). Since less substrate was respired to carbon dioxide, the oxygen consumption per carbon-mole of substrate was also lower for butyrate than for acetate: 0.19 vs. 0.25 mol·Cmol^{-1}. However, due to the increased specific carbon uptake rate, the specific oxygen uptake rate did not change. During the famine phase, when all external substrate had been depleted, the accumulated PHB was degraded and used for biomass synthesis and maintenance.

To indicate the accuracy of the measurements carbon and electron balances were setup over the complete cycle experiment. On average 99% (±4.4) of the carbon in the substrate could be found back as active biomass, PHB, or carbon dioxide. Of the electrons present in the substrate on average 97% (±3.8) was traced back in the active biomass, PHB, and oxygen consumption.

2.3.3. SUBSTRATE PREFERENCES: SBR PERFORMANCE ON AN ACETATE BUTYRATE MIXTURE

The substrate uptake pattern in SBR 2 (Figure 2.2c,d) showed that the uptake of butyrate was strongly preferred over that of acetate. While both substrates were present in the medium, butyrate accounted for 82% of the substrate (mole based) taken up, whereas its fraction within the total substrate mixture was only 0.33 mol·mol^{-1}. As a result of the prevalence of butyrate uptake during the first ten minutes of the feast phase, the kinetic behavior of the enrichment culture (Table 2.4) closely resembled that of SBR 1. The specific substrate uptake rate was 1.8 mol·Cmol^{-1}·h^{-1}, which lies between the values found for the culture on sole butyrate (SBR 1: 1.7 mol·Cmol^{-1}·h^{-1}) and sole acetate (Jiang et al., 2011c: 2.2 mol·Cmol^{-1}·h^{-1}). The fraction of butyrate in the total carbon uptake (f_{Bu}) was 0.90 Cmol·Cmol^{-1}, leading to a specific butyrate uptake rate of 6.0 Cmol·Cmol^{-1}·h^{-1} and a specific acetate uptake rate of only 0.67 Cmol·Cmol^{-1}·h^{-1}. A major share of the consumed substrate (0.91 Cmol·Cmol^{-1}) was converted to PHB, and the remaining carbon (0.08 Cmol·Cmol^{-1}) was respired to carbon dioxide. The contribution of growth to the total substrate consumption was negligible.

Due to the difference in uptake rate, butyrate was depleted before acetate. Immediately after butyrate depletion the acetate uptake rate increased strongly, implying that butyrate competes with the acetate. A similar preference for butyrate was observed by Albuquerque et al. (2013) for an enrichment culture on fermented sugar cane molasses, and by Jiang et al. (2012) for an enrichment culture on fermented paper mill wastewater

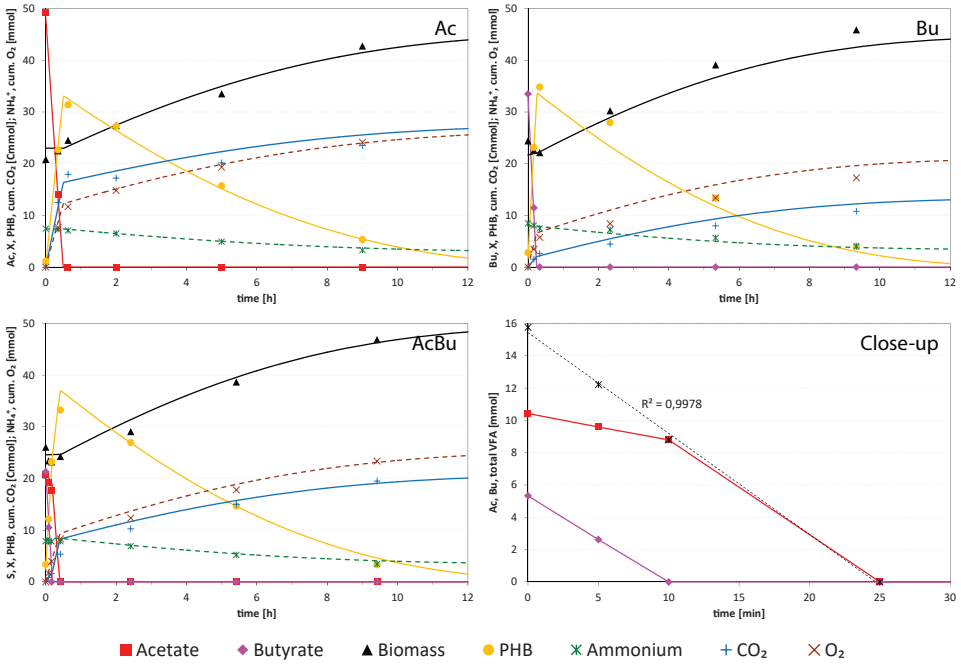

Figure 2.2: Results for the cycle experiments on acetate (Ac), butyrate (Bu), and mixed acetate and butyrate (AcBu). Data for the cycle experiment on acetate was adapted from Jiang et al. (2011c). The symbols represent measured data, the lines modeled data. In addition a close-up of the measured substrate uptake in the SBR on mixed acetate and butyrate is shown (Close-up). The black asterisks indicate the total amount of VFAs in the reactor (in mmol), which decreases almost linearly as indicated by the dashed line and its R^2 value.

dominated by the same microorganism, *P. acidivorans*. There butyrate accounted for 90% of the substrate (mole based) taken up, whereas its fraction in the total substrate was 0.62 mol·mol^{-1}.

During the second part of the feast phase acetate was the only external substrate. The maximum specific substrate uptake rate remained 1.8 mol·Cmol^{-1}·h^{-1}, resulting in a specific acetate uptake rate of 3.7 Cmol·Cmol^{-1}·h^{-1}. This is more than five times as high as during the first part of the feast phase. Around two-third of the consumed carbon was converted to PHB and the remaining carbon (0.33 Cmol·Cmol^{-1}) was respired to carbon dioxide. Growth still hardly contributed to the total substrate uptake. At the end of the feast phase the intracellular PHB content reached 54 wt.% of the TSS. The accumulated PHB was used for growth and maintenance during the famine phase.

Again, carbon and electron balances were setup to indicate the accuracy of the measurements in the cycle experiment. On average 95% (±3.4) of the carbon in the substrate was found back as active biomass, PHB, or carbon dioxide. Of the electrons in the substrate 96% (±1.7) could be traced back in the active biomass, PHB, and oxygen consumption.

2.3.4. CARBON VERSUS SUBSTRATE UPTAKE

Interestingly, the maximum specific substrate uptake rate ($q_{S,max}$) of the enrichment culture in SBR 2 was 1.8 mol·Cmol^{-1}·h^{-1} throughout the feast phase, independent of the prevalence of either butyrate or acetate uptake (Figure 2.2d). Albuquerque et al. (2013) and Jiang et al. (2012) reported that the substrate uptake rate decreased significantly after butyrate had been depleted. As in many other papers on PHA production by microbial enrichment cultures (e.g., Albuquerque et al., 2007; Bengtsson et al., 2010; Jiang et al., 2011b; Lemos et al., 2006) the specific substrate uptake rate was expressed as Cmol·Cmol^{-1}·h^{-1}. Also in this study the specific carbon uptake rate, and PHB production rate, showed an immediate and strong decrease after the depletion of butyrate. When expressed as mol·Cmol^{-1}·h^{-1}, however, the substrate uptake rate remained constant throughout the feast phase. Based on the reported specific uptake rates of individual VFAs, the same holds for, e.g., the microbial enrichment culture of Albuquerque et al. (2013).

The fact that the molar substrate uptake rate remains constant when butyrate gets depleted – whereas the oxygen uptake rate increases and the PHB production rate decreases – suggests that uptake or activation of the substrate is the rate-limiting process. In combination with the increasing acetate uptake rate after butyrate depletion this implies that acetate and butyrate share a transporter or coenzyme A transferase, with a higher affinity for butyrate.

2.3.5. PHA ACCUMULATION

To evaluate the PHB production rate and capacity of the enrichment cultures, fed-batch accumulation experiments were performed. The measured and modeled results of these experiments are shown in Figure 2.3 and Table 2.4. During the experiments the carbon source (i.e., butyric acid or mixed acetic and butyric acid) was continuously supplied to the reactor via pH control. As the prevention of growth, for example by limiting the ammonium, has been reported to be a prerequisite to obtaining high PHB contents (Bengtsson et al., 2008b; Johnson et al., 2010; Serafim et al., 2004), the presence of ammonium was limited to the small amount remaining from the preceding SBR cycle.

During the first 4.5 h of the accumulation experiment on sole butyrate (SBR 1), ammonium was still present in the reactor and the kinetic behavior was highly similar to that in the feast phase of the SBR. The high product yield and carbon uptake rate resulted in a maximum specific PHB production rate ($q_{PHB,max}$) of 3.6 Cmol·Cmol^{-1}·h^{-1}, which is twice the value reported for acetate (Jiang et al., 2011c). As a result, the intracellular PHB content reached 83 wt.% in only 3.4 h.

Also during the first hour of the accumulation experiment on mixed acetate and butyrate (SBR 2) the conversions were dominated by butyrate uptake and highly similar to those described for the feast phase of the SBR. The maximum specific PHB production rate ($q_{PHB,max}$) was 3.7 Cmol·Cmol^{-1}·h^{-1}, and the intracellular PHB content reached 74 wt.% within this first hour. After the first hour the butyrate concentration in the reactor reached zero, and its consumption became limited by the dosage of new substrate. As a result, the butyrate fraction in the total substrate uptake (f_{Bu}) dropped from 0.97 to 0.48 Cmol·Cmol^{-1}. In correspondence with that the product yield ($Y_{PHB,S}$) decreased to 0.75 Cmol·Cmol^{-1} and the fraction of respired carbon ($Y_{CO2,S}$) increased to 0.21 Cmol·Cmol^{-1}. Both yields are the average of those observed for acetate and butyrate individually (Table 2.4).

Both the enrichment culture on sole butyrate and the enrichment culture on mixed acetate and butyrate reached a maximum PHB content of 88 wt.% after 9 h. This is the same as previously reported for the enrichment culture on acetate (Jiang et al., 2011c) and was to be expected since all three cultures were dominated by the same bacterial species.

Although the amount of ammonium was limited, it remained present in the medium for 4.5 h. During that period the PHB content of both enrichment cultures reached already 83-85 wt.% of the TSS. This result suggests that, when butyrate is the dominant substrate, the presence of ammonium is less detrimental to achieving a high PHB content than presumed for acetate-fed cultures. Results presented by Dionisi et al. (2005b) and Johnson et al. (2010) also show that initially similar amounts of PHB were accumulated in experiments with and without ammonium present. Only after this first period of 1 or 2 h an increasing fraction of the substrate was used for growth instead of PHB

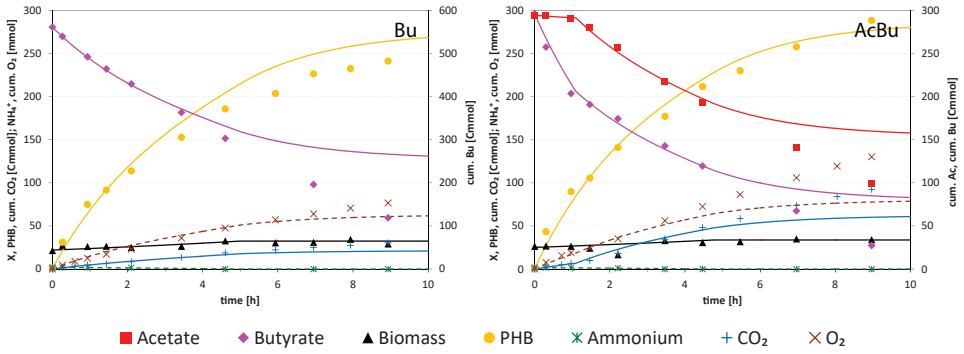

Figure 2.3: Results for the accumulation experiments on butyrate (Bu) and mixed acetate and butyrate (AcBu). The symbols represent measured data, the lines modeled data.

production if ammonium was available. Therefore, as long as the specific PHB production rate is high enough, the presence of ammonium does not necessarily impede obtaining a high intracellular PHB content. This broadens the range of organic waste streams suitable for PHA production by microbial enrichment cultures, and specifically by *P. acidivorans*. Further research on this topic is required to obtain a conclusive answer on the impact of ammonium on the accumulation of large amounts of PHA.

To evaluate the accuracy of the measurements during these accumulation experiments, carbon and electron balances were setup. During the first 4.5 h, i.e., while ammonium was present in the reactors, on average 99% of the consumed carbon (±4.3 for SBR 1 and ±1.4 for SBR 2) could be found back as active biomass, PHB, or carbon dioxide. For SBR 1, on average 97% (±6.4) of the electrons present in the consumed substrate was traced back in the active biomass, PHB, and oxygen consumption during this period. For SBR 2, 99% (±1.1) of the electrons was traced back. The gap in the carbon and electron balance was however increasing with time and became significant (<90% recovery) during the second half of the accumulation experiments. This may have arisen from the production of an unknown extracellular compound. Analysis of the broth liquid by HPLC showed emerging, unidentified peaks at 13.4, 14.5, and 25.6 min (data not shown).

2.3.6. BUTYRATE AS PREFERRED SUBSTRATE FOR PHB PRODUCTION

The ideal substrate for PHB production should yield a microbial enrichment culture with a high maximum PHB content, a high specific PHB production rate, and a high product yield. The enrichment cultures on butyrate had all three. The dominant bacterial species in these cultures, *P. acidivorans*, can accumulate up to 89 wt.% PHB (Johnson et al., 2009a), which is still the highest PHB content reported for a microbial enrichment on one or more VFAs. The maximum specific PHB production rate was significantly higher on

butyrate than on acetate due to the increased carbon uptake rate, and because as much as 90% of the carbon in the substrate was converted to PHB. This high yield of PHB on butyrate results from the lowered need for ATP to convert butyrate to PHB (per Cmol). Where the conversion of acetate to PHB requires NADH, the conversion of butyrate to PHB generates NADH. The NADH generation during PHB production from butyrate is almost sufficient to generate the required ATP, resulting in reduced respiration requirements for butyrate as compared to acetate. This makes that, in order to optimize the PHB production process, the acidogenic pre-fermentation step should be directed towards the production of butyrate, for example by adjusting the pH and retention time.

Several researchers have reported a clear shift in the product distribution of acidogenic fermentation around pH 6 (Albuquerque et al., 2007; Reis et al., 1991; Temudo et al., 2007; Zoetemeyer et al., 1982). Below pH 6 mainly butyric and acetic acid are produced. At higher pH values the concentration of butyric acid decreases, whereas the concentration of acetic acid and ethanol increases (Temudo et al., 2007; Zoetemeyer et al., 1982). The transition from the production of longer chain VFAs to that of short VFAs with increasing pH was also observed for valerate and propionate (Albuquerque et al., 2007; Reis et al., 1991). Hence, the organic waste should ideally be pre-fermented at a pH around 5.5. This will not only promote the production of butyrate, but also prevent the growth of methanogens and reduce the need for alkaline addition. For chemostat systems, a short retention time (<10 h) has also been reported to enhance the production of butyric acid (Bengtsson et al., 2008a; Reis et al., 1991; Zoetemeyer et al., 1982). By shortening the retention time the reactor size can be reduced. It may however lower the degree of acidification, another crucial parameter for optimization of the PHB production process (Jiang et al., 2012). Determination of an optimal retention time for the production of VFA-rich product streams with a high butyrate fraction will therefore be necessary.

2.4. CONCLUSION

The results of this study show that butyrate is a highly suitable substrate for the production of PHB by microbial enrichment cultures. The product yield and specific carbon uptake rate are significantly higher for butyrate than for acetate, resulting in a doubling of the specific PHB production rate. Butyrate is therefore preferred over acetate as substrate for PHB production. Future work should aim at maximizing the butyrate yield over the acetate yield from organic waste fermentations.

NOMENCLATURE

α	exponent of the PHB inhibition term	[-]
δ	efficiency of the oxidative phosphorylation	[mol ATP/mol NADH]

f_{Bu}	fraction butyrate in total substrate uptake	[Cmol·Cmol^{-1}]
k	rate constant for PHB degradation	[Cmol$^{1/3}$·Cmol$^{-1/3}$·h^{-1}]
μ	modeled biomass-specific growth rate	[Cmol·Cmol^{-1}·h^{-1}]
μ_{max}	maximum biomass-specific growth rate	[Cmol·Cmol^{-1}·h^{-1}]
m_{ATP}	biomass-specific ATP requirement for maintenance	[mol·Cmol^{-1}·h^{-1}]
q_i	modeled biomass-specific production rate of compound i	[(C)mol·Cmol^{-1}·h^{-1}]
$q_{i,max}$	maximum biomass-specific production rate of compound i	[(C)mol·Cmol^{-1}·h^{-1}]
$Y_{i,j}$	modeled actual yield of compound i on j	[(C)mol·Cmol^{-1}]

3

IMPACT OF NON-STORING BIOMASS ON PHA PRODUCTION

The use of enrichment cultures for polyhydroxyalkanoate (PHA) production from substrate mixtures such as wastewater inevitably results in the establishment of a non-PHA-storing population besides the PHA-producing bacteria. This reduces the maximum PHA content that can be established, and increases downstream-processing costs. The aim of this study was to investigate the impact of non-storing biomass on the PHA production process. A microbial culture was enriched in a sequencing batch reactor fed with acetate and methanol. Methanol served as model substrate for compounds unsuitable for PHA production. The enrichment was dominated by Plasticicumulans acidivorans*, a known PHA producer, and* Methylobacillus flagellatus*, an obligate methylotroph that cannot store PHA. As expected, the presence of the non-storing population lowered the maximum PHA content of the culture, from more than 80 to 66 wt.%. To mimic a nitrogen-rich waste stream, additional accumulation experiments were performed with continuous supply of carbon and ammonium. In these experiments* P. acidivorans *still accumulated large amounts of PHA, but unrestricted growth of the non-storing, methylotrophic population reduced the maximum overall PHA content to 52 wt.%. Besides ammonium limitation, other strategies to restrict the fraction of non-storing biomass should be developed. The mixture of acetate and methanol is a useful model substrate for the development of such strategies.*

Published as: L. Marang, Y. Jiang, M.C.M. van Loosdrecht, and R. Kleerebezem. 2014. Impact of non-storing biomass on PHA production: An enrichment culture on acetate and methanol. International Journal of Biological Macromolecules 71, 74-80.

3.1. INTRODUCTION

Polyhydroxyalkanoates (PHAs) are storage polymers accumulated by a large variety of bacteria as an intracellular reserve of carbon and energy (Steinbüchel, 1991). The chemical properties of the polymer make it an interesting, biodegradable bioplastic. Moreover, the methyl esters of its monomers could be used as a biofuel (Chen, 2009), and, since the polymer is enantiomerically pure, its hydroxyl fatty acid monomers could serve as chiral building blocks for the production of various biochemicals (Chen, 2009).

The commercially available PHA is generally produced using pure cultures of *Ralstonia eutropha* or recombinant *Escherichia coli*, and glucose and propionic acid as substrate (Chen, 2009). The use of enrichment cultures of natural bacteria and waste organic carbon as substrate forms a more sustainable and economical alternative for PHA production (Reis et al., 2003). Organic waste streams (possibly fermented) typically contain a mixture of compounds that are highly suitable for PHA production – e.g., volatile fatty acids (VFAs), lactate and glycerol – and compounds that are less suitable. The presence of the latter category compounds leads to the co-enrichment of non-PHA-storing bacteria that will lower the overall PHA content of the culture, as reported by, e.g., Albuquerque et al. (2007), Jiang et al. (2012) and Morgan-Sagastume et al. (2010). If the final PHA content becomes too low, increased downstream-processing cost may undo the cost reduction achieved by using a cheaper substrate and open, continuously operated bioreactors.

For an optimized PHA production process it is important to understand the exact impact of these non-PHA-storing populations, and develop strategies to reduce their impact on the overall PHA content of the culture. The aim of this study was to investigate the impact of non-storing biomass on the overall PHA production process, using a simple substrate mixture to mimic the agro-industrial waste stream. To that end, a sequencing batch reactor (SBR) operated under feast-famine conditions was fed with a mixture of acetate and methanol. Methanol was used as model substrate for compounds that do not give rise to PHA production in a feast-famine process. PHA production from methanol has been reported for both pure cultures of *Methylobacterium* species (Bourque et al., 1992; Kim et al., 1996; Yezza et al., 2006) and microbial enrichment cultures (Dobroth et al., 2011; Mockos et al., 2008), but only under nutrient-limited conditions and only relatively small amounts. There is no report on microbial enrichment cultures storing industrially relevant amounts of PHA on methanol. Since methanol is a toxic compound (Bourque et al., 1992; Yezza et al., 2006) the impact of this compound on the kinetic behavior, i.e., growth and PHA production, of *Plasticicumulans acidivorans* was studied as well.

3.2. MATERIALS AND METHODS

3.2.1. SBR FOR ENRICHMENT OF A PHA-PRODUCING CULTURE

To enrich and maintain the PHA-producing microbial culture, a double-jacket glass bioreactor with a working volume of 2 L (Applikon, Netherlands) was used. The basic setup and operation of the reactor were the same as described by Johnson et al. (2009a). The reactor was operated as a non-sterile SBR with 12-h cycles, each consisting of a start phase (5 min), feeding phase (10 min), reaction phase (685 min), and effluent phase (20 min). The exchange volume was 1 L and there was no settling phase, so the solids retention time (SRT) equaled the hydraulic retention time (HRT) and both were 1 day. The air flow rate to the reactor was set to 0.2 $L_N \cdot min^{-1}$ using a mass flow controller (Brooks Instrument, USA). The total gas flow rate through the reactor was increased to 1.4 $L_N \cdot min^{-1}$ by partial recirculation of the off-gas. The temperature in the reactor was controlled at 30±1°C using a thermostat bath (Lauda, Germany), and the pH was maintained at 7.0±0.1 by the addition of 1 M HCl and 1 M NaOH. Controlling of the pumps and pH was done by a biocontroller (ADI 1030, Applikon, Netherlands).

Aerobic activated sludge from the municipal wastewater treatment plant Kralingseveer in Rotterdam (Netherlands) was used to inoculate the SBR. During each cycle 1 L of fresh medium was dosed into the reactor. The carbon source herein was a mixture of sodium acetate and methanol (13.5 and 27 mM respectively). The other chemical compounds in the medium were: 6.75 mM NH_4Cl, 2.49 mM KH_2PO_4, 0.55 mM $MgSO_4 \cdot 7H_2O$, 0.72 mM KCl, 1.5 $mL \cdot L^{-1}$ trace elements solution according to Vishniac and Santer (1957), and 5 $mg \cdot L^{-1}$ allylthiourea (to prevent nitrification).

The enrichment culture was considered stable, or at stable operational performance, when the length of the feast phase and the concentration of total suspended solids (TSS) at the end of the cycle had become constant for at least 5 days. After several weeks of stable operation cycle experiments (in duplicate) were conducted to characterize the operational performance of the SBR. In addition, biomass from the SBR was collected for accumulation experiments and analysis of the microbial community structure.

3.2.2. FED-BATCH REACTOR FOR PHA ACCUMULATION

To evaluate the PHA storage capacity of the obtained enrichment culture, accumulation experiments were performed, in duplicate, in another double-jacket glass bioreactor (Applikon, Netherlands) operated as a non-sterile fed-batch reactor. The reactor, with a working volume of 2 L, was operated at the same aeration rate, pH, and temperature as the SBR. At the beginning of each experiment the reactor was filled with 1 L biomass from the enrichment SBR, and 1 L of carbon- and ammonium-free medium (otherwise the same composition). The production of PHA was initiated by feeding a pulse of the substrate mixture on which the culture had been enriched: 25 mmol sodium acetate and 50 mmol methanol. Further carbon source was continuously supplied to the reactor via pH

control, using a solution of 1.5 M acetic acid and 1.5 M methanol instead of the 1 M HCl solution used in the SBR (Johnson et al., 2009a). In the nitrogen-limited experiments, no further ammonium was supplied and microbial growth was limited by the amount of ammonium remaining from the preceding SBR cycle. During the two nitrogen-excess experiments, ammonium (0.56 M) was dosed along with the acetic acid and methanol in a C:N ratio of 8. When necessary a few drops of antifoam B (Sigma-Aldrich) were added. After 8 h the experiments were stopped.

3.2.3. ANALYTICAL METHODS

During the cycle and accumulation experiments the reactor was monitored closely by both online (dissolved oxygen, temperature, pH, acid and base dosage, off-gas O_2 and CO_2) and offline (substrate, ammonium, TSS, PHA) measurements.

Samples taken to determine the substrate and ammonium concentration in the reactor were immediately filtered with a 0.45 µm pore size filter (PVDF membrane, Millipore, Ireland) to remove the biomass. The ammonium concentration in the supernatant was determined spectrophotometrically using a commercial cuvette test kit (Hach Lange, Germany). The acetate concentration was analyzed using a high-performance liquid chromatograph (HPLC) with a BioRad Aminex HPX-87H column and a UV detector (Waters 484, 210 nm). The mobile phase, 1.5 mM H_3PO_4 in Milli-Q water, had a flow rate of 0.6 mL·min^{-1} and a temperature of 59°C. The methanol concentration was determined using a gas chromatograph (Thermo Scientific Focus GC, USA) equipped with a flame ionization detector (FID) and a HP-INNOWax column. Pentanol was used as internal standard.

The biomass concentration in the reactor was measured as TSS. The samples were collected in 15 mL tubes with five drops of formaldehyde (37%) to stop all biological activity and centrifuged at 4500 rpm (3850*g*) for 10 minutes. After removing the supernatant and pre-freezing the samples (-20°C) the samples were freeze dried overnight (-40°C, 10^{-1} atm). Subsequently, the PHA content of the freeze-dried biomass was determined using a gas chromatograph (Agilent 6890N, USA) equipped with a flame ionization detector (FID) and a HP-INNOWax column. A detailed description of the procedure can be found elsewhere (Johnson et al., 2009a). The PHA content of the cells, expressed as the weight percentage PHA of TSS, was calculated using pure PHB (Sigma-Aldrich, CAS 26063-00-3) as standard, and benzoic acid as internal standard. The determined PHA content was subtracted from the TSS to obtain the concentration of active biomass in the reactor. The biomass composition was assumed to be $CH_{1.8}O_{0.5}N_{0.2}$ and its molecular weight 25.1 g·Cmol^{-1} (including ash).

3.2.4. DATA TREATMENT AND CALCULATIONS

The gathered online and offline data were corrected for effects of sampling, the addition of liquids, and inorganic carbon dissolution, according to the approach proposed by Johnson et al. (2009b). After correcting the data using Microsoft Excel, carbon and electron balances were setup to assess the accuracy of the measurements.

Average biomass-specific rates (q-rates) during the feast and famine phase were calculated from the change in a compound's concentration (c_i) over a certain period and the average biomass concentration (c_X) during this period, as shown in Eq. 3.1.

$$q_i = \left(\sum_{1}^{n} \frac{c_i(t_{n+1}) - c_i(t_n)}{0.5 \cdot (c_X(t_{n+1}) + c_X(t_n))} \right) / (t_n - t_1) \tag{3.1}$$

An estimate of the PHA content in *P. acidivorans* specifically ($PHA_{P.a.}$) was obtained from the measured overall PHA content (PHA_{total}) and the fraction of *P. acidivorans* in the overall biomass ($f_{P.a.}$) using Eq. 3.2, previously published by Jiang et al. (2012).

$$PHA_{total} = -\frac{PHA_{Other} - PHA_{P.a.} \cdot PHA_{Other} + PHA_{P.a.} \cdot f_{P.a.} - PHA_{Other} \cdot f_{P.a.}}{PHA_{P.a.} - PHA_{P.a.} \cdot f_{P.a.} + PHA_{Other} \cdot \left(f_{P.a.}\right)^{-1}} \tag{3.2}$$

3.2.5. MICROBIAL COMMUNITY ANALYSIS

In order to analyze the microbial composition of the enrichment culture, biomass samples were collected from the SBR and fed-batch reactor, and washed with TE buffer. The genomic DNA was extracted using the Ultra Clean Soil DNA extraction kit (MoBio Laboratories, USA) and subsequently used as template DNA for PCR-DGGE (biomass samples SBR) or qPCR (samples fed-batch reactor).

For identification of the different community constituents by DGGE, 16S rRNA gene fragments were obtained using a "touchdown" PCR program with the primers 341F-GC and 907R (Table 3.1) (Schäfer and Muyzer, 2001). The 16S rRNA gene amplicons were loaded onto 8% polyacrylamide gels with a denaturing gradient from 20% to 70% DNA denaturants (100% denaturants is a mixture of 5.6 M urea and 32% formamide) (Schäfer and Muyzer, 2001). The DNA was visualized by UV illumination after staining with SYBR® Safe, and photographed with a digital camera. Individual bands were excised from the gel with a sterile razor blade and incubated overnight in 50 µL water at 4°C. Re-amplification was performed using the same primer pair (Table 3.1) and the PCR products were sequenced by a commercial company (Macrogen, South Korea). The sequences have been stored in GenBank under accession numbers: KJ198897– KJ198899.

During the accumulation experiments the relative abundance of *P. acidivorans* in the total enrichment culture ($f_{P.a.}$) was analyzed by qPCR. The extracted genomic DNA was amplified using two primer pairs: 518F/907R and 518F/UCB823R (Table 3.1). The first was used to quantify the total amount of bacteria in the samples, and the second to

Table 3.1: Oligonucleotide probes for FISH analysis and primers for (q)PCR analysis used in this study.

Code	Function	Sequence (5'-3')	Specificity	Reference
EUB338 I	Probe	gct gcc tcc cgt agg agt	Bacteria	Amann et al. (1990)
EUB338 II	Probe	gca gcc acc cgt agg tgt	Bacteria	Daims et al. (1999)
EUB338 III	Probe	gct gcc acc cgt agg tgt	Bacteria	Daims et al. (1999)
UCB823	Probe	cct ccc cac cgt cca gtt	*P. acidivorans*	Johnson et al. (2009a)
341F-GC	Primer	cct acgg gag gca gcag*	Bacteria	Schäfer and Muyzer (2001)
518F	Primer	cca gca gcc gcg gta at	Bacteria	Muyzer et al. (1993)
907R	Primer	ccg tca att cmt ttg agt tt	Bacteria	Schäfer and Muyzer (2001)
UCB823R	Primer	cct ccc cac cgt cca gtt	*P. acidivorans*	Jiang et al. (2011a)

* Contains GC-clamp (5'-cgcccgccgcgccccgcgcccgtcccgccgcccccgcccg-3') at the 5' end of the primer.

quantify *P. acidivorans*. The qPCR was performed with the iQ™ SYBR® Green Supermix Kit (Bio-Rad, USA). Each reaction system was composed of 10 µL SYBR® Green Mastermix, 0.2 µL forward primer, 0.2 µL reverse primer, 0.4 µL DNA template, and 9.2 µL H_2O. The PCR program comprised: 5 min at 95°C, 40 cycles of 30 s at 94°C, 30 s at 57°C and 1 min at 72°C, followed by a final elongation step for 10 min at 72°C, and termination at 4°C. DNA of *P. acidivorans* was used to make calibration curves for both primer pairs, relating the SYBR® fluorescence signal to the amount of DNA.

In addition to the PCR-DGGE and qPCR, FISH was performed to validate the results. A detailed description of the procedure can be found in Johnson et al. (2009a). The probes used in this study are listed in Table 3.1. They were commercially synthesized and 5' labeled with either FLUOS or the sulfoindocyanine dye Cy5 (Thermo Hybaid interactive, Ulm, Germany). The general probe mixture EUB338I-III was used to visualize all bacteria in the sample, and the specific probe UCB823 to indicate the presence of *P. acidivorans*. Post-staining with Nile blue A was performed to identify the bacterial species involved in PHA synthesis (Johnson et al., 2009a).

3.3. RESULTS

3.3.1. CULTURE ENRICHMENT AND CHARACTERIZATION

The SBR was fed with a 1:1 Cmol mixture of sodium acetate and methanol, and operated at an SRT of 1 day and a cycle length of 12 h. The reactor was operated for 4.5 months (≈ 135 SRTs). Few cycles after inoculation with activated sludge, the typical feast-famine profile of dissolved oxygen (DO) was established. The feast phase was characterized by a stepwise increase of the DO (Figure 3.1). When the reported experiments were performed – during the last month of operation – the first increase was observed after 36 (±3) min, when acetate was depleted. The second increase, caused by the depletion of methanol, followed roughly 1.5 h later: after 125 (±8) min. These values reflect the strongly different acetate and methanol uptake rate in the system. The small standard

deviations for the length of the feast phases (only 7%) demonstrate the operational stability.

During the first 36 min of the feast phase, the average biomass-specific substrate uptake rate was 1.7 Cmol·Cmol^{-1}·h^{-1}. Acetate – taken up much faster than the methanol – accounted for 83% of the carbon consumption during this period. Around half of the consumed carbon (49%) was converted to PHA, and the PHA content of the overall culture reached 30 wt.%. Besides for PHA production a significant fraction of the substrate was used for growth (11%) and another 30% of the substrate was traced back as carbon dioxide.

The second part of the feast phase was characterized by fast growth. The only external substrate available was methanol: 80% of the initially dosed methanol still remained in the reactor liquid and was taken up at an average specific rate of 0.3 Cmol·Cmol^{-1}·h^{-1}. This was similar to its uptake rate during the first part of the feast phase. In addition, PHA started to be degraded. The simultaneous growth on PHA and methanol led to an increase of the average biomass-specific growth rate and 44% of the total ammonium consumption occurred during this period (Figure 3.1). After methanol depletion, i.e. during the famine phase, only the growth on stored PHA continued and the average specific growth rate dropped to 0.02 Cmol·Cmol^{-1}·h^{-1}.

Analysis of the enrichment culture by FISH and DGGE (Figure 3.2a,b) showed the presence of two dominant bacterial species: *Plasticicumulans acidivorans* (band 2, 100% similarity) and *Methylobacillus flagellatus* (band 1, 98.6% similarity). The first has been found in several PHA-producing enrichment cultures on acetate before (Johnson et al., 2009a; Jiang et al., 2011b,a,c) and can produce up to 89 wt.% PHA. It was isolated and characterized by Jiang et al. (2011d), and cannot use methanol as carbon and energy source. The second, *M. flagellatus*, is an obligate methylotroph using the ribulose monophosphate (RuMP) pathway for carbon assimilation (Chistoserdova et al., 2007). It has a high biomass yield and growth rate compared to methylotrophs using the serine cycle, but cannot store PHA (Baev et al., 1992; Chistoserdova et al., 2007; Föllner et al., 1993), as confirmed by post-staining with Nile blue A (Figure 3.2c). Band 3 is likely an artifact (Schäfer and Muyzer, 2001) and yielded a noisy sequence identical to that of band 1.

3.3.2. SHORT-TERM EXPERIMENTS WITH SINGLE SUBSTRATES

To determine if the kinetics of *P. acidivorans* are affected by methanol, duplicate short-term cycle experiments with sole acetate were performed (Figure 3.3a). The specific acetate uptake rate (1.2 Cmol·Cmol^{-1}·h^{-1}) was comparable to that during a normal cycle and after 35 min the acetate was depleted. The overall PHA content reached 29 wt.% at this point. Different from a normal SBR cycle, when both acetate and methanol are fed, little growth was observed. Of the dosed carbon, 66% was found back in PHA, 33% in carbon dioxide, and only 2% in active biomass. After acetate depletion, the accumulated

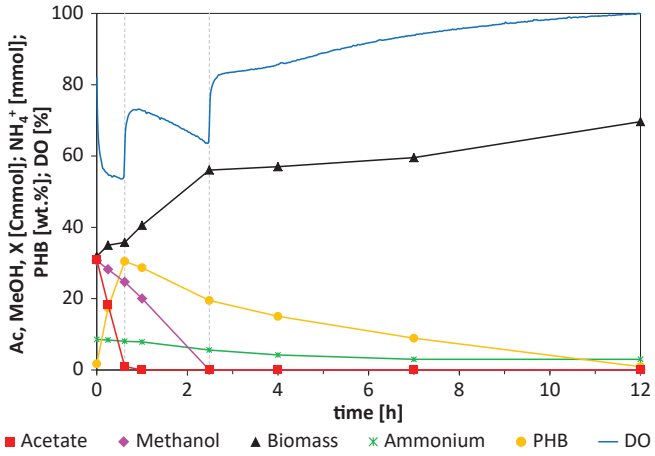

Figure 3.1: Results of a cycle experiment during normal operation of the SBR. The acetate present in the reactor (Cmmol) is represented by red squares, methanol (Cmmol) by pink diamonds, active biomass (Cmmol) by black triangles, ammonium (mmol) by green asterisks, and PHB (wt.%) by yellow circles. The blue line displays the dissolved oxygen level (%) in the reactor liquid.

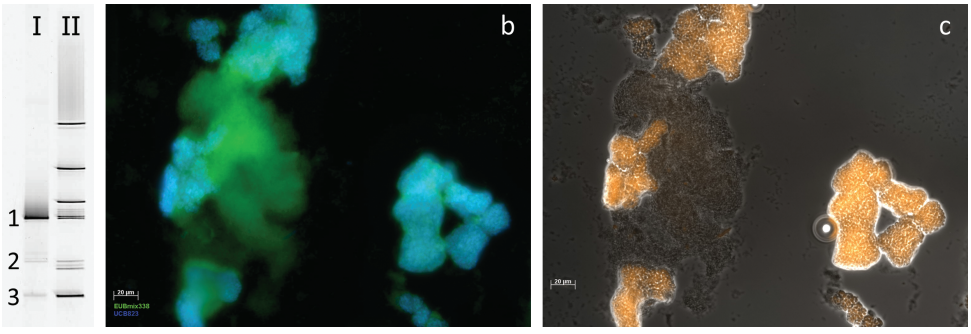

Figure 3.2: DGGE gel and FISH microscopic photographs of the enrichment culture on mixed acetate and methanol. (a) DGGE gel of PCR-amplified 16S rRNA gene fragments from the enrichment culture in lane I. SmartLadder (Eurogentec) was loaded in lane II. The bands labeled 1-3 were excised and re-amplified for microbial identification. (b) Fluorescence microscopy image of a sample taken from the SBR at the end of the feast phase. The biomass was stained with a FLUOS-labelled probe for Eubacteria (EUB338I-III, green) and Cy5-labelled probe for *P. acidivorans* (UCB823, blue). (c) An overlay of a phase contrast image and fluorescence microscopy image of the same field post-stained with Nile blue A to indicate the presence of PHA.

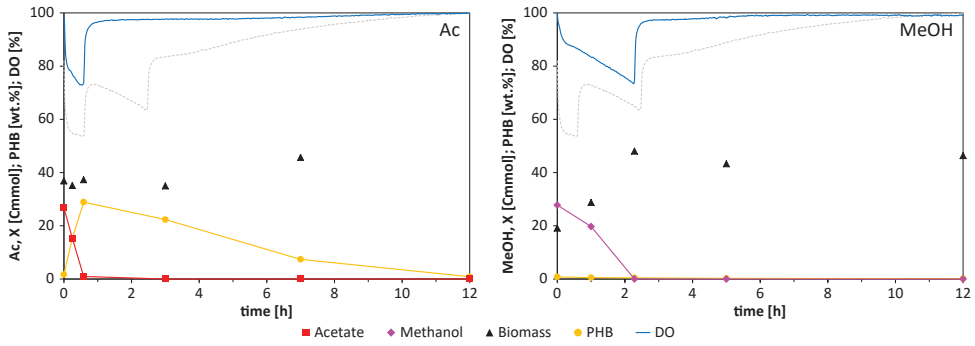

Figure 3.3: Results of short-term cycle experiments using sole acetate (Ac) or sole methanol (MeOH) as substrate. The acetate present in the reactor (Cmmol) is represented by red squares, methanol (Cmmol) by pink diamonds, active biomass (Cmmol) by black triangles, and PHB (wt.%) by yellow circles. The blue line displays the dissolved oxygen level (%) in the reactor liquid. The dashed, grey line shows the dissolved oxygen level in the reactor liquid during a normal cycle of the SBR (see Figure 3.1).

PHA was used for biomass synthesis.

Similarly, two short-term cycle experiments were performed with sole methanol (Figure 3.3b). Like in a normal SBR cycle, methanol was consumed in 137 min, at an average specific uptake rate of 0.4 Cmol·Cmol^{-1}·h^{-1}. No PHA formation was observed: all methanol was directly used for growth and maintenance. After methanol depletion, biomass formation stopped and the respiration rate dropped to around 5% of its initial value. Growth or maintenance on PHA was considered negligible, since the overall PHA content at the start of the experiment was less than 1 wt.%.

These short-term experiments with sole acetate and sole methanol confirmed that the kinetic behavior of the overall culture was a summation of two separate populations: a PHA-producing population on acetate and a non-PHA-storing population on methanol. This has previously also been observed for a microbial enrichment culture on mixed acetate and lactate (Jiang et al., 2011c). In that case both populations did store PHA.

3.3.3. PHA MAXIMIZATION IN PRESENCE AND ABSENCE OF AMMONIUM

To evaluate the PHA production rate and capacity of the enrichment culture, fed-batch accumulation experiments were performed. Initial experiments were performed under N-limited conditions, while the carbon source, 1.5 M HAc and 1.5 M MeOH, was continuously supplied to the reactor via pH control. The acetate concentration in the reactor was thus maintained at 14 (±1) mM, while the methanol concentration slowly increased from 25 to 45 mM at the end of the experiment. During the first hour of the experiment, the small amount of ammonium remaining from the preceding SBR cycle was consumed and used for biomass synthesis (Figure 3.4). After that, only a limited increase in active –

i.e. non-PHA – biomass was observed. After 6 h, a maximum PHA content of 66 wt.% was obtained in the overall culture (Figure 3.5). The production of PHA was fully ascribed to *P. acidivorans*. Although methanol consumption accounted for almost a quarter of the total carbon uptake, Nile blue A staining confirmed that the methylotrophic population did also not accumulate PHA under nutrient-limited conditions (data not shown). Based on the theoretical yields for growth on methanol (0.66 Cmol·Cmol^{-1}, van Dien and Lidstrom, 2002) and growth via PHA on acetate (0.45 Cmol·Cmol^{-1}, Johnson et al., 2009b) the fraction of *P. acidivorans* in the enrichment culture ($f_{P.a.}$) was estimated at 0.4 Cmol·Cmol^{-1}. This value was consistent with the FISH (Figure 3.2 and 3.6) and qPCR results (Figure 3.7). Assuming that the fraction was constant throughout the experiment, due to the ammonium limitation, the PHA content of *P. acidivorans* could be calculated using Eq. 3.2. As shown in Figure 3.5 by the red, dashed line, the final PHA content in *P. acidivorans* was around 83 wt.%.

To mimic the use of a nitrogen-rich waste stream additional accumulation experiments were performed in which ammonium was dosed together with the carbon, in a C:N ratio identical to that in the SBR feed (8 Cmol·mol^{-1}). Due to the presence of ammonium in the feed, its supply to the reactor via pH control did not fully maintain the acetate concentration in the reactor: it slowly decreased from 14 mM to almost zero when the experiment was stopped after 7 h. The methanol concentration in the reactor initially increased slightly, from 25 to 27 mM, as also observed during the N-limited accumulation experiments. After 2 h, the methanol concentration started to decrease, to 2 mM when the experiment was stopped. In these N-excess experiments, the maximum PHA content of the overall enrichment culture was lower and reached earlier: 52 wt.% after 4 h (Figure 3.5). Afterwards the amount of PHA in the reactor kept increasing. As shown in Figure 3.4, *P. acidivorans* still accumulated large amounts of PHA under N-excess conditions and the absolute amounts of PHA accumulated during both experiments were comparable. That the PHA content of the culture started to decrease after 4 h, was due to unrestricted growth of the methylotrophic population: the methanol and ammonium uptake rate (mol·h^{-1}) increased over time, while the acetate uptake rate was more or less constant (Figure 3.4).

The fraction of *P. acidivorans* in the overall culture ($f_{P.a.}$) was analyzed by qPCR throughout both sets of accumulation experiments (Figure 3.7). Where under N-limited conditions the fraction of *P. acidivorans* was more or less constant, this clearly decreased under N-excess conditions. This was consistent with the FISH results (Figure 3.6).

3.4. DISCUSSION

3.4.1. *P. acidivorans* UNAFFECTED BY PRESENCE METHANOL

The experiments in this study showed that *P. acidivorans* was unaffected by the presence of methanol at concentrations of 15 to 45 mM. The cycle experiments with sole acetate

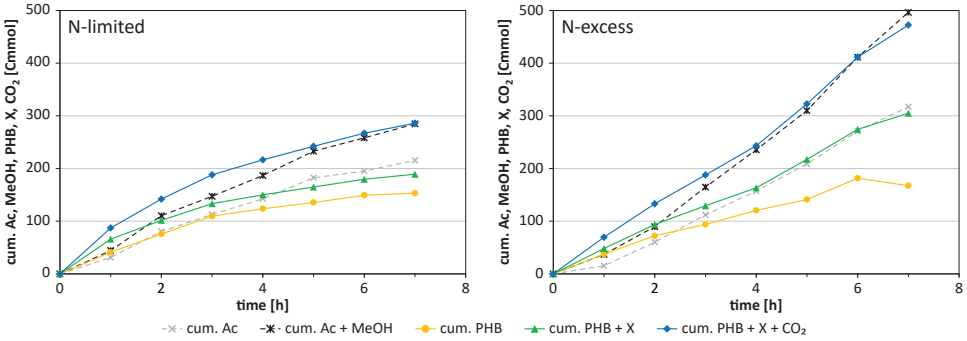

Figure 3.4: Results of a representative accumulation experiment with acetate and methanol under N-limited and N-excess conditions, respectively. The cumulative consumption of acetate (Cmmol) and carbon (acetate plus methanol, Cmmol) is represented by grey crosses and black asterisks, respectively. The cumulative production of PHA is represented by yellow circles, PHA and active biomass by green triangles, and PHA, active biomass and carbon dioxide by blue circles.

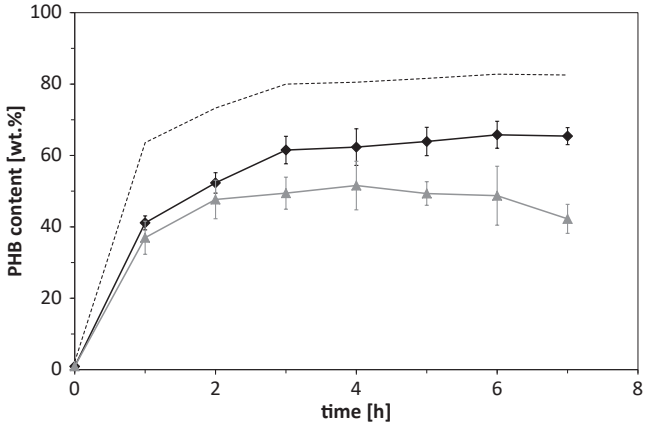

Figure 3.5: Accumulation of PHB, as weight percentage of TSS, in the overall culture under N-limited (black diamonds) and N-excess conditions (grey triangles). The dashed, black line indicates the estimated PHB content in *P. acidivorans* under N-limited conditions – these values were calculated using Eq. 3.2 and assuming a constant $f_{P.a.}$ of 0.4 Cmol·Cmol^{-1}. Shown data are the average of duplicate experiments, with error bars indicating standard deviations.

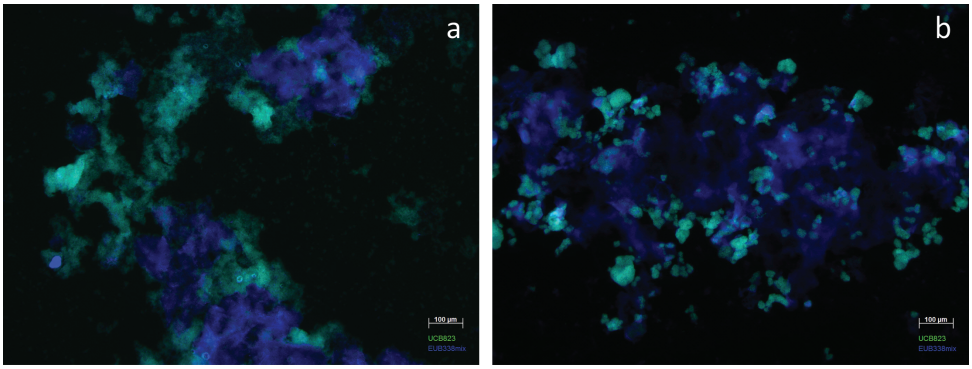

Figure 3.6: FISH microscopic photographs of the enrichment culture on mixed acetate and methanol. The samples were taken at the end of an accumulation experiment under N-limited (a) and N-excess conditions (b), respectively. The biomass was stained with a Cy5-labelled probe for Eubacteria (EUB338I-III, blue) and FLOUS-labelled probe for *P. acidivorans* (UCB823, green).

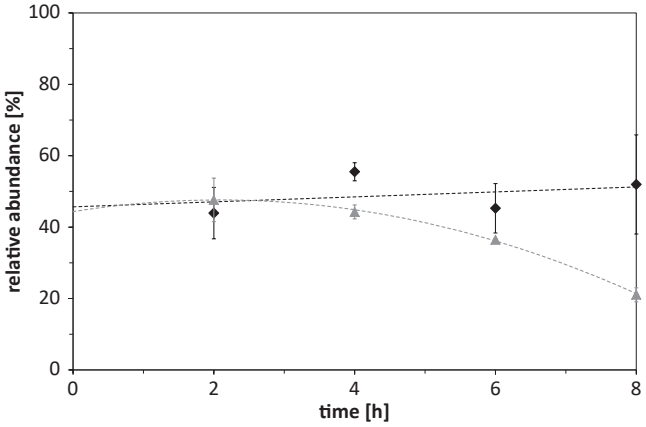

Figure 3.7: Relative abundance of *P. acidivorans* in the total biomass during accumulation experiments under N-limited (black diamonds) and N-excess conditions (grey triangles), as determined by qPCR. Shown data are the average of duplicate experiments, with error bars indicating standard deviations. The dashed lines indicate the trend.

(Figure 3.3a) and mixed acetate and methanol (Figure 3.1) gave similar results: under both conditions the dosed acetate was consumed in around 36 min. This is also the same as reported for previous enrichment cultures on acetate, dominated by *P. acidivorans* (Johnson et al., 2009a; Jiang et al., 2011a,c). To allow comparison of the specific acetate uptake rate and maximum PHA content of *P. acidivorans* during an SBR cycle, it has to be taken into account that *P. acidivorans* forms only part of the total culture. If the overall specific acetate uptake rate (1.4 Cmol·Cmol^{-1}·h^{-1}) and PHA content (30 wt.%) measured during the SBR cycle are corrected for the estimated fraction of *P. acidivorans* in the total biomass (40%), an estimated specific acetate uptake rate of 3.5 Cmol·Cmol^{-1}·h^{-1} and PHA content of 52 wt.% are found for *P. acidivorans* specifically. Both values are highly similar to those reported in previous, *P. acidivorans* dominated, enrichment cultures on acetate (Johnson et al., 2009a; Jiang et al., 2011a,c).

3.4.2. FEAST-FAMINE SELECTS NON-STORING METHYLOTROPHS

Although the presence of methanol did not affect the PHA production by *P. acidivorans*, the enriched methylotroph in this study, *M. flagellatus*, did not store PHA. *M. flagellatus* is an obligate methylotroph that uses the RuMP pathway for carbon assimilation. The production of PHA from methanol has been associated with facultative methylotrophs, using the serine cycle for carbon assimilation (Föllner et al., 1993; Pieja et al., 2011). It is to be disputed whether it is possible to enrich these PHA-producing methylotrophs in an SBR operated under true feast-famine conditions, i.e. when the competition is purely based on substrate uptake rate. The serine cycle includes a carboxylation step, where in the RuMP pathway all carbon is assimilated at the level of formaldehyde (Chistoserdova and Lidstrom, 2013). This difference makes that methylotrophs using the RuMP pathway have a 30% higher theoretical biomass yield (Anthony, 1978; van Dien and Lidstrom, 2002) and a significantly higher growth rate than those using the serine cycle (Schrader et al., 2009). Since the serine cycle is likely the rate-determining step in both methylotrophic growth and PHA production (Šmejkalová et al., 2010), these organisms cannot increase their substrate uptake rate (q_S) by diverting the methanol to the synthesis of PHA instead of biomass. This is unlike *P. acidivorans*, which can take up and store acetate much faster than it can use it for growth. The reported maximum specific growth and substrate uptake rate of *Methylobacterium extorquens*, a well-known PHA-producing methylotroph, are 0.2 Cmol·Cmol^{-1}·h^{-1} and 0.4 mol·Cmol^{-1}·h^{-1}, for example (Bourque et al., 1995; Peyraud et al., 2011). This organism will easily be outcompeted by *M. flagellatus*, which can reach a specific growth rate of 0.7 Cmol·Cmol^{-1}·h^{-1} (Baev et al., 1992) and therefore at least double the substrate uptake rate.

The enrichment of PHA-producing methylotrophs has been reported, for example by Dobroth et al. (2011) and Mockos et al. (2008). In both enrichment cultures the availability of an essential growth nutrient was limited: feast-famine conditions alone were

reported insufficient to induce PHA production. Similarly, Pieja et al. (2011) and Pfluger et al. (2011) studied the selection of PHA-producing methanotrophs, and reported the use of N_2 as sole nitrogen source, copper limitation, a low DO and low pH as ways to select for type II, PHA-producing methanotrophs. Although such additional measures are no problem when using a (virtually) single substrate, the limitation of an essential growth nutrient might be neither possible nor desired when using a real waste stream, containing many different compounds with different uptake rates. It remains to be elucidated if it is possible to select for PHA-producing methylotrophs without compromising the selection pressure for other PHA-producing bacteria when using a complex substrate mixture, like wastewater.

3.4.3. IMPACT AMMONIUM ON PHA MAXIMIZATION

Various researchers have reported the prevention of growth, for example by ammonium limitation, as essential to obtain high intracellular PHA contents (Bengtsson et al., 2008b; Johnson et al., 2010; Serafim et al., 2004). The presence of ammonium indeed reduced the maximum PHA content of the culture from 66 wt.% to 52 wt.%, but this reduction was due to growth of the non-storing, methylotrophic population: the fraction of *P. acidivorans* in the total biomass was shown to decrease significantly during accumulation experiments with excess ammonium (Figure 3.7). *P. acidivorans* itself accumulated large amounts of PHA (>80 wt.%) under both N-limited and N-excess conditions. Previous experiments with a PHA-producing enrichment culture on butyrate already suggested that also without nutrient limitation *P. acidivorans* stores large amounts of PHA (Marang et al., 2013). In those experiments 83-85 wt.% PHA was obtained while ammonium was present in the reactor. We, therefore, suggest that the negative effect of ammonium availability during the accumulation step can merely be ascribed to unrestricted growth of the non-storing population and not to behavior of *P. acidivorans* under these conditions. In other words, in the case of microbial enrichment cultures obtained under feast-famine conditions, nutrient limitation is not a prerequisite for obtaining a high PHA content, but a way to restrict the growth of non-storing bacteria. If the final fraction of non-storing bacteria in the culture can be restricted in a different way, the presence of ammonium in itself is not a problem and high PHA contents can still be obtained.

3.4.4. REDUCING THE NON-STORING POPULATION

In previous reports on the co-enrichment of non-storing bacteria on waste and the resulting reduction in overall PHA content (Albuquerque et al., 2007; Jiang et al., 2012; Morgan-Sagastume et al., 2010), optimization of the pre-fermentation step, i.e. increasing the fraction of VFAs, has been proposed as strategy to reduce the non-storing population. Depending on the waste stream it may not always be possible to achieve full organic carbon conversion to VFAs. Additional strategies will, therefore, be necessary.

Such a strategy could be the inclusion of a concentration step directly after depletion of the compounds suitable for PHA production (VFAs, lactate, etc.). It was observed in this study that when acetate was depleted, 80% of the dosed methanol still remained in the reactor liquid. If a solid-liquid separation step would be included at this point, partial discharge of the supernatant can remove a large part of the remaining external substrate – methanol – from the system. Thus reducing the availability for and thereby the size of the methylotrophic population. Since less methylotrophic biomass is formed, the next cycle less methanol will be consumed. This strategy enables the selective removal of substrates unsuitable for PHA production, and is currently being investigated in our lab. The simple substrate mixture of acetate and methanol is a useful model substrate for the development of such strategies.

3.5. CONCLUSION

The enrichment culture on acetate and methanol was dominated by two bacterial species: *P. acidivorans*, a known PHA producer, and *M. flagellatus*, an obligate methylotroph. PHA production by *P. acidivorans* was not impeded by the presence of methanol, but the presence of a non-storing, methylotrophic population reduced the PHA content of the overall culture. Especially when ammonium was present during the accumulation experiments, unrestricted growth of the methylotrophic population caused a significant reduction of the overall PHA content. For successful PHA production from fermented waste streams, strategies to restrict the size of the non-storing population need to be developed. The simple substrate mixture of acetate and methanol is a useful model substrate for the development of such strategies.

NOMENCLATURE

c_i	concentration of compound i	[(C)mmol·L^{-1}]
$f_{P.a.}$	fraction *P. acidivorans* in the total active biomass	[Cmol·Cmol^{-1}]
PHA_{Other}	PHA content of the flanking microbial population	[g·g^{-1}]
$PHA_{P.a.}$	PHA content of *P. acidivorans*	[g·g^{-1}]
PHA_{total}	PHA content of the total biomass	[g·g^{-1}]
q_i	average biomass-specific production rate of compound i	[(C)mol·Cmol^{-1}·h^{-1}]

4

COMBINING THE ENRICHMENT AND ACCUMULATION STEP

The process for non-axenic polyhydroxyalkanoate (PHA) production from organic waste generally comprises three steps: acidogenic fermentation of the waste stream, enrichment of a PHA-producing culture, and production of the PHA. This study assesses the feasibility of combining the enrichment and production step. Harvesting PHA-rich biomass directly from the sequencing batch reactor (SBR) used for enrichment of the microbial culture reduces capital cost, but may increase downstream-processing cost if the PHA content is significantly lowered. Operating an acetate-fed SBR at a volume exchange ratio of 0.75 (18 h cycles, 1 d SRT) allowed the production of biomass with 70 wt.% poly(3-hydroxybutyrate) (PHB) in a single-step process. By increasing the exchange ratio to 0.83 (20 h cycles) the PHB content of the harvested biomass increased to 75 wt.%, but the operational stability decreased. SBR operation at these high exchange ratios makes that bacteria have to increase their growth rate and external substrate is available for relatively long periods. This allows the establishment of larger flanking populations and negatively affected the kinetic properties of Plasticicumulans acidivorans*, the predominant organism. Maximizing the volume exchange ratio is, therefore, a suitable strategy to produce large amounts of PHA in the SBR, but does not ensure the enrichment of a culture with superior PHA productivity.*

Published as: L. Marang, M.C.M. van Loosdrecht, and R. Kleerebezem. 2016. Combining the enrichment and accumulation step in non-axenic PHA production: Cultivation of *Plasticicumulans acidivorans* at high volume exchange ratios. Journal of Biotechnology 231, 260-267.

4.1. INTRODUCTION

Polyhydroxyalkanoates (PHAs) are microbial storage polymers accumulated by many different prokaryotes as an intracellular carbon and energy reserve (Steinbüchel, 1991; Tan et al., 2014). The chemical properties of the polymer make it an interesting bioplastic that is fully biodegradable (Chen, 2009). Moreover, the PHA monomers could serve as chiral building blocks for the production of various biochemicals, and the hydroxy fatty acid methyl esters could be used as a biofuel (Chen, 2009).

The commercially available PHA is generally produced using pure cultures of *Cupriavidus necator* – formerly *Ralstonia eutropha* (Vandamme and Coenye, 2004) – or recombinant *Escherichia coli*, and glucose and propionic acid as substrate(Chen, 2009). To reduce the production cost of PHA and allow broad application, various researchers investigated the use of open microbial communities and waste organic carbon as substrate (Albuquerque et al., 2010b; Bengtsson et al., 2008b; Coats et al., 2007; Dionisi et al., 2005a; Jiang et al., 2012). The process for non-axenic PHA production from organic waste consists of three steps: (1) acidogenic fermentation of the waste stream, (2) enrichment of a PHA-producing culture, and (3) production of the PHA (Dionisi et al., 2004; Serafim et al., 2008). The first or acidogenic fermentation step (Temudo et al., 2007) aims to convert the waste organic carbon, primarily carbohydrates, to a mixture of volatile fatty acids. These acids are a more suitable substrate for PHA production (Reis et al., 2003) and will be used as such in the following two steps. In the second step, an open microbial community is enriched in bacteria with a high PHA storage capacity. This enrichment step is performed in a sequencing batch reactor (SBR) operated under feast-famine conditions, as intermittent substrate availability creates a competitive advantage for bacteria that store substrate inside their cell as a reserve (Reis et al., 2003). Once a stable culture is obtained, the SBR will be operated as a biomass production step and the excess sludge used in step three: maximization of the PHA content of the biomass in a (nitrogen-limited) fed-batch reactor (Johnson et al., 2009a). PHA contents of 70-80 wt.% have been reported for the production of PHA from fermented waste streams like molasses and paper or food industry effluents (Albuquerque et al., 2010b; Jiang et al., 2012; Tamis et al., 2014a). The highest PHA contents reported for microbial enrichment cultures are around 90 wt.% and were obtained when using sole acetate or lactate as substrate (Jiang et al., 2011c; Johnson et al., 2009a).

PHA-rich biomass could also be harvested directly from the enrichment reactor (Dionisi et al., 2007; Reis et al., 2003). During the feast phase of each SBR cycle, external substrate is taken up and stored as PHA before it is used for growth. At the end of the feast phase, part of the PHA-rich biomass could be harvested. Eliminating the separate accumulation step (step 3) reduces the capital cost, but may lead to increased downstream-processing cost as the maximum PHA content obtained in the SBR is generally much lower (≤50 wt.%) than that obtained after the fed-batch accumulation step. Jiang et al.

(2011a) demonstrated that the PHA content at the end of the feast phase increases if the number of cycles per solids retention time (SRT) is reduced. When they operated the SBR at a volume exchange ratio of 0.5 (12 h cycles and 1 d SRT), 53 wt.% PHA was accumulated during the SBR cycle. At a volume exchange ratio of 0.75 (18 h cycles), up to 71 wt.% PHA was accumulated (Jiang et al., 2011a). Operating the SBR at a maximized volume exchange ratio might, therefore, lead to sufficiently high PHA contents and allow a reduction in capital cost that outweighs increased downstream-processing costs.

The aim of this study was to assess the feasibility of combining the enrichment and accumulation step in non-axenic PHA production. To that end, an aerobic SBR inoculated with activated sludge was operated at a volume exchange ratio of 0.75, and later 0.83. The reactor was fed with acetate, and broth removal took place at the end of the feast phase in order to harvest biomass rich in poly(3-hydroxybutyrate) (PHB). To promote growth on stored PHB, the dosage of carbon and nutrients was uncoupled: growth nutrients, including ammonium, were supplied after the effluent phase. The effect of these operational conditions on the enrichment and kinetic performance of *Plasticicumulans acidivorans* (Jiang et al., 2011d) was studied.

4.2. MATERIALS AND METHODS

4.2.1. SBR FOR CULTURE ENRICHMENT AND PHB PRODUCTION

The enrichment and maintenance of a PHB-producing culture and the production of PHB were performed in a single double-jacket glass bioreactor with a working volume of 2 L (Applikon, Netherlands). The reactor was operated as a non-sterile SBR with, initially, 18-h cycles. The exchange volume was 1.5 L, resulting in a volume exchange ratio of 0.75 and hydraulic retention time (HRT) of 1 day. As there was no settling phase, the SRT equaled the HRT. To allow the harvest of PHB-rich biomass, biomass was withdrawn from the reactor at the end of the feast phase. Each SBR cycle consisted of a carbon feed phase (15 min), reaction phase (125 min), effluent phase (20 min), nutrient feed phase (15 min), and second reaction phase (905 min). During the carbon feed phase 150 mL concentrated sodium acetate solution (0.83 M) was dosed into the reactor. After the effluent phase, the reactor was refilled with 1.35 L fresh medium comprising 5.82 mM NH_4Cl, 2.77 mM KH_2PO_4, 0.62 mM $MgSO_4 \cdot 7H_2O$, 0.80 mM KCl, 1.67 mL·L^{-1} trace elements solution according to Vishniac and Santer (1957), and 5.5 mg·L^{-1} allylthiourea (to prevent nitrification).

The reactor was equipped with a stirrer with three standard geometry six-blade turbines, operated at 900 rpm. The air flow rate to the reactor was set to 0.5 $L_N \cdot min^{-1}$ using a mass flow controller (Brooks Instrument, USA). The total gas flow rate through the reactor was increased to 3.0 $L_N \cdot min^{-1}$ by partial recirculation of the off-gas. The temperature in the reactor was controlled at 30±1°C using a thermostat bath (Lauda, Germany), and the pH was maintained at 7.0±0.1 by the addition of 1 M HCl and 1 M

NaOH. Controlling of the pumps, stirrer, airflow, temperature, and pH was done by a biocontroller (Biostat Bplus, Sartorius Stedim Biotech, Germany).

Aerobic activated sludge from the municipal wastewater treatment plant Kralingseveer (Rotterdam, Netherlands) was used to inoculate the SBR. The reactor was operated for almost 4 years and cleaned once or twice a week to remove biofilm from the walls, electrodes, and other submerged reactor parts. The performance was monitored online by the length of the feast phase, which can be derived from the dissolved oxygen profile Jiang et al. 2011c. Periodically, samples were collected to determine the biomass and PHB concentration at the end of the feast phase, and cycle experiments were conducted to characterize the enrichment culture in more detail. Moreover, biomass was collected from the SBR for accumulation experiments and analysis of the microbial community structure.

After 3 years and 4 months of continuous operation, the cycle was prolonged to 20 h and the volume exchange ratio increased to 0.83 – maintaining an HRT and SRT of 1 day. The new SBR cycle consisted of a carbon feed phase of 17 min, reaction phase of 223 min, effluent phase of 18 min, nutrient feed phase of 17 min, and second reaction phase of 925 min. The carbon feed consisted of 167 mL concentrated sodium acetate solution (1.25 M), and after the effluent phase 1.50 L fresh medium (unchanged composition) was added. The reactor was operated at 20-hour cycles for 6.5 months and monitored as before.

4.2.2. FED-BATCH REACTOR FOR ACCUMULATION EXPERIMENTS

To evaluate the maximum PHB storage capacity of the enrichment culture, accumulation experiments were conducted in a similar double-jacket glass bioreactor (Applikon, Netherlands) operated as a non-sterile fed-batch reactor. At the beginning of each experiment the reactor was filled with 1.5 L effluent from the SBR, and 0.5 L carbon- and ammonium-free medium (otherwise the same composition). If the effluent did not contain residual acetate, the production of PHA was initiated by feeding a pulse of 60 mmol sodium acetate. Further carbon source was continuously supplied to the reactor via pH control, using a 1.5 M acetic acid solution instead of the 1 M HCl solution used in the SBR (Johnson et al., 2009a). As the ammonium concentration in the effluent was zero, microbial growth was prevented throughout the experiment. When necessary a few drops of antifoam B (Sigma-Aldrich) were added and after 10 h the experiments were stopped.

4.2.3. ANALYTICAL METHODS

During cycle and accumulation experiments the reactor was monitored closely by both online (dissolved oxygen, temperature, pH, acid and base dosage, off-gas O_2 and CO_2) and offline (acetate, ammonium, TSS, PHB) measurements.

Samples taken to determine the acetate and ammonium concentration in the reactor were immediately filtered with a 0.45 µm pore size filter (PVDF membrane, Millipore, Ireland) to remove the biomass. The ammonium concentration in the supernatant was determined spectrophotometrically using a commercial cuvette test kit (Hach Lange, Germany). The acetate concentration was analyzed using a high-performance liquid chromatograph (HPLC) with a BioRad Aminex HPX-87H column and a UV detector (Waters 484, 210 nm). The mobile phase – 1.5 mM H_3PO_4 in Milli-Q water – had a flow rate of 0.6 mL·min^{-1} and a temperature of 59°C.

Samples taken to determine the total suspended solids (TSS) and PHB concentration in the reactor were collected in 15 mL tubes with five drops of formaldehyde (37%) to stop all biological activity. The samples were centrifuged for 10 min at 4500 rpm (3850*g*) before removing the supernatant and freezing the samples (-20°C). The samples were subsequently freeze-dried for 24 h (-40°C, 10^{-4} atm) to yield the TSS. The PHB content of the freeze-dried cells was determined using a gas chromatograph (Agilent 6890N, USA) equipped with a flame ionization detector (FID) and a HP-INNOWax column. A detailed description of the procedure can be found elsewhere (Johnson et al., 2009a). The PHB content, expressed as the weight percentage PHB of TSS, was calculated using pure PHB (Sigma-Aldrich, CAS 26063-00-3) as standard, and benzoic acid as internal standard. The determined PHB content was subtracted from the TSS to obtain the concentration of active biomass in the reactor. The biomass composition (excl. PHB) was assumed to be $CH_{1.8}O_{0.5}N_{0.2}$ and its molecular weight 25.1 g·Cmol^{-1} (including ash).

4.2.4. DATA TREATMENT AND MODELING

The data collected during cycle and accumulation experiments was evaluated according to the approach proposed by Johnson et al. (2009b). The gathered online and offline measurements were corrected for the air pressure and effects of sampling, the addition of liquids, and inorganic carbon dissolution. After correction, carbon and electron balances were setup to assess the accuracy of the measurements. On average 96% (±5) of the carbon and 99% (±6) of the electrons present in the substrate could be traced back in the active biomass, PHB, and carbon dioxide production or oxygen consumption. Finally, the corrected data was evaluated using a metabolic model to determine the biomass-specific reaction rates and other kinetic parameters. The metabolic reactions, stoichiometry, and kinetic equations can be found in Johnson et al. (2009b). The efficiency of the oxidative phosphorylation (P:O ratio) was assumed to be 2.0 mol ATP/mol NADH. The half-saturation constants for acetate (K_{Ac}) and ammonium (K_N) – both acting merely as a switch function – were set to 0.2 Cmmol·L^{-1} and 0.0001 mmol·L^{-1}, respectively.

The initial data treatment was performed in Microsoft Excel. The metabolic model was written in Matlab™ (Mathworks, USA), where the built-in function *ode113* was used

to solve the differential equations and *fmincon* was used to minimize the sum of the squared relative error (SSqRE) between the measured and modeled data. For each compound (acetate, biomass, PHB, NH_4^+, CO_2, and O_2) the SSqRE was calculated according to Eq. 4.1. These squared relative errors were subsequently summated to yield the overall error.

$$SSqRE_i = \sum_0^t \left(\frac{c_i^{measure}(t) - c_i^{model}(t)}{c_i^{model}(t)} \right)^2 \tag{4.1}$$

4.2.5. MICROBIAL COMMUNITY ANALYSIS

In order to analyze the microbial community structure by PCR-DGGE, biomass samples were collected from the SBR and washed with TE buffer. The genomic DNA was extracted using the Ultra Clean Soil DNA extraction kit (MoBio Laboratories, USA) and subsequently used as template DNA. 16S rRNA gene fragments of the different community constituents were obtained using a touchdown PCR program with the primers 341F-GC and 907R (Table 4.1) (Schäfer and Muyzer, 2001). The 16S rRNA gene amplicons were loaded onto 8% polyacrylamide gels with a denaturing gradient from 20 to 70% DNA denaturants (100% denaturants is a mixture of 5.6 M urea and 32% formamide) (Schäfer and Muyzer, 2001). The DNA was visualized by UV illumination after staining with SYBR® Safe, and photographed with a digital camera. Individual bands were excised from the gel with a sterile razor blade and incubated overnight in 50 µL water at 4°C. Re-amplification was performed using the same primer pair (Table 4.1) and the PCR products were sequenced by a commercial company (BaseClear, Netherlands). The sequences have been stored in GenBank under accession numbers: KT634309–KT634310.

In addition to the PCR-DGGE analysis, FISH was performed to confirm the predominance of *P. acidivorans* on a more regular basis. A detailed description of the procedure can be found in Johnson et al. (2009a). The general probe mixture EUB338I-III was used to visualize all bacteria in the sample and the specific probe UCB823 to indicate the presence of *P. acidivorans*. The probes (Table 4.1) were commercially synthesized and 5' labeled with respectively FLUOS and the sulfoindocyanine dye Cy5 (Thermo Hybaid interactive, Germany).

4.3. RESULTS

4.3.1. CULTURE ENRICHMENT AND MICROBIAL CHARACTERIZATION

The SBR operated in this study – serving the simultaneous enrichment of a PHB-producing culture and production of PHB – was fed with acetate as model substrate. It was, initially, operated at a volume exchange ratio of 0.75 (i.e. 18 h cycles and 1 d SRT). The typical feast-famine response established immediately after inoculation with acti-

Table 4.1: Oligonucleotide probes for FISH analysis and primers for PCR-DGGE analysis used in this study.

Code	Function	Sequence (5'-3')	Specificity	Reference
EUB338 I	Probe	gct gcc tcc cgt agg agt	Bacteria	Amann et al. (1990)
EUB338 II	Probe	gca gcc acc cgt agg tgt	Bacteria	Daims et al. (1999)
EUB338 III	Probe	gct gcc acc cgt agg tgt	Bacteria	Daims et al. (1999)
UCB823	Probe	cct ccc cac cgt cca gtt	*P. acidivorans*	Johnson et al. (2009a)
341F-GC	Primer	cct acg gga ggc agc ag*	Bacteria	Schäfer and Muyzer (2001)
907R	Primer	ccg tca att cmt ttg agt tt	Bacteria	Schäfer and Muyzer (2001)

* Contains GC-clamp (5'-cgcccgccgcgccccgcgcccgtcccgccgcccccgcccg-3') at the 5' end of the primer.

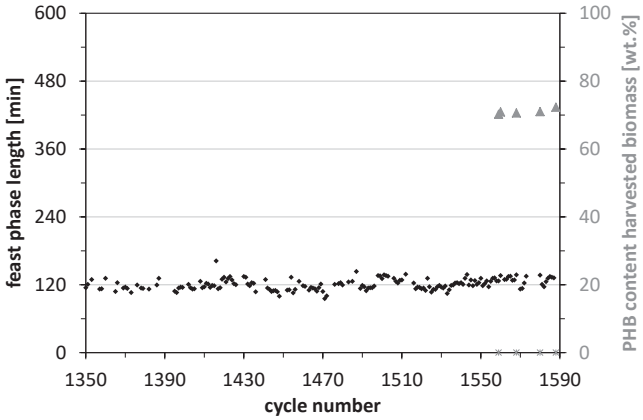

Figure 4.1: Performance of the SBR during the final six months of operation at 18 h cycles. Black diamonds indicate the length of the feast phase (min), grey triangles the PHB content of the harvested biomass (wt.% of TSS). The grey asterisks on the x-axis indicate when cycle and/or accumulation experiments were conducted.

vated sludge, but the feast phase length remained relatively long and variable (5.5±0.9 h) throughout the first months of operation (not shown). After eight months the feast phase length had decreased to around 180 min. It took almost two years (23 months), though, to reach a stable and final feast phase length of 128 (±12) min. During the 16-month operational period thereafter, the reactor performance remained stable. Figure 4.1 shows the feast phase length during the last six months of operation.

Analysis of the microbial community structure by FISH after 9 and 20 months of operation showed that the enrichment culture was dominated by *P. acidivorans* (Figure 4.2a,b). Small but not negligible fractions of other bacteria were also present, especially in the first sample. At the end of the stable operational period, the continued predominance of *P. acidivorans* was confirmed by PCR-DGGE analysis (Figure 4.2c, band B1, 99.8% similarity).

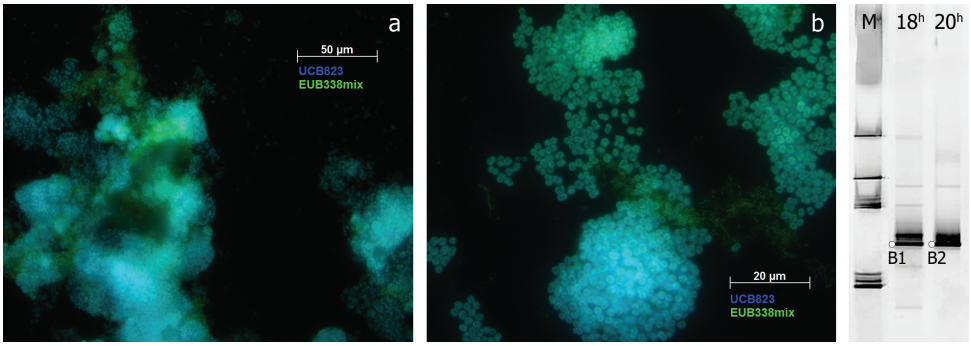

Figure 4.2: FISH microscopic photographs and DGGE gel. (a,b) Fluorescence microscopy images of the enrichment culture after respectively 9 months (40× magnification) and 20 months (100× magnification) of reactor operation at 18-h cycles. The biomass was stained with a FLUOS-labeled probe for Eubacteria (EUB338I-III, green) and Cy5-labeled probe for *P. acidivorans* (UCB823, blue). (c) DGGE gel of PCR-amplified 16S rRNA gene fragments from the enrichment culture collected during operation at 18 h (lane 18^h) and 20 h cycles (lane 20^h). SmartLadder SF (Eurogentec) was loaded in lane M. The bands labeled B1-2 were excised and re-amplified for microbial identification. Previous analyses have shown that the bands just above B1-2 also belong to *P. acidivorans* (Jiang et al., 2011a).

4.3.2. SBR PERFORMANCE AT 18-HOUR CYCLES

To evaluate the kinetic performance of the enrichment culture in detail, multiple cycle experiments – covering the feast (10) and/or famine phase (4) – were conducted throughout the final 16-month operational period. Table 4.2 gives an overview of the main observed and model-derived variables that were obtained, while Figure 4.3 shows the results of a single, representative feast and famine experiment.

The maximum biomass-specific acetate uptake rate ($q_{Ac,max}$) of the culture was 2.15 (±0.17) Cmol·Cmol^{-1}·h^{-1}. The consumed acetate was primarily stored as PHB ($Y_{PHB,Ac}$ = 0.59 Cmol·Cmol^{-1}) and at the end of the feast phase the PHB content reached 70±1 wt.%. To promote the growth on stored PHB, growth nutrients – including ammonium – were supplied after the feast phase and nitrogen availability during the feast phase was limited. Direct growth on acetate was not prevented since the ammonium concentration reached zero only shortly before substrate depletion. The maximum biomass-specific growth rate on acetate (μ_{max}) was found to be 0.12 (±0.03) Cmol·Cmol^{-1}·h^{-1} (Table 4.2). Five percent of the consumed carbon was traced back as active biomass ($Y_{X,Ac}$ = 0.05 Cmol·Cmol^{-1}) and around 30% of the total ammonium consumption occurred during the feast phase.

After 140 minutes, 75% of the broth liquid was removed from the reactor – to harvest the PHB – and replaced by fresh medium. In the period between substrate depletion and fresh nutrient supply (±0.5 h) already a slight reduction in the PHB content was observed (1-2 wt.%, data not shown). After nutrient supply, the accumulated PHB was rapidly degraded and used for biomass synthesis. The initial biomass-specific growth rate was

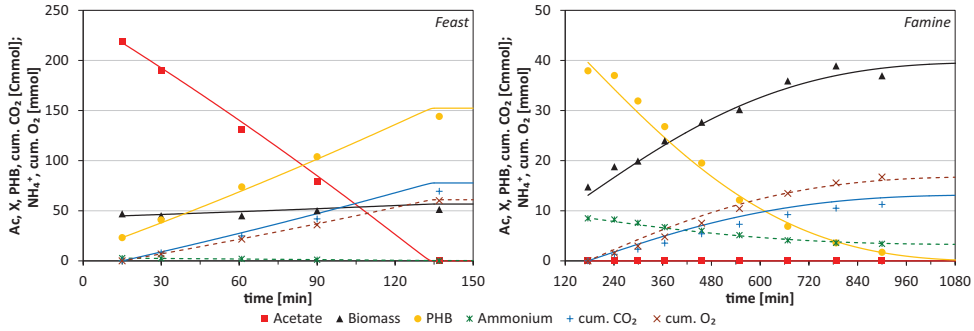

Figure 4.3: Results of a cycle experiment during normal SBR operation at 18 h cycles. The symbols represent measured data, the lines modeled data.

around 0.2 Cmol·Cmol^{-1}·h^{-1}, but this slowed down as the intracellular PHB content decreased towards 3±1 wt.% at the end of the cycle. The average biomass-specific growth rate during the famine phase was 0.07 Cmol·Cmol^{-1}·h^{-1} (Table 4.2).

4.3.3. SBR PERFORMANCE AT 20-HOUR CYCLES

After 39 months of operation the volume exchange ratio of the reactor was increased to 0.83 (i.e. 20 h cycles and 1 d SRT). The reactor was not re-inoculated with activated sludge and no clear adaptation period was observed (Figure 4.4). The feast phase length and its variability increased considerably: throughout reactor operation (6.5 months) the feast phase length was 354±40 min. Analysis of the microbial community structure by PCR-DGGE (after 2 months, Figure 4.2c) and FISH (after 6 months, not shown) showed that *P. acidivorans* remained the predominant microbial species. The sequence derived from band B2 (Figure 4.2c) showed 99.8% similarity to that of *P. acidivorans*.

As before, cycle experiments – covering the feast (6) and/or famine phase (3) – were conducted to evaluate the kinetic parameters of the enrichment culture. The results of a representative feast and famine experiment are shown in Figure 4.5, and an overview of the observed and model-derived variables is given in Table 4.2. The acetate was taken up slower than in the first, 18 h setup: the maximum biomass-specific acetate uptake rate ($q_{Ac,max}$) was only 1.34 (±0.14) Cmol·Cmol^{-1}·h^{-1}. Nevertheless, the consumed acetate was largely stored as PHB ($Y_{PHB,Ac}$ = 0.56 Cmol·Cmol^{-1}) and upon substrate depletion the PHB content reached 75±3 wt.%. The nitrogen availability during the feast phase was limited and ammonium got depleted after roughly 3 h. Despite the absence of ammonium during a significant part of the feast phase, the role of biomass growth increased: 40% of the overall ammonium consumption occurred during the feast phase. The biomass yield ($Y_{X,Ac}$) and maximum specific growth rate on acetate (μ_{max}) increased slightly to 0.07 Cmol·Cmol^{-1} and 0.14 (±0.02) Cmol·Cmol^{-1}·h^{-1}, respectively.

The effluent phase started 4 h after the start of the cycle. At that point, not all acetate

Table 4.2: Overview of observed variables, and model-derived yields and biomass-specific rates during normal SBR operation and accumulation experiments. The presented average values and standard deviation for the SBR are based on the results of at least three experiments. The accumulation experiments were performed in duplicate.

	SBR 1	SBR 2	SBR 3
	12 h cycle	**18 h cycle**	**20 h cycle**
	Jiang et al. (2011c)	*This study*	*This study*
SBR operation/Cycle experiments			
Observed			
Length feast phase [min]	38	128 ± 12	354 ± 40
Length feast phase [% of CL]	5	12 ± 1	30 ± 3
PHB max. feast [wt.%]	52	70 ± 1	75 ± 3
PHB max. feast [Cmol·Cmol^{-1}]	1.3	2.8 ± 0.2	3.6 ± 0.6
Model-derived (feast)			
$Y_{PHB,Ac}^{feast}$ [Cmol·Cmol^{-1}]	0.67	0.59 ± 0.01	0.56 ± 0.02
$Y_{X,Ac}^{feast}$ [Cmol·Cmol^{-1}]	0.00	0.05 ± 0.01	0.07 ± 0.02
$Y_{CO2,Ac}^{feast}$ [Cmol·Cmol^{-1}]	0.33	0.36 ± 0.00	0.37 ± 0.01
$q_{Ac,max}$ [Cmol·Cmol^{-1}·h^{-1}]	4.38	2.15 ± 0.17	1.34 ± 0.14
μ_{max}^{feast} [Cmol·Cmol^{-1}·h^{-1}]	0.00	0.12 ± 0.03	0.14 ± 0.02
m_{ATP}^{feast} [mol·Cmol^{-1}·h^{-1}]	0.00	0.00 ± 0.01	0.00 ± 0.01
Model-derived (famine)			
k [Cmol$^{1/3}$·Cmol$^{-1/3}$·h^{-1}]	-0.16	-0.17 ± 0.01	-0.14 ± 0.02
μ^{famine}, max. [Cmol·Cmol^{-1}·h^{-1}]	0.14	0.20 ± 0.04	0.20 ± 0.06
μ^{famine}, average [Cmol·Cmol^{-1}·h^{-1}]	0.06	0.07 ± 0.01	0.08 ± 0.01
m_{ATP}^{famine} [mol·Cmol^{-1}·h^{-1}]	0.00	0.00 ± 0.00	0.01 ± 0.01
Accumulation experiments			
Observed			
PHB max. acc [wt.%]	88	86 ± 1	83 ± 1
PHB max. acc [Cmol·Cmol^{-1}]	8.3	7.1 ± 0.4	5.9 ± 0.3
Time PHB max. [h]	9.2	10-12	11-14
Time PHB >80 wt.% [h]	4.2	4-5	6-7

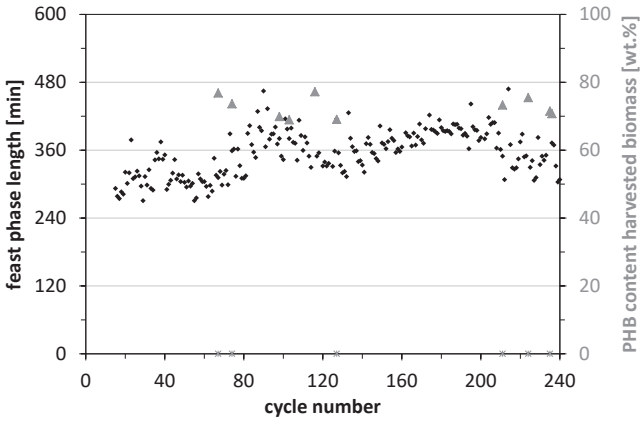

Figure 4.4: Performance of the SBR during operation at 20 h cycles (6.5 months). Black diamonds indicate the length of the feast phase (min), grey triangles the PHB content of the harvested biomass (wt.% of TSS). The grey asterisks on the x-axis indicate when cycle and/or accumulation experiments were conducted.

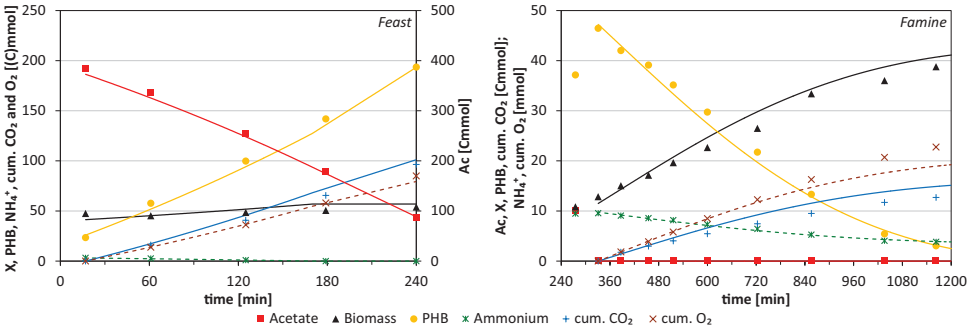

Figure 4.5: Results of a cycle experiment during normal SBR operation at 20 h cycles. The symbols represent measured data, the lines modeled data.

had been consumed yet and the PHB content of the harvested biomass was 73±3 wt.%. As afterwards the reactor was being refilled with ammonium-rich medium, the remaining acetate was used for PHB production as well as fast biomass growth (Figure 4.5). Once the acetate had been depleted, stored PHB was degraded and used for biomass synthesis. The maximum and average biomass-specific growth rate during the famine phase were, respectively, 0.2 and 0.08 Cmol·Cmol^{-1}·h^{-1}. At the end of the famine phase the PHB content had decreased to 9±4 wt.%. This is somewhat higher than observed in the 18 h setup (this study) or previous studies (Jiang et al., 2011a), and suggests that the growth rate on PHB has approached its maximum.

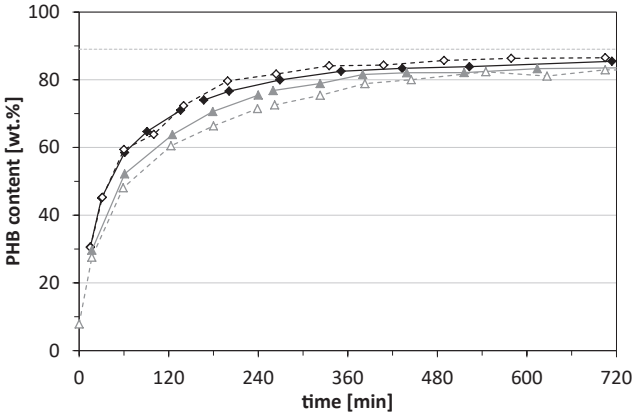

Figure 4.6: The production of PHB (wt.% of TSS) during accumulation experiments with biomass enriched at 18 h (black diamonds) and 20 h cycles (grey triangles). The filled and open symbols present the results obtained during duplicate experiments. The horizontal grey, dashed line indicates the maximum PHB storage capacity of *P. acidivorans* (Johnson et al., 2009a).

4.3.4. PHB STORAGE CAPACITY

In addition to characterization of the normal SBR performance at 18 and 20 h cycle length, the maximum PHB storage capacity of the enrichment culture was determined in fed-batch accumulation experiments. Part of the SBR effluent was transferred to another bioreactor, where additional carbon source (acetic acid) was supplied via pH control. As the ammonium concentration in the SBR effluent was zero, these experiments were conducted under ammonium-limited conditions. Figure 4.6 shows the accumulation of PHB during duplicate feast and accumulation experiments with biomass from the SBR operated at 18 and 20 h cycles, respectively.

Biomass harvested from the 18 h setup had a maximum PHB storage capacity of 86±1 wt.% (Table 4.2). This is slightly lower than the PHB storage capacities previously reported for *P. acidivorans* predominated enrichment cultures (88-89 wt.%) by, e.g., Johnson et al. (2009a) and Jiang et al. (2011c). The maximum PHB content reached in the culture enriched at 20 h cycles was further reduced: 83±1 wt.% after 11 h or more. Aside from the lowered maximum PHB content, the PHB production rate also decreased considerably. Where the culture enriched at 18 h cycles still accumulated 80 wt.% PHB in 4-5 h, the culture enriched at 20 h cycles required 6-7 h to reach this level (Figure 4.6 and Table 4.2).

4.4. DISCUSSION

4.4.1. ENRICHMENT PROGRESS

The enrichment of *P. acidivorans* in an acetate-fed SBR operated at 18 h cycles and 1 d SRT has been studied once before. Jiang et al. (2011a) reported a feast phase length similar to that observed in this study, namely 137 min. However, contrary to the long enrichment period in the present study (23 months), they reached this feast phase length within a few weeks after inoculation with activated sludge. The fast stabilization of their system may well be ascribed to the bioaugmentation with 1% *P. acidivorans* predominated biomass. The inoculated biomass originated from an enrichment reactor (SBR, 12 h cycles, 1 d SRT, 30°C) that had been running for several years and for which the gradual increase of the culture's kinetic performance has also been reported (Johnson et al., 2009a). Johnson et al. (2009a) presented three accumulation experiments – conducted after respectively 2, 7, and 16 months of operation – that show a clear increase of the biomass-specific PHB production rate and the PHB storage capacity over time. Furthermore, the feast phase was reported to last 50 min (Johnson et al., 2009a), while later a feast phase length of 38 min has been reported for the same enrichment culture (Jiang et al., 2011c).

The timescale of the current enrichment period (2 years), together with the continued predominance of *P. acidivorans* (Figure 4.2) and significant reduction of the feast phase length, suggests that the enrichment process involved more than just the wash-out of flanking populations. To explain the reduction of the feast phase length from 180 to 128 min solely by the wash-out of bacteria, the flanking population should have formed at least 30% of the culture. Assuming that the flanking population is competing with *P. acidivorans* for the acetate at around half the biomass-specific rate of *P. acidivorans*, more than 50% of the culture should have consisted of bacteria other than *P. acidivorans*. Although other bacteria were present (roughly 10%, Figure 4.2a,b), the flanking population was not large enough to fully explain the long feast phase lengths. The kinetic properties of *P. acidivorans* itself – especially its maximum biomass-specific acetate uptake rate – will likely have changed as well. In the future, analysis of the genome and/or gene expression of *P. acidivorans* in biomass samples collected throughout the enrichment period may reveal what changed and provide more insight into possible cellular adaptation occurring alongside the microbial selection.

4.4.2. IMPACT OF THE EXCHANGE RATIO

As the SBR was operated at higher volume exchange ratios, the relative feast phase length increased significantly. In previous acetate-fed SBRs that were dominated by *P. acidivorans* and operated at volume exchange ratios between 0.04 and 0.50 (i.e., 1-12 h cycles) the feast phase occupied around 5% of the total cycle (Figure 4.7) (Jiang et al., 2011a,c). At an exchange ratio of 0.75 (18 h cycles) the relative feast phase length increased to 12%.

This was observed in the present study as well as in the study by Jiang et al. (2011a). SBR operation at an exchange ratio of 0.83 (20 h cycles), finally, resulted in the presence of external substrate during 30% of the cycle (Figure 4.7 and Table 4.2). The increase of the relative feast phase length along with an increase of the volume exchange ratio or cycle length is partially due to the increased substrate-to-biomass (F/M) ratio. Assuming a constant biomass-specific substrate uptake rate ($q_{Ac,max}$), the relative feast phase length will increase as shown by the dashed line in Figure 4.7. However, as the biomass-specific substrate uptake rate of the enrichment culture decreased (Table 4.2), the actual increase was more pronounced – especially for the highest exchange ratio.

Compared to the SBR previously operated at 12 h cycles (Jiang et al., 2011c) the specific substrate uptake rate in the 18 h setup was roughly half, and that in the 20 h setup only one-third (Table 4.2). Just as for the speed of the enrichment process (section 4.4.1), the flanking population alone (roughly 10%) cannot explain these differences. There is no conclusive answer as to why the substrate uptake rate of *P. acidivorans* decreased so much, though. Cellular stress caused by elevated acetate concentrations (up to 100 mM) or the storage of large amounts of PHB (up to 75 wt.%) forms one possible explanation, but no specific indications for this were found. The overall substrate uptake rate was still reasonably constant throughout the feast phase and the small increase could well be explained by biomass growth (Figure 4.3 and 4.5). The repeated storage of large amounts of PHB may also have affected the size of the bacterial cells. The cell-size has previously been reported to increase significantly during the accumulation of PHB (Jiang et al., 2011c; Pedrós-Alió et al., 1985). An increased cell-size will reduce the specific surface area and may thus result in a lower biomass-specific substrate uptake rate.

Another possible explanation for *P. acidivorans*' decreased substrate uptake rate is the increased growth rate. In contrast to the growth in a continuous stirred-tank reactor (CSTR), the average growth rate (μ) in an SBR does not simply equal the dilution rate. Instead, the average growth rate of the culture increases with the applied cycle length or volume exchange ratio – at the same SRT (μ = ln[1/(1-CL/SRT)]/CL). To prevent being washed-out, the average growth rate of a culture in an SBR operated at 20 h cycles has to be 55% higher than in a similar SBR operated at 12 h cycles. While increasing the volume exchange ratio, increasing growth rates were indeed observed for the feast as well as the famine phase (Table 4.2). The average growth rate during the famine phase, for example, increased from 0.06 Cmol·Cmol^{-1}·h^{-1} in the 12 h setup to 0.07 and 0.08 Cmol·Cmol^{-1}·h^{-1} in the 18 and 20 h setup, respectively. The increased growth rates reduce the cellular overcapacity that can be used for PHB production and may affect the overall biomass-specific substrate uptake rate.

4.4.3. HIGH EXCHANGE RATIO AS ENRICHMENT STRATEGY

Jiang et al. (2011a)previously suggested that the number of cycles per SRT should be

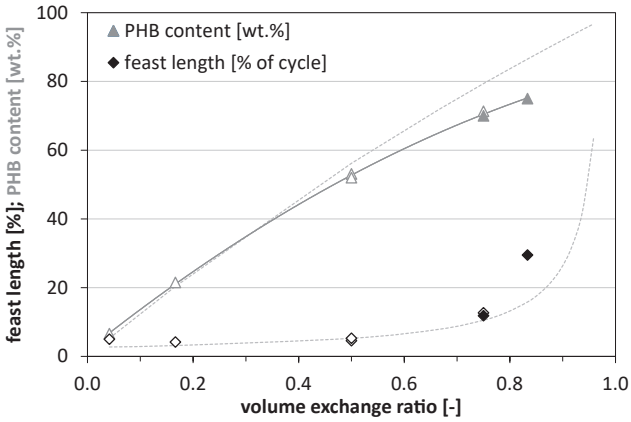

Figure 4.7: Impact of the volume exchange ratio on the PHB content obtained upon substrate depletion (grey triangles, wt.% of TSS) and the relative feast phase length (black diamonds, % of the cycle length). The filled symbols are data points obtained in this study, the open symbols data points from literature (Jiang et al., 2011a,c). The grey, dashed lines show the theoretical impact of the volume exchange ratio on the PHB content and the feast phase length, assuming negligible biomass growth during the feast and a constant biomass-specific acetate uptake rate (using the 12 h cycle (Jiang et al., 2011c) as reference point).

minimized to enrich bacteria with a high PHA storage capacity. Operating the SBR at higher volume exchange ratios – increasing the F/M ratio – leads to higher maximum PHA contents in the SBR itself. This was observed in the present study, as well as by Jiang et al. (2011a) and Valentino et al. (2014). However, it does not necessarily select for the highest PHA storage capacity or for a higher substrate uptake and PHA production rate. Although Jiang et al. (2011a) reported increasing rates for SBRs operated at cycle lengths increasing from 1 to 12 h, the specific substrate uptake rate in the SBR operated at 18 h cycles was considerably lower again – just as in this study (Table 4.2). Moreover, Valentino et al. (2014) reported decreasing uptake and storage rates for SBRs operated at increasing cycle lengths (2-8 h). For successful PHA production, both high biomass-specific rates and a high PHA storage capacity are important. Maximization of the volume exchange ratio is, therefore, a suitable strategy for the production of PHA-rich biomass in the SBR, but not necessarily the best strategy to enrich a microbial culture with a superior PHA productivity. At very high volume exchange ratios, bacteria will have to increase their growth rate and external substrate will be available for growth for a relatively long period (Section 4.4.2).

4.4.4. FEASIBILITY OF COMBINING ENRICHMENT AND ACCUMULATION

Operating the SBR at a high volume exchange ratio (0.75) allowed the production of biomass with 70 wt.% PHB in a single-step process from acetate. The reactor was operated for more than three years and already before the final 16-month operational period

biomass with a high PHB content could be harvested (66-70 wt.%, not shown). The PHB content reached upon substrate depletion was lower than the theoretical maximum that can be calculated from the applied volume exchange ratio (79 wt.%, Figure 4.7) (Jiang et al., 2011a). The calculation is based on the assumption that growth and maintenance during the feast phase can be neglected, while in reality biomass growth did occur. As a result, the PHB yield decreased (Table 4.2) and lower PHB contents were obtained (Figure 4.7). Still, the PHB content of the harvested biomass ranks among the higher values reported for non-axenic PHB production (Jiang et al., 2012; Serafim et al., 2008).

All in all, it does not seem feasible to produce much more than this 70 wt.% PHA when omitting the accumulation step. The PHB content of the harvested biomass was increased up to 75 wt.% by further increasing the volume exchange ratio, but this reduced the operational stability (Figure 4.4). Moreover, fermented organic waste streams – containing also compounds that are less suitable for PHA production – will ultimately be used as substrate. This will lead to the co-enrichment of non-PHA-storing bacteria and thereby to a reduction of the culture's PHA content (Jiang et al., 2012; Tamis et al., 2014a).

Depending on the intended application and required product purity, recovery of the PHA may still be economically feasible (Koller et al., 2013). However, besides the lower PHA content, combining the enrichment and accumulation step in a single reactor also showed other drawbacks: the storage rate, yield, and capacity of the enrichment culture were severely compromised (Table 4.2) and the existing imbalance in the oxygen transfer required during the feast and the famine phase – becoming apparent from the typical dissolved oxygen profile for feast-famine systems (Jiang et al., 2011c) – was enlarged. As biomass is withdrawn from the reactor after the feast phase, the reactor contains least biomass during the period with the lowest biomass-specific oxygen uptake: the famine phase. To guarantee an efficient and robust PHA production process and the enrichment of a culture with a high productivity, the initial SBR setup with 12 h cycles and 1 d SRT (Johnson et al., 2009a) seems more optimal. To save on the equipment cost, the feast and accumulation step could be combined in a single reactor, while the growth on stored PHA is facilitated in a separate famine reactor.

NOMENCLATURE

k	rate constant for PHB degradation	[Cmol$^{1/3}$·Cmol$^{-1/3}$·h^{-1}]
μ_{max}	maximum biomass-specific growth rate	[Cmol·Cmol^{-1}·h^{-1}]
m_{ATP}	biomass-specific ATP requirement for maintenance	[mol·Cmol^{-1}·h^{-1}]
$q_{Ac,max}$	maximum biomass-specific substrate uptake rate	[Cmol·Cmol^{-1}·h^{-1}]
$Y_{i,j}$	modeled actual yield of compound i on j	[Cmol·Cmol^{-1}]

5

MODELING THE COMPETITION IN FEAST-FAMINE SYSTEMS

Although the enrichment of specialized microbial cultures for the production of PHA is generally performed in sequencing batch reactors (SBRs), the required feast-famine conditions can also be established using two or more continuous stirred-tank reactors (CSTRs) in series with partial biomass recirculation. The use of CSTRs offers several advantages, but will result in distributed residence times and a less strict separation between feast and famine conditions. The aim of this study was to investigate the impact of the reactor configuration, and various process and biomass-specific parameters, on the enrichment of PHA-producing bacteria. A set of mathematical models was developed to predict the growth of Plasticicumulans acidivorans *– as a model PHA producer – in competition with a non-storing heterotroph. A macroscopic model considering lumped biomass, and an agent-based model considering individual cells were created to study the effect of residence time distribution and the resulting distributed bacterial states. The simulations showed that in the 2-stage CSTR system the selective pressure for PHA-producing bacteria is significantly lower than in the SBR, and strongly affected by the chosen feast-famine ratio. This is the result of substrate competition based on both the maximum specific substrate uptake rate and substrate affinity. Although the macroscopic model overestimates the selective pressure in the 2-stage CSTR system, it provides a quick and fairly good impression of the reactor performance and the impact of process and biomass-specific parameters.*

Published as: L. Marang, M.C.M. van Loosdrecht, and R. Kleerebezem. 2015. Modeling the competition between PHA-producing and non-PHA-producing bacteria in feast-famine SBR and staged CSTR systems. Biotechnology and Bioengineering 112 (12), 2475-2484.

5.1. INTRODUCTION

Polyhydroxyalkanoates (PHAs) are microbial storage polymers accumulated by many different groups of bacteria as an intracellular carbon and energy reserve (Steinbüchel, 1991). The chemical properties of the polymer make it an interesting bioplastic that is fully biodegradable (Chen, 2009). Besides the use as a bioplastic, the PHA monomers could serve as chiral building blocks for the production of various biochemicals, and the hydroxy fatty acid methyl esters could be used as a biofuel (Chen, 2009). To reduce the production cost – and allow broad application – various researchers investigated the use of open, microbial communities for the production of PHA from organic waste streams (Albuquerque et al., 2010b; Bengtsson et al., 2008b; Coats et al., 2007; Dionisi et al., 2005a; Jiang et al., 2012). By applying feast-famine conditions the communities can be enriched in PHA-producing bacteria (Reis et al., 2003). Using a single fatty acid as substrate, Johnson et al. (2009a) and Jiang et al. (2011c) thus enriched microbial cultures with a superior storage capacity of up to 90 wt.% PHA. If more complex substrate mixtures are used, such as fermented molasses or paper mill wastewater, maximum PHA contents range from 70 to 80 wt.% (Albuquerque et al., 2010b; Jiang et al., 2012).

In the past year, results of the first pilot studies on PHA production by microbial enrichment cultures have been published (Anterrieu et al., 2014; Morgan-Sagastume et al., 2014; Tamis et al., 2014a). These pilot facilities were directly based on the systems used in the lab, and all comprised a sequencing batch reactor (SBR) of a few hundred liters for the enrichment of PHA-producing bacteria. Although the SBR is a very convenient system at small scale, the discontinuous nature of the SBR – the periodic feed and discharge – requires relatively large buffer volumes and pumping capacity. Moreover, the large difference between the oxygen transfer rate required during the feast phase and the famine phase of the SBR cycle – becoming apparent from the typical dissolved oxygen profile for feast-famine systems (Jiang et al., 2011c) – leads to intrinsic scale-up problems with respect to aeration. The high oxygen requirements during the feast phase determine the reactor design, while during the significantly longer famine phase the requirements are much lower.

Alternatively, feast-famine conditions can be established using two or more continuous stirred-tank reactors (CSTRs) in series, with a partial biomass recycle (Reis et al., 2003). Such a staged CSTR system has a continuous in- and effluent stream, and a feast and famine phase separated in space instead of time. The physical separation facilitates the inclusion of a solid-liquid separation step between the feast and famine reactor, allowing the independent design of the feast and famine reactor(s) and the selective removal of substrates unsuitable for PHA production (Marang et al., 2014). However, in a 2-stage CSTR system with excess substrate availability in the first reactor (i.e., feast conditions), the subsequent, second reactor will have a small, continuous inflow of substrate. This will result in substrate-limited conditions, but not in the absence of external

substrate. And, while the SBR is an ideal plug flow reactor, a staged CSTR system introduces distributed residence times and consequently distributed bacterial states (Gujer, 2002; Schuler, 2006). Both factors may affect the selective pressure for PHA-producing bacteria. Experimental research on the use of staged CSTR systems for PHA production is limited to that of Bengtsson et al. (2008b) and Albuquerque et al. (2010a). Although the latter reported the feast-famine ratio and residual carbon concentration in the feast reactor as essential factors for the effective enrichment of PHA-producing bacteria, an in-depth discussion on the differences between the SBR and staged CSTR system, and the impact on the process performance is lacking.

The aim of this study was to investigate the impact of the reactor configuration, and various process (e.g., feast-famine ratio) and biomass-specific parameters (e.g., substrate uptake rate and affinity), on the enrichment of PHA-producing bacteria. To that end, a mathematical model simulating the growth of *Plasticicumulans acidivorans* – as a model PHA producer – in competition with a non-storing heterotroph has been developed for both SBR and staged CSTR systems. Besides a macroscopic model considering lumped biomass, an agent-based model considering individual (groups of) cells was created to study the effect of residence time distribution, and the resulting distribution in intracellular PHA content.

5.2. MODEL DESCRIPTION

5.2.1. METABOLIC MODEL

The metabolic reactions considered in this study (Table 5.1) were adapted from the model published by Johnson et al. (2009b). The six reactions involved are as follows: (1) acetate uptake and activation to acetyl-CoA, (2) catabolism, (3) polyhydroxybutyrate (PHB) production, (4) biomass synthesis, (5) PHB degradation, and (6) oxidative phosphorylation. Balances of the conserved moieties (ATP, NADH, acetyl-CoA) in these reactions were used to derive the maximum stoichiometric yields (Table 5.2). To simplify the model, acetate was considered to be the sole substrate and the efficiency of the oxidative phosphorylation (δ) was assumed to be 2.0 mol ATP/mol NADH for all microbial species in the model.

To model the kinetics of growth and PHB production in a 2-stage CSTR system, a new set of kinetic equations was required (Table 5.3, Eq. 5.1–5.8). SBR systems have a distinct feast phase – with presence of excess substrate – and famine phase – with absence of external substrate. The period of limiting substrate availability is negligible, and the simultaneous uptake of external substrate and degradation of PHB is, therefore, not considered in existing models (Dias et al., 2005; Johnson et al., 2009b). In a 2-stage CSTR system with excess substrate availability in the first or "feast" reactor, the second or "famine" reactor will have a small, continuous inflow of substrate. Under the resulting substrate-limited conditions, bacteria are likely to grow on their stored PHB and com-

Table 5.1: Reactions considered in the metabolic model on a carbon-mole base (adapted from Johnson et al., 2009b). The efficiency of the oxidative phosphorylation (δ) was assumed to be 2.0 mol ATP/mol NADH for both species in the model.

	Reaction	**Stoichiometry**
1.	Acetate uptake, activation	1 HAc + 1 ATP → 1 AcCoA
2.	Catabolism	1 AcCoA → 1 CO_2 + 2 NADH
3.	PHB production	1 AcCoA + 0.25 NADH → 1 PHB
4.	Anabolism	1.267 AcCoA + 0.2 NH_3 + 2.16 ATP → 1 $CH_{1.8}O_{0.5}N_{0.2}$ + 0.267 CO_2 + 0.434 NADH
5.	PHB consumption	1 PHB + 0.25 ATP → 1 AcCoA + 0.25 NADH
6.	Oxid. phosphorylation	1 NADH + 0.5 O_2 → δ ATP

pete for the remaining external substrate. Rather than using a conditional statement to switch between two different sets of kinetic equations, as used by Dias et al. (2005) and Johnson et al. (2009b), the here proposed kinetic model (Table 5.3) consists of a single set of kinetic equations and uses a Monod-like switch function ($c_i/(c_i+K_i)$) for the gradual transition between the use of external (acetate) and internal substrate (PHB). The acetate uptake rate (Eq. 5.1) and PHB degradation rate (Eq. 5.7) are considered to be rate determining, while the PHB production rate (Eq. 5.6) follows from the amount of acetate not used for growth (Eq. 5.2) or maintenance (Eq. 5.4). To prevent the over-accumulation of PHB, a PHB inhibition term is incorporated in the definition of the substrate uptake rate. To limit the impact of this term at moderate PHB contents, the exponent of the PHB inhibition term (α) is set to 3.0 (Table 5.2). This value is based on previous accumulation experiments with *P. acidivorans* (Jiang et al., 2011c; Marang et al., 2013), indicating that the substrate uptake and accumulation of PHB is linear up to PHB contents of at least 70 wt.%.

When neither external nor internal substrate is available, the assumed, constant maintenance requirement (m_{ATP}) will give rise to biomass decay: a negative growth rate and ammonium release. For the non-PHB-producing bacteria, biomass decay – an inversion of the growth reaction (Table 5.1) – is explicitly defined (m_X, Eq. 5.12). For bacteria that do produce PHB, biomass decay is defined implicitly: as a result of ceasing PHB degradation (Eq. 5.7) and continued maintenance requirements (Eq. 5.5), the growth (Eq. 5.3) and ammonium uptake rate (Eq. 5.8) will become negative. In the proposed model, biomass decay will also occur when in absence of external substrate the ammonium availability becomes limited (despite possible presence of PHB). This situation is unlikely to occur when modeling a feast-famine reactor system for the enrichment of PHB-accumulating bacteria.

Table 5.2: Overview of the model input: process values and biomass-specific parameters.

Parameter	Description	Value	
Process parameters			
HRT	hydraulic retention time	24	h
	recycle/volume exchange ratio	0.5	-
f:f ratio	feast-famine ratio (for 2-stage CSTR only)	0.065	$h \cdot h^{-1}$
OLR	organic loading rate	2.25	$Cmmol \cdot L^{-1} \cdot h^{-1}$
C:N ratio	carbon-to-nitrogen ratio	8	$Cmol \cdot mol^{-1}$
V	working volume (largest) reactor	2	L
Stoichiometric yields [a]			
$Y_{PHB,Ac}$	PHB yield on acetate	0.67	$Cmol \cdot Cmol^{-1}$
$Y_{X,Ac}$	biomass yield on acetate	0.47	$Cmol \cdot Cmol^{-1}$
$Y_{X,PHB}$	biomass yield on PHB	0.67	$Cmol \cdot Cmol^{-1}$
$Y_{N,X}$	yield of ammonium on biomass	0.20	$mol \cdot Cmol^{-1}$
$Y_{ATP,Ac}$	yield of ATP on acetate	3.00	$mol \cdot Cmol^{-1}$
$Y_{ATP,PHB}$	yield of ATP on PHB	4.25	$mol \cdot Cmol^{-1}$
Kinetic parameters *P. acidivorans* [b]			
$q_{Ac,max}$	maximum biomass-specific acetate uptake rate	3.5	$Cmol \cdot Cmol^{-1} \cdot h^{-1}$
μ^{max}	maximum biomass-specific growth rate	0.1	$Cmol \cdot Cmol^{-1} \cdot h^{-1}$
m_{ATP}	biomass-specific ATP requirement maintenance	0.001	$mol \cdot Cmol^{-1} \cdot h^{-1}$
$f_{PHB,max}$	maximum fraction of PHB on active biomass	8.5	$Cmol \cdot Cmol^{-1}$
α	exponent of the PHB inhibition term	3.0	-
k	rate constant for PHB degradation	0.16	$Cmol^{1/3} \cdot Cmol^{-1/3} \cdot h^{-1}$
K_{Ac}	half-saturation constant for acetate	0.3	$Cmmol \cdot L^{-1}$
K_N	half-saturation constant for ammonium	0.001	$mmol \cdot L^{-1}$
Kinetic parameters non-PHB-storing heterotroph			
μ_{max}	maximum biomass-specific growth rate [c]	0.47	$Cmol \cdot Cmol^{-1} \cdot h^{-1}$
m_{ATP}	biomass-specific ATP requirement maintenance	0.001	$mol \cdot Cmol^{-1} \cdot h^{-1}$
K_{Ac}	half-saturation constant for acetate	0.1	$Cmmol \cdot L^{-1}$
K_N	half-saturation constant for ammonium	0.001	$mmol \cdot L^{-1}$

[a] derived from the metabolic reactions (Table 5.1) and balances of the conserved moieties

[b] based on experimental data reported by Johnson et al. (2009a) and Jiang et al. (2011c)

[c] based on kinetic data for *Acinetobacter* spp. (Hao and Chang, 1987)

Table 5.3: Kinetic model for *P. acidivorans* (Eq. 5.1–5.8) and the non-storing heterotroph (Eq. 5.9–5.13). In absence of (internal and external) substrate, the ATP required for maintenance is supplied by biomass decay. For *P. acidivorans* this is implicitly defined in Eq. 5.3.

Process	**Biomass-specific rate equation**	
P. acidivorans		
Acetate uptake	$q_{Ac} = q_{Ac}^{max} \cdot \frac{c_{Ac}}{K_{Ac} + c_{Ac}} \cdot \left(1 - \left(\frac{f_{PHB}}{f_{PHB}^{max}}\right)^{\alpha}\right)$	(5.1)
Growth on acetate	$\mu_{Ac} = \mu_{Ac}^{max} \cdot \frac{c_{Ac}}{K_{Ac} + c_{Ac}} \cdot \frac{c_N}{K_N + c_N}$	(5.2)
Growth on PHB	$\mu_{PHB} = \left(-q_{PHB}^{degra} - m_{PHB}\right) \cdot Y_{X,PHB}$	(5.3)
Maintenance on acetate	$m_{Ac} = \frac{m_{ATP}}{Y_{ATP,Ac}} \cdot \frac{c_{Ac}}{K_{Ac} + c_{Ac}}$	(5.4)
Maintenance on PHB	$m_{PHB} = \frac{m_{ATP}}{Y_{ATP,PHB}} \cdot \left(1 - \frac{c_{Ac}}{K_{Ac} + c_{Ac}}\right)$	(5.5)
PHB production	$q_{PHB}^{prod} = \left(q_{Ac} - \frac{\mu_{Ac}}{Y_{X,Ac}} - m_{Ac}\right) \cdot Y_{PHB,Ac}$	(5.6)
PHB degradation	$q_{PHB}^{degra} = k \cdot \left(f_{PHB}\right)^{2/3} \cdot \frac{c_N}{K_N + c_N} \cdot \left(1 - \frac{c_{Ac}}{K_{Ac} + c_{Ac}}\right)$	(5.7)
Ammonium uptake	$q_N = \left(\mu_{Ac} + \mu_{PHB}\right) \cdot Y_{N,X}$	(5.8)
Non-PHB-storing heterotroph		
Acetate uptake	$q_{Ac} = \frac{\mu_{Ac}}{Y_{X,Ac}} + m_{Ac}$	(5.9)
Growth on acetate	$\mu_{Ac} = \mu_{Ac}^{max} \cdot \frac{c_{Ac}}{K_{Ac} + c_{Ac}} \cdot \frac{c_N}{K_N + c_N}$	(5.10)
Maintenance on acetate	$m_{Ac} = \frac{m_{ATP}}{Y_{ATP,Ac}} \cdot \frac{c_{Ac}}{K_{Ac} + c_{Ac}}$	(5.11)
Biomass decay	$m_X = \frac{m_{ATP}}{Y_{ATP,Ac}} \cdot Y_{X,Ac} \cdot \left(1 - \frac{c_{Ac}}{K_{Ac} + c_{Ac}}\right)$	(5.12)
Ammonium uptake	$q_N = \left(\mu_{Ac} - m_X\right) \cdot Y_{N,X}$	(5.13)

5.2.2. MICROBIAL SPECIES

The model considers the competition between two types of bacteria: a PHB producer and a non-storing heterotroph. *Plasticicumulans acidivorans* was used as model PHB producer. This bacterium accumulates large amounts of PHB and has previously been enriched in multiple SBR systems fed with acetate or wastewater and operated under feast-famine conditions (Jiang et al., 2011c; Johnson et al., 2009a; Marang et al., 2013; Tamis et al., 2014a). Most of the required kinetic parameters have been reported in these studies: the maximum specific acetate uptake rate ($q_{Ac,max}$, 3.5 Cmol·Cmol^{-1}·h^{-1}), the maximum specific growth rate on external substrate (μ_{max}, 0.1 Cmol·Cmol^{-1}·h^{-1}), the maximum fraction of PHB ($f_{PHB,max}$, 8.5 Cmol·Cmol^{-1}), and the rate constant for PHB degradation (k, 0.16 Cmol$^{1/3}$·Cmol$^{-1/3}$·h^{-1}). The specific ATP requirement for maintenance (m_{ATP}) was generally found to be low and assumed to be 0.001 mol·Cmol^{-1}·h^{-1} in this study. The half-saturation constants for acetate (K_{Ac}) and ammonium (K_N) have not been determined previously. Since they play a minimal role in SBR systems, hypothetical values – chosen to avoid numerical problems and acting merely as switch function – have been used before (Johnson et al., 2009b). For ammonium, which should be present in excess throughout the operation of the reactor, this approach can be maintained and the half-saturation constant (K_N) was set to 0.001 mmol·L^{-1}. In an attempt to measure the half-saturation constant for acetate (K_{Ac}), an enrichment culture predominated by *P. acidivorans* was fed with acetate at half its maximum acetate uptake rate (data not shown). The residual acetate concentration in the reactor was found to be below the detection limit of the HPLC (<0.5 Cmmol·L^{-1}), and the half-saturation constant K_{Ac} was, therefore, assumed to be 0.3 Cmmol·L^{-1}. Table 5.2 gives an overview of all values used for the kinetic description of *P. acidivorans*.

The second organism is a hypothetical, non-storing heterotroph. Although PHB storage is a common bacterial trait (Steinbüchel, 1991), the accumulation of PHB by this organism was assumed to be negligible. This reduces the kinetic model to Eq. 5.9–5.13 (Table 5.3). The specific substrate uptake rate (Eq. 5.9) was defined as the sum of the acetate required for growth (Eq. 5.10) and maintenance (Eq. 5.11). In absence of external substrate, the ATP required for maintenance is supplied by biomass decay (Eq. 5.12). The kinetic parameters of the non-storing heterotroph were partially based on literature data for the genus *Acinetobacter*. Bacteria of this genus are common, fast-growing organisms in soil, water and activated sludge systems (Towner, 2006; Wagner et al., 1994). Supported by experimental data on the growth of *Acinetobacter* spp. at 30°C (Hao and Chang, 1987), the maximum specific growth rate (μ_{max}) was set to 0.47 Cmol·Cmol^{-1}·h^{-1}. The ATP requirement for maintenance (m_{ATP}) was assumed to be the same as for *P. acidivorans* (Table 5.2). The same holds for the half-saturation constant for ammonium (K_N), which acts merely as switch function. The non-storer's half-saturation constant for acetate (K_{Ac}) was assumed to be slightly lower than that of *P. acidivorans*, and set to 0.1

Cmmol·L^{-1}. This value is similar to that used in, for example, ASM3 (Gujer et al., 1999).

5.2.3. MACROSCOPIC MODEL SBR

Matlab™ (Mathworks, USA) was used to simulate the competition between PHB-producing and non-PHB-producing bacteria. The frequently studied setup of Johnson et al. (2009a) served as reference scenario: a fully aerobic SBR with a working volume of 2 L, operated at a hydraulic retention time (HRT) of 1 day and feast-famine cycles of 12 h, that is, at a volume exchange ratio of 0.5. There is no biomass retention. The temperature in the reactor is controlled at 30°C and the pH at 7.0. The organic loading rate (OLR) is 2.25 Cmmol·L^{-1}·h^{-1} and the carbon to nitrogen ratio (C:N ratio) in the feed 8 Cmol·mol^{-1}. The feeding of fresh medium and removal of broth are both modeled to occur instantaneously.

At the start of a simulation, the microbial community is composed of a 50/50 mixture of the two bacterial species: *P. acidivorans* (with an intracellular PHB content of 1 Cmol·Cmol^{-1}) and the other, non-storing heterotroph. The development of the reactor is simulated over a period of 480 h (40 cycles), tracking the amount of acetate (Ac), ammonium (N), PHB-accumulating biomass ($X_{P.a.}$), non-storing biomass (X_{Other}) and PHB (PHB) in the reactor over time. To do so, a mass balance is set up for each of these compounds. Since, outside the feeding and effluent phase, an SBR is simply a batch reactor, the mass balances contain no transport terms but only the microbial conversions (Table 5.3). The macroscopic model uses a lumped biomass concentration, assuming that all bacteria within one species have the same composition. The built-in function *ode45* was used to solve the differential equations. The general structure of the macroscopic model for the SBR system is as follows:

I. Define process and biomass-specific parameters (Table 5.2)

II. Set initial conditions

- No substrate (Ac) or ammonium (N) present.
- 5 Cmmol $X_{P.a.}$, 5 Cmmol X_{Other}, and 5 Cmmol PHB.

III. Run simulation

- For 40 cycles:
  - Feed substrate and ammonium: 54 Cmmol Ac and 6.75 mmol N.
  - Solve mass balances (Eq. 5.14–5.18) over a period of 12 h.

$$dAc/dt = -X_{P.a.} \cdot q_{Ac,P.a.} - X_{Other} \cdot q_{Ac,Other} \tag{5.14}$$

$$dX_{P.a.}/dt = X_{P.a.} \cdot \left(\mu_{Ac,P.a.} + \mu_{PHB,P.a.}\right) \tag{5.15}$$

$$dX_{Other}/dt = X_{Other} \cdot \left(\mu_{Ac,Other} - m_{X,Other}\right) \tag{5.16}$$

$$dPHB/dt = X_{P.a.} \cdot \left(q^{prod}_{PHB,P.a.} - q^{degra}_{PHB,P.a.}\right) \tag{5.17}$$

$$dN/dt = -Y_{N,X} \cdot (dX_{P.a.}/dt + dX_{Other}/dt) \tag{5.18}$$

– Broth removal: half the amount of each compound in the reactor.

IV. Create output

- Total amounts of Ac, N, $X_{P.a.}$, X_{Other}, and PHB in the reactor over time.

5.2.4. MACROSCOPIC MODEL STAGED CSTR SYSTEM

The macroscopic model for a 2-stage CSTR system is largely similar to that for the SBR. The first important difference is the fact that the CSTR setup consists of two reactors instead of one. Hence, the ratio between the residence time in the first and the second reactor (feast-famine ratio) is added as process parameter (Table 5.2). In combination with a fixed working volume (2 L) of the largest, that is, famine reactor, the working volume of the feast reactor and the influent, effluent and recycle flow rates (i.e., to and from the famine reactor) can be calculated. The amount of acetate, ammonium, PHB-accumulating biomass ($X_{P.a.}$), non-storing biomass (X_{Other}) and PHB is recorded for both reactors (1 and 2) individually. The size and composition of the initial microbial community is the same as for the SBR but distributed over the two reactors: at the start of a simulation 5% of the community resides in reactor 1. Where it was assumed that in the SBR no substrate or ammonium was present at the start of a simulation, it was assumed that in the 2-stage CSTR initially 5 Cmmol acetate is present in reactor 1, and 5 mmol ammonium is present in reactor 2.

The second difference is that the process is fully continuous instead of a series of batches. This means that the mass balances can be numerically solved over the full simulation period (480 h), without discontinuities like the feeding of substrate and removal of broth in an SBR. As a result of the two differences, the mass balances (Eq. 5.14–5.18) are doubled (one set for each reactor) and extended with transport terms ($Q_{\text{in}} \cdot c_{\text{i,in}} - Q_{\text{out}} \cdot c_{\text{i,out}}$).

5.2.5. AGENT-BASED MODEL STAGED CSTR SYSTEM

To be able to take the residence time distribution and the resulting distribution in intracellular PHB content into account, the biomass has to be modeled as individual (groups of) cells. Each individual is described by four variables: location (reactor 1 or 2), time to leave the current reactor (h), amount of active biomass (Cmmol), and amount of stored PHB (Cmmol). Other than the consideration of individual cells, the macroscopic and agent-based model are kept similar: the process and biomass-specific parameters, kinetic equations, initial conditions, and mass balances are identical. Different is the way the mass balances are solved: like in the model of Johnson et al. (2009b), a simple first-order method with a fixed step size (0.005 h) is used to obtain the amounts of acetate, ammonium, PHB-accumulating biomass, non-storing biomass and PHB in the reactor over time. The full program code is found in Appendix A. The general structure of the agent-based model is given below.

I. Define process and biomass-specific parameters (Table 5.2)
   - Calculate reactor volumes.
   - Calculate influent, effluent, and recycle flow rates.

II. Set initial conditions
   - Create 5,000 individuals of *P. acidivorans*: all consist of 0.001 Cmmol biomass and 0.001 Cmmol PHB, 5% is located in reactor 1 and 95% in reactor 2. For each individual, the time spent in the current reactor is randomly assigned from an exponential distribution with the average residence time of the reactor as mean.
   - Similarly, create 5,000 individuals of the non-storing heterotroph (no PHB).
   - Total amounts reactor 1: 5 Cmmol Ac, 0 mmol N, 0.25 Cmmol $X_{P.a.}$, 0.25 Cmmol X_{Other}, and 0.25 Cmmol PHB.
   - Total amounts reactor 2: 0 Cmmol Ac, 5 mmol N, 4.75 Cmmol $X_{P.a.}$, 4.75 Cmmol X_{Other}, and 4.75 Cmmol PHB.

III. Run simulation
   - For t = 0 until 480 h (in steps of 0.005 h):
     - For each individual:
       - ◇ Run kinetic conversions, update properties of the individual, and determine impact on the overall amounts of Ac, N, $X_{P.a.}$, X_{Other}, and PHB.
       - ◇ If it is time to leave the reactor:

- Split individual in equal parts of ≥0.001 Cmmol biomass (if large enough).
- Randomly discard 50% of the individuals leaving reactor 1.
- Move individual(s) to the other reactor and assign a new "time to leave".
- Determine impact on the overall amounts of $X_{P.a.}$, X_{Other}, and PHB.

– Update overall amount of Ac, N, $X_{P.a}$, X_{Other}, and PHB in both reactors at t.

IV. Create output

- Total amounts of Ac, N, $X_{P.a.}$, X_{Other}, and PHB in the reactors over time.
- Final composition microbial community (properties of each individual at t = 480 h).

5.3. RESULTS

5.3.1. COMPETITION IN THE SBR AND 2-STAGE CSTR SYSTEM

Simulation of the growth of *P. acidivorans* in competition with a non-storing heterotroph confirms the strong selective pressure for PHB-producing bacteria in the feast-famine SBR system. Starting from a 50/50 mixture of PHB-producing and non-PHB-producing bacteria, the predicted fraction of *P. acidivorans* in the total biomass rapidly increases to 1.0 Cmol·Cmol^{-1} (Figure 5.1). Since the introduction of new bacteria is not included in the model, all non-storing bacteria will eventually be washed out. The feast-famine conditions are reflected in the seesaw pattern of the fraction *P. acidivorans* in the reactor. During the feast phases, *P. acidivorans* is outgrown by its competitor and the fraction in the total biomass decreases. During the famine phases, only *P. acidivorans* can grow, using its stored PHB as substrate, and the fraction in the total biomass increases again.

Also in the 2-stage CSTR system *P. acidivorans* is predicted to win the competition with the non-storing heterotroph and dominate the reactor, but it takes much longer to reach this (Figure 5.1). To be able to compare different reactor configurations, the predicted time (h) for *P. acidivorans* to reach 95% of the total active biomass is used as a measure for the selective pressure. If the setup consists of multiple reactors, as in the staged CSTR system, the fraction of *P. acidivorans* in the last reactor is used. In the SBR, *P. acidivorans* is predicted to reach 95% of the total biomass in 78 h. In the 2-stage CSTR system, the macroscopic model predicts that *P. acidivorans* requires twice this time: 164 h. This suggests that the selective pressure for PHB-producing bacteria is significantly reduced.

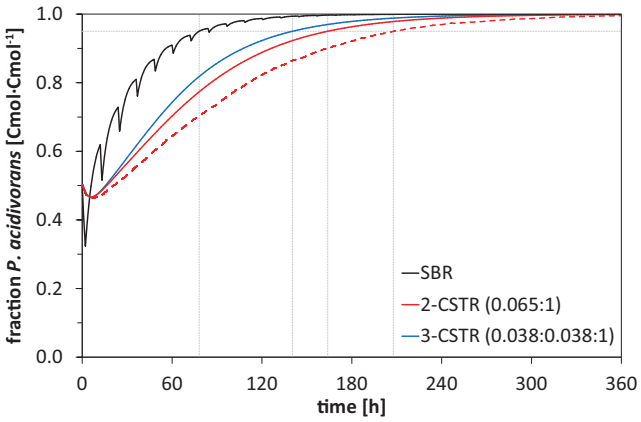

Figure 5.1: Fraction of *P. acidivorans* in the overall biomass (Cmol·Cmol^{-1}) over time, as modeled for the SBR (black), 2-stage CSTR (red, feast-famine ratio 0.065 h·h^{-1}), and 3-stage CSTR system (blue, feast-famine ratio 0.075 h·h^{-1}). The solid lines represent data obtained by the macroscopic model, the dashed line data obtained by the agent-based model. The time (h) needed for *P. acidivorans* to reach 95% of the total biomass was used as a measure for the selective pressure.

5

5.3.2. IMPACT OF THE FEAST-FAMINE RATIO

The selective pressure for PHB-producing bacteria in the 2-stage CSTR system is strongly dependent on the chosen feast-famine ratio, that is, the ratio between the residence time of the feast reactor and the famine reactor (Figure 5.2). Figure 5.1 shows the development of *P. acidivorans* in a 2-stage CSTR system operated at its optimal feast-famine ratio: 0.065 h·h^{-1}. This value is similar to the feast-famine ratio predicted and observed for the SBR system (Jiang et al., 2011c; Johnson et al., 2009a). If the average residence time of the feast reactor is shorter, not all acetate will be consumed (Figure 5.2). The residual acetate will end up in the famine reactor and allow growth on external substrate throughout the process. If the residence time is longer, the leaching of acetate to the famine reactor is prevented but the acetate concentration in the feast reactor becomes limiting (Figure 5.2). As a result, the competition for substrate is no longer primarily based on the maximum specific substrate uptake rate ($q_{Ac,max}$) of the bacteria but also, increasingly, on the substrate affinity (K_{Ac}).

Based on experimental results also Albuquerque et al. (2010a) reported the feast-famine ratio as an important factor for the effective enrichment of PHA-producing bacteria. In that study, the 2-stage CSTR system was operated at a feast-famine ratio of 0.22 h·h^{-1}. Although higher than the optimal feast-famine ratio found in this study, the applied feast-famine ratio was again similar to that of the comparable SBR system (Albuquerque et al., 2010b). Operation at a higher feast-famine ratio (0.50 h·h^{-1}) resulted in carbon-limited conditions in the feast reactor and did not effectively enrich PHA-producing bacteria.

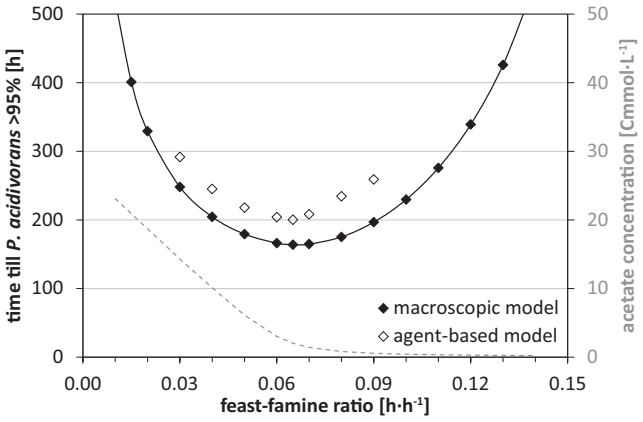

Figure 5.2: Impact of the feast-famine ratio ($h \cdot h^{-1}$) on the selective pressure for *P. acidivorans* in a 2-stage CSTR system. The black, filled and open diamonds represent the time (h) needed for *P. acidivorans* to reach 95% of the total biomass, as predicted by the macroscopic and agent-based model, respectively. The corresponding residual acetate concentration in the feast reactor ($Cmmol \cdot L^{-1}$) is plotted as a grey dashed line.

A third reactor could be added to ensure excess substrate conditions in the feast reactor and, at the same time, prevent leaching of substrate to the famine reactor. For a 3-stage CSTR system where the feast reactor is split in two equal, smaller reactors, the optimal feast-famine ratio is 0.075 $h \cdot h^{-1}$ – that is, a residence time ratio of 0.038:0.038:1. Compared to the 2-stage CSTR system, such a 3-stage system improves the selective pressure for PHB-producing bacteria by 14%. The macroscopic model predicts that the time *P. acidivorans* needs to reach 95% of the overall biomass is reduced from 164 to 140 h (Figure 5.1).

5.3.3. IMPACT OF THE RESIDENCE TIME DISTRIBUTION

So far, the results were obtained from simulations with macroscopic models, assuming that all bacteria within one species are identical. However, in an ideal CSTR the residence times of individual cells are exponentially distributed (Danckwerts, 1953). For a famine reactor with an average residence time of 11.3 h this means that 11% of the bacteria resides in the famine reactor for more than the average residence time of the overall system (24 h). If the residence time distribution and the resulting distribution of intracellular PHB contents are taken into account, it is predicted that *P. acidivorans* needs 204 h to reach 95% of the total biomass: the selective pressure for PHB-producing bacteria in a 2-stage CSTR system is further reduced than predicted by the macroscopic model (Figure 5.1). The overestimation of the competitive advantage of PHB-producing bacteria by the macroscopic model is due to an overestimation of the growth on stored PHB in the famine reactor. Figure 5.3 shows the development of the culture as predicted by the macroscopic and the agent-based model. The agent-based model predicts a lower

concentration of *P. acidivorans* biomass and higher concentration of PHB for the famine reactor. The cause of this becomes apparent from Figure 5.4, showing the distribution of the intracellular PHB content of *P. acidivorans* in the feast and famine reactor. The cells in the feast reactor contain a wide range of intracellular PHB contents, but only a minor fraction contains extremely low or high amounts of PHB. In the famine reactor, a major fraction of the *P. acidivorans* cells (46%) contains virtually no PHB and will, therefore, not contribute to the overall PHB degradation rate. This reduces the overall growth rate in the famine reactor.

5.3.4. PARAMETER SENSITIVITY ANALYSIS

To evaluate the impact of assumptions and uncertainties in the input values on the model outcome, a parameter sensitivity analysis was performed for all three models (Figure 5.5). The original value of each of the kinetic parameters in Table 5.2 was increased and decreased by 20% to determine the impact on the selective pressure. As to be expected for feast-famine systems, the maximum specific substrate uptake rates of *P. acidivorans* ($q_{Ac,max}$) and the non-storing heterotroph (directly related to its μ_{max}) are the most important parameters in both the SBR and the 2-stage CSTR system. In the latter a reduction in the ratio between the maximum acetate uptake rate of *P. acidivorans* and that of the non-storing heterotroph has a disastrous impact on the time needed for *P. acidivorans* to reach 95% of the total biomass (Figure 5.5). This suggests that the modeled 2-stage CSTR system is operating close to the limit for a successful enrichment of *P. acidivorans*.

The impact of the half-saturation constants for acetate (K_{Ac}) is highly different for the two types of systems. In the SBR the impact on the model outcome is negligible, whereas in the 2-stage CSTR system a 20% change in the K_{Ac} value for either of the two species results in a similar in- or decrease of the selective pressure (10-25%). Like for the substrate uptake rate, changing one of the K_{Ac} values induces a change in the K_{Ac} ratio between *P. acidivorans* and the non-storing heterotroph. This change in the K_{Ac} ratio is the main cause of the impact shown in Figure 5.5. If the K_{Ac} values of the two species are simultaneously in- or decreased by 20% the effect on the selective pressure is less than 3% for all three models (data not shown).

A third parameter of significance is the rate constant for PHB degradation (k). In both systems a lower value for k reduces the selective pressure (Figure 5.5). Since the PHB degradation is rate-determining for the growth of *P. acidivorans*, a minimal value for k is needed to ensure the full conversion of stored PHB to biomass in the famine phase or reactor. Once above this value, cells in an SBR do not benefit from a further increase of the rate constant k, since the length of the famine period is fixed. In a 2-stage CSTR system, there is a continuous in- and outflow of PHB and an increased rate constant k – that is, an increased conversion of PHB to biomass – will reduce the outflow of PHB.

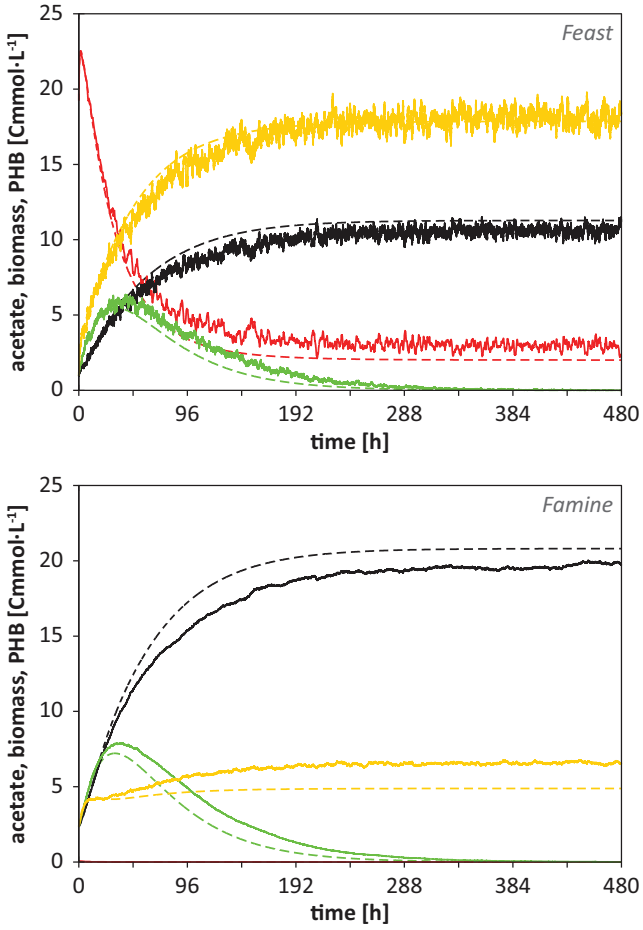

Figure 5.3: Development of the acetate, biomass, and PHB concentrations (Cmmol·L^{-1}) in the feast (top) and famine reactor (bottom) over time, as predicted by the macroscopic model (dashed lines) and agent-based model (solid lines) for a 2-stage CSTR system operated at a feast-famine ratio of 0.065 h·h^{-1}. The acetate concentration is shown in red, the biomass concentration of *P. acidivorans* in black, the non-storing biomass concentration in green, and the PHB concentration in orange.

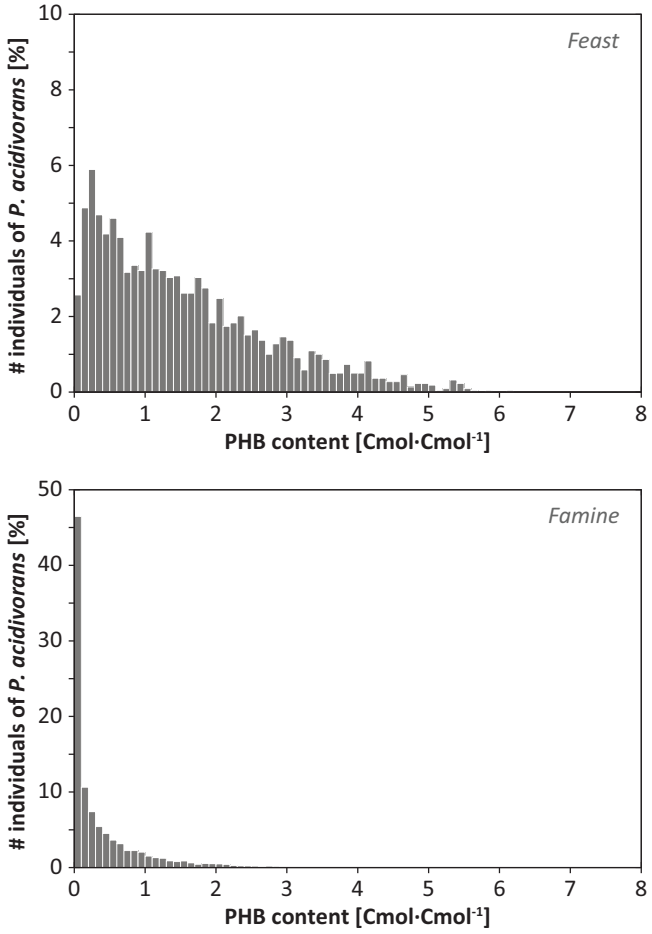

Figure 5.4: Distribution of the intracellular PHB content (Cmol·Cmol^{-1}) over the individuals of *P. acidivorans* in the feast (top) and famine reactor (bottom) of the 2-stage CSTR system in Figure 5.3, at the end of the 480 h simulation period.

Therefore, the cells do benefit from a higher PHB degradation rate (Figure 5.5).

The parameter sensitivity analyses of the macroscopic and agent-based model for the 2-stage CSTR system give a comparable outcome (Figure 5.5). The slightly elevated impacts predicted by the agent-based model are, at least partially, inherent to the model itself. The model outcome will differ for each simulation due to the random cell discharge and sampling of individual residence times from an exponential probability distribution. Ten simulations of the 2-stage CSTR system with the agent-based model yielded an average and standard deviation of 204±4 h for the time needed until *P. acidivorans* reaches 95% of the total biomass. This variation largely explains the changed impacts, as simulations for the parameter sensitivity analysis were run just once.

5.3.5. SUBSTRATE UPTAKE RATE AND SUBSTRATE AFFINITY

Motivated by the outcome of the parameter sensitivity analysis, the impact of the K_{Ac} ratio and q_{Ac} ratio between *P. acidivorans* and its competitor was studied in more detail (Figure 5.6). The filled and open symbols in Figure 5.6 show, respectively, the results obtained by varying the parameter value for *P. acidivorans* while keeping the value for the non-storing heterotroph constant, and vice versa. The impact of the absolute parameter values is thus illustrated by a divergence between the two.

In the SBR, neither the ratio between the half-saturation constant for acetate (K_{Ac}) of *P. acidivorans* and the non-storing heterotroph nor the absolute parameter value has a significant impact on the selective pressure (Figure 5.6). In the 2-stage CSTR system, both the K_{Ac} ratio and the absolute K_{Ac} values do play a role. When the substrate affinity of *P. acidivorans* is significantly lower than that of its competitor – at K_{Ac} ratios above 4 – the predictions become clearly dependent on the absolute parameter values. Higher K_{Ac} values make that a larger fraction of the total substrate will be competed for based on $q_{Ac,max}/K_{Ac}$ instead of primarily $q_{Ac,max}$. At high K_{Ac} ratios, high absolute values for K_{Ac} will thus enhance the negative impact on the selective pressure for PHB-producing bacteria.

Absolute parameter values play a minimal role in the impact of the ratio between the maximum substrate uptake rate ($q_{Ac,max}$) of *P. acidivorans* and its competitor. The competitive advantage of *P. acidivorans* over the non-storing heterotroph obviously increases with an increasing q_{Ac} ratio. At high ratios the impact on the selective pressure is, however, limited. Only when the q_{Ac} ratio approaches its lower limit, the time needed for *P. acidivorans* to reach 95% of the total biomass increases rapidly (Figure 5.6). As a result of the K_{Ac} ratio, the lower limit for the 2-stage CSTR system lies at a higher q_{Ac} ratio than for the SBR system.

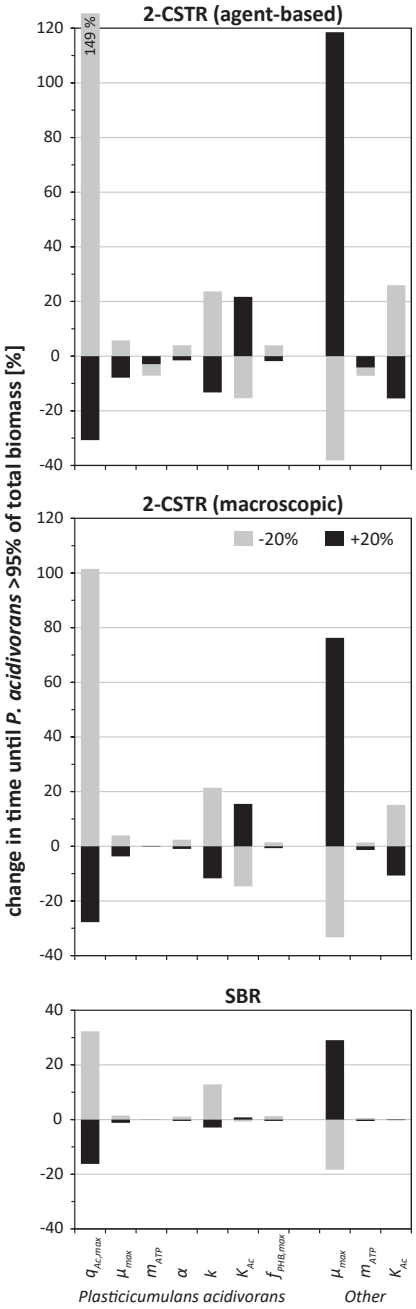

Figure 5.5: Parameter sensitivity analysis: the change in the time needed for *P. acidivorans* to reach 95% of the total biomass when the original value of one of the kinetic parameters is increased (black) or decreased (grey) by 20%, as predicted by the model for the SBR (bottom), and macroscopic (middle) and agent-based model (top) for the 2-stage CSTR.

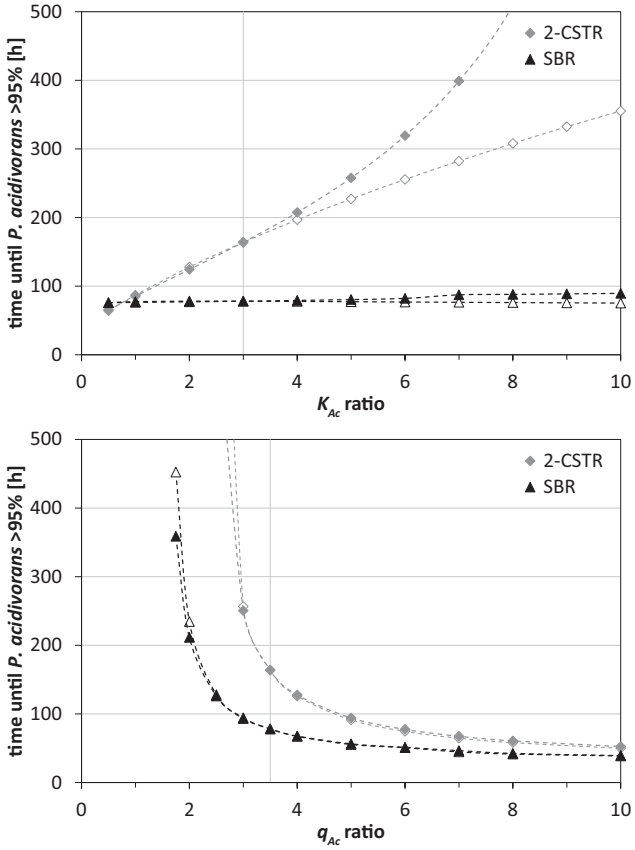

Figure 5.6: Impact of the K_{Ac} ratio (top) and q_{Ac} ratio (bottom) between *P. acidivorans* and the non-storing heterotroph on the selective pressure for PHB-producing bacteria in the SBR (black triangles) and 2-stage CSTR system (grey diamonds), as predicted by the macroscopic model. The filled and open symbols show the results obtained by varying the parameter value for *P. acidivorans*, while keeping the value for the non-storing heterotroph constant, and vice versa. Differences between the two indicate the impact of the absolute parameter values. The vertical line indicates the original K_{Ac} or q_{Ac} ratio.

5.4. DISCUSSION

5.4.1. THE COMPETITIVE ADVANTAGE OF PHB-PRODUCING BACTERIA

The timescale at which *P. acidivorans* is predicted to be enriched in the SBR system is similar to that experimentally observed. When starting the simulation with 0.1 instead of 50% *P. acidivorans*, the model predicts that *P. acidivorans* predominates the SBR system after 259 h (11 SRTs). In previous research a stable feast phase length was observed within 15 SRTs after inoculation (Jiang et al., 2011c). Detailed experimental data for the 2-stage CSTR system is currently unavailable. However, Albuquerque et al. (2010a) reported that the storage yield and maximum storage capacity decreased after transferring the enrichment culture from an SBR to a comparable 2-stage CSTR system. This supports the reduction in selective pressure predicted by the model.

The reduced competitive advantage of PHB-producing bacteria in the 2-stage CSTR system is due to the half-saturation constants for acetate (K_{Ac}). Figure 5.6 clearly illustrates that, where the microbial competition in the SBR is based solely on the maximum substrate uptake rate ($q_{Ac,max}$) of the bacteria, in a 2-stage CSTR system also the half-saturation constant K_{Ac} plays an important role. Since experimental values for the K_{Ac} of *P. acidivorans* are lacking, it forms one of the most important unknowns in the model. If the substrate affinity of *P. acidivorans* would be comparable to that of its competitor, the selective pressure in a 2-stage CSTR system will not be compromised and suffice to enrich PHB-producing bacteria. If it would be significantly lower though, the impact of K_{Ac} will have to be reduced. Increasing the number of CSTRs in series will narrow the residence time distribution and give rise to a (dispersed) plug flow. As shown in Figure 5.1 and expected from the fact that the SBR is an ideal plug flow reactor, this will reduce the impact of the half-saturation constant and strengthen the competitive advantage of PHB-producing bacteria.

The maximum specific substrate uptake rate ($q_{Ac,max}$) and half-saturation constant for acetate (K_{Ac}) of both species, *P. acidivorans* and the non-storing heterotroph, are crucial for the model outcome. Continued research should provide more information on the identity of the close competitors of *P. acidivorans*, and the missing $q_{Ac,max}$ and K_{Ac} values. In order to validate the model, the here presented modeling results can be used to design lab-scale experiments with the staged CSTR system.

5.4.2. MACROSCOPIC VERSUS AGENT-BASED MODELING

The different prediction by the macroscopic and agent-based model (Figure 5.3) is due to non-linearity in the PHB kinetics. As PHB is an intracellular compound, it is only accessible to a specific cell. In the case of non-first-order kinetics, the result obtained by adding up the behavior of individual cells will, therefore, differ from that obtained by assuming an averaged biomass composition (Gujer, 2002; Schuler, 2005). In the presented model, such non-linearity is found in the PHB inhibition term of the substrate

uptake and the $2/3^{th}$ reaction order for PHB degradation (Table 5.3, Eq. 5.1 and 5.7). If the kinetic description for PHB degradation is replaced by a first-order reaction and the PHB inhibition term eliminated, the macroscopic and agent-based model predict that *P. acidivorans* reaches 95% of the total biomass in the 2-stage CSTR system after 190 and 200 h, respectively. The small, remaining difference between the two models (5%) can be ascribed to the random sampling of cell residence times and applied integration method.

Although the macroscopic model overestimates the growth on PHB in the famine reactor, and thereby the selective pressure, the applied kinetic equations are still quite close to linear and the macroscopic model provides a good impression of the reactor performance. The parameter sensitivity analysis (Figure 5.5) showed that the macroscopic and agent-based model predict a similar impact for the various biomass-specific parameters. The same is observed for the process parameters: studying the impact of the feast-famine ratio on the selective pressure for PHB-producing bacteria resulted in different values when the macroscopic or agent-based model was used, but the shape and optimum of the curve were highly similar (Figure 5.2). Considering that the agent-based model is computationally much more demanding – where the macroscopic model runs a simulation (480 h) in 17 s, the agent-based model takes 17 h on the same computer – the added value of the agent-based model for these kind of general evaluations seems limited.

5.4.3. IMPLICATIONS FOR WASTE-BASED PHA PRODUCTION

The successful production of PHA from organic waste using microbial enrichment cultures requires a robust process and strong selective pressure for PHA-producing bacteria. The SBR system has clear advantage over the 2-stage CSTR system on both criteria. Fermented organic waste streams typically comprise volatile fatty acids but also, for example, lactic acid and ethanol (Temudo et al., 2007; Zoetemeyer et al., 1982). The use of these different compounds for the production of PHA has previously been shown to result in the enrichment of distinct microbial communities (Jiang et al., 2011c). If waste is used as substrate, the importance of an optimized feast-famine ratio in the staged CSTR system (Figure 5.2) makes that the optimal feast-famine ratio needs to be set for each of the enriched species. This requires a plug flow system. Rather than the temporal plug flow in an SBR, this could be a spatial plug flow reactor with partial biomass recirculation. Such a plug flow reactor would, just like the 2-stage CSTR system, allow a truly continuous process and the separation of periods with highly distinct oxygen requirements over different reactors.

5.5. CONCLUSION

The model predicts that both the SBR and the staged CSTR system are selective for PHA-producing bacteria, but the selective pressure in the 2-stage CSTR system is significantly lower than in the SBR. While microbial competition in the SBR is based solely on the maximum substrate uptake rate, in the staged CSTR system it is based on both the maximum substrate uptake rate and substrate affinity. For an accurate description of the staged CSTR system, individual (groups of) cells need to be considered. However, for general evaluations the macroscopic model – considering lumped biomass – is accurate enough.

NOMENCLATURE (SUBSCRIPTS)

Ac	acetate
N	ammonium
Other	non-storing hetertroph
P.a.	*Plasticicumulans acidivorans*
X	active biomass

6

ENRICHMENT OF PHA-PRODUCERS UNDER CONTINUOUS SUBSTRATE SUPPLY

To enrich polyhydroxyalkanoate (PHA) producing microbial communities, generally, a feast-famine regime is applied. Here we investigated the impact of continuous substrate feeding on the enrichment of PHA-producing bacteria in two sequencing batch reactors (SBRs). In the first reactor, the substrate (acetate) was dosed continuously and Zoogloea *sp. was enriched. The culture accumulated PHA upon exposure to excess carbon, but the PHA production rate and storage capacity (53 wt.%) were one-fifth of that observed for enrichment cultures in a standard, pulse-fed SBR dominated by the PHA producer* Plasticicumulans acidivorans. *In the second reactor, half the acetate was dosed at the beginning of the cycle and the other half continuously. Having a true feast phase, the enrichment of* P. acidivorans *was not impeded by the continuous supply of acetate and the culture accumulated 85 wt.% PHA. This shows that for the enrichment of bacteria with a superior PHA-producing capacity periodic substrate excess – a true feast phase – is essential, while periodic substrate absence – a true famine phase – is not.*

Under review at New Biotechnology: L. Marang, M.C.M. van Loosdrecht, and R. Kleerebezem. Enrichment of PHA-producing bacteria under continuous substrate supply.

6.1. INTRODUCTION

Polyhydroxyalkanoates (PHAs) are microbial storage polymers, accumulated by many different prokaryotes as an intracellular carbon and energy reserve (Steinbüchel, 1991; Tan et al., 2014). They are synthesized when excess carbon is present during intermittent substrate feeding, or when the microorganisms are exposed to a nutrient or oxygen limitation (Reis et al., 2003; Steinbüchel, 1991). The chemical properties of the polymer make PHA an interesting bioplastic that is fully biodegradable (Chen, 2009). Moreover, the PHA monomers could serve as chiral building blocks for the production of various biochemicals and the hydroxy fatty acid methyl esters could be used as a biofuel (Chen, 2009).

The natural function of PHA as storage polymer can be exploited to enrich open, microbial communities in bacteria that have a high PHA storage capacity (Johnson et al., 2009a). Intermittent substrate availability – as achieved in a sequencing batch reactor (SBR) with a feast-famine regime – creates a competitive advantage for bacteria that quickly store substrate inside their cell during the feast phase and use this to grow during the famine phase (Reis et al., 2003). The enriched microbial culture can be used to accumulate large amounts of PHA in a separate step: biomass from the enrichment SBR is transferred to a (nitrogen-limited) fed-batch reactor where the PHA content of the biomass is maximized (Johnson et al., 2009a; Serafim et al., 2008). PHA contents up to 90 wt.% have been reported for microbial enrichment cultures fed with carboxylic acids like acetate or lactate (Jiang et al., 2011c; Johnson et al., 2009a). These values are comparable to those obtained using pure cultures of natural PHA producers – *Cupriavidus necator* (Vandamme and Coenye, 2004), for example – or recombinant *Escherichia coli*, while the kinetic properties of the enrichment cultures are better than those of the pure cultures (Chen, 2009).

The use of microbial enrichment cultures eliminates the need for axenic fermentation conditions (Reis et al., 2003). The fact that the reactor and the liquid streams entering the process do not have to be sterile, allows the use of waste organic carbon as substrate instead of the glucose used in pure culture processes (Chen, 2009). As a way to significantly reduce the production cost of PHA and allow broad application, various researchers investigated the use of microbial enrichment cultures for the production of PHA from fermented waste streams of the paper and food industry (Albuquerque et al., 2010b; Bengtsson et al., 2008b; Coats et al., 2007; Dionisi et al., 2005a; Jiang et al., 2012).

The discontinuous nature of the enrichment SBR – the periodic feed and discharge – requires relatively large buffer volumes and pumping capacity. Furthermore, there is a large difference between the oxygen transfer rate required during the feast and famine phase of the SBR cycle, which becomes apparent from the typical dissolved oxygen profile for feast-famine systems (Jiang et al., 2011c). These issues inhibit the economic scale-up of the process, and could be addressed by establishing the feast-famine conditions in

two continuous stirred-tank reactors (CSTRs) in series, with a partial biomass recycle (Marang et al., 2015; Reis et al., 2003). Such a 2-stage CSTR system has a continuous in- and effluent stream, and a feast and famine phase that are separated in space instead of time. The physical separation facilitates the inclusion of a solid-liquid separation step between the feast and famine reactor, and thus allows the optimal design of both reactors. However, as a result of the feast conditions (i.e., excess substrate availability) in the first reactor, small amounts of substrate will continuously enter the second or 'famine' reactor. This may affect the selective pressure for PHA-producing bacteria: the competition for the substrate leaching to the 'famine' reactor will not merely be based on the maximum substrate uptake rate of the bacteria ($q_{S,max}$) but also on their substrate affinity (K_S).

Experimental research on the enrichment of PHA-producing bacteria in a 2-stage CSTR system is limited to that of Bengtsson et al. (2008b) and Albuquerque et al. (2010a), and does not answer how the chosen reactor configuration affects the microbial competition. In a previous study (Marang et al., 2015) a mathematical model was developed to investigate the impact of a 2-stage CSTR system and the leaching of substrate on the competition between PHA-producing and non-PHA-producing bacteria. The substrate affinities (K_S) of the main microbial species were identified as important, but also at that stage unknown (Marang et al., 2015).

The aim of the current study was to experimentally investigate the impact of continuous carbon supply, and thereby the continuous presence of residual substrate, on the enrichment of PHA-producing bacteria. To that end, two SBRs were operated. In the first, the substrate (acetate) was dosed continuously, throughout the cycle. This removes the selective pressure for PHA-producing bacteria. In the second reactor, the leaching of acetate – as it will occur in a 2-stage CSTR system – was mimicked by dosing half of the substrate at the beginning of the cycle (creating a true feast phase) and the other half of the substrate continuously (creating a 'famine' phase with extra substrate supply). For both enrichment cultures the kinetic properties, PHA storage capacity, and dominant organism were determined.

6.2. MATERIALS AND METHODS

6.2.1. CULTURE ENRICHMENT IN A SEQUENCING FED-BATCH REACTOR

The enrichment and maintenance of the two microbial cultures was performed in double-jacket glass bioreactors with a working volume of 2 L (Applikon, Netherlands). The reactors were operated as a sequencing fed-batch reactor (SFBR): a sequencing batch reactor with a continuous feed stream. The length of the SFBR cycle was 12 h and each cycle consisted of a influent phase (10 min), reaction phase (695 min), and effluent phase (15 min). The exchange volume was 1 L, resulting in a hydraulic retention time (HRT) of 1 day. As there was no settling phase, the solids retention time (SRT) equaled the HRT.

Both reactors were equipped with a stirrer with two standard geometry six-blade turbines, operated at 750 rpm. The air flow rate to the reactor was set to 0.5 $L_N \cdot min^{-1}$ using a mass flow controller (Brooks Instrument, USA). The total gas flow through the reactor was increased to 1.0 $L_N \cdot min^{-1}$ by partial recirculation of the off-gas. The temperature in the reactor was controlled at 30±1°C using a thermostat bath (Lauda, Germany), and the pH was maintained at 7.0±0.1 by the addition of 1 M HCl and 1 M NaOH. Controlling of the pumps, stirrer, airflow, temperature, and pH was done by a biocontroller (Biostat Bplus, Sartorius Stedim Biotech, Germany).

During the influent phase 1.0 L fresh medium was dosed into the reactor. The medium comprised 9.0 mM NH_4Cl, 2.49 mM KH_2PO_4, 0.55 mM $MgSO_4 \cdot 7H_2O$, 0.72 mM KCl, 1.5 $mL \cdot L^{-1}$ trace elements solution according to Vishniac and Santer (1957), and 5 $mg \cdot L^{-1}$ allylthiourea (to prevent nitrification). In the first setup (SFBR100) the medium did not contain a carbon source. Instead, carbon was supplied throughout the SFBR cycle via the continuous feed stream: a concentrated sodium acetate solution (0.74 M) dripping into the reactor at 100 $mL \cdot day^{-1}$. In the second setup (SFBR50) half of the carbon was supplied continuously, whereas the other half was dosed during the influent phase. To maintain an organic loading rate of 3 $Cmmol \cdot L^{-1} \cdot h^{-1}$, the acetate concentration of the continuous feed stream in SFBR50 was reduced to 0.37 M and the composition of the medium extended with 18 mM sodium acetate.

Aerobic activated sludge from the municipal wastewater treatment plant Harnaschpolder (Delft, Netherlands) was used to inoculate the SFBRs. The inoculum was bioaugmented with ±1% (w/w) *P. acidivorans* dominated biomass (Marang et al., 2016). The reactors were operated for 3-4 months and cleaned once a week to remove biofilm from the walls, electrodes, and other submerged reactor parts. The enrichment progress was monitored by regular microscopy and biomass sampling to determine the total suspended solids (TSS) and poly(3-hydroxybutyrate) (PHB) concentration. For the second setup (SFBR50), the performance of the enrichment culture was also monitored online by identifying the length of the feast phase, which can be derived from the dissolved oxygen profile (Jiang et al., 2011c).

After obtaining a stable operational performance, (fed-)batch experiments were conducted to evaluate the kinetic properties of the enrichment culture. During these experiments the reactor was monitored closely by both online (dissolved oxygen, temperature, pH, acid and base dosage, off-gas O_2 and CO_2) and offline (acetate, ammonium, TSS, PHB) measurements. The analytical procedures for the offline measurements have been described in detail by Marang et al. (2016).

6.2.2. FED-BATCH REACTOR FOR ACCUMULATION EXPERIMENTS

To evaluate the maximum PHB storage capacity of the enrichment cultures, accumulation experiments were conducted in a similar double-jacket glass bioreactor (App-

likon, Netherlands) operated as a non-sterile fed-batch reactor. The same stirring speed, aeration rate, pH, and temperature were applied as in the SFBR. At the beginning of each experiment the reactor was filled with 1 L effluent from the SFBR, and 1 L carbon- and ammonium-free medium (otherwise the same composition). In this way, microbial growth in the fed-batch reactor was limited by the amount of ammonium remaining from the previous SFBR cycle. The production of PHB was initiated by feeding a pulse of 40 mmol sodium acetate. Further carbon source was continuously supplied to the reactor via pH control (set to pH 7.0±0.1), using a 1.5 M acetic acid solution instead of the 1 M HCl solution used in the SFBR (Johnson et al., 2009a). Thus, non-limiting acetate concentrations (10-30 mM) could be maintained throughout the experiment. When necessary a few drops of antifoam B (Sigma-Aldrich) were added and after 12 h the experiments were stopped.

6.2.3. DATA TREATMENT AND MODELING

The data collected during (fed-)batch experiments was corrected and evaluated according to the approach proposed by Johnson et al. (2009b). The accuracy of the measurements was assessed by setting up carbon and electron balances: on average 100% (±3) of the carbon and 103% (±5) of the electrons present in the substrate was traced back in the active biomass, PHB, and carbon dioxide production or oxygen consumption. Furthermore, a metabolic model was fitted to the corrected, experimental data to identify the kinetic parameters (e.g., biomass-specific conversion rates). The metabolic model was written in Matlab™ (Mathworks, USA) and has been described by Marang et al. (2016). To account for simultaneous acetate uptake and PHB degradation during the 'famine' phase, the metabolic reactions, stoichiometry, and kinetic equations previously published by Marang et al. (2015) were used. The biomass-specific carbon dioxide production and oxygen consumption rate were calculated from the other specific rates and the respective stoichiometric yields for carbon dioxide and oxygen – i.e., similar to the equation for ammonium uptake in Marang et al. (2015). As in Marang et al. (2016), the efficiency of the oxidative phosphorylation (P:O ratio) was assumed to be 2.0 mol ATP/mol NADH, and the half-saturation constants for acetate (K_S) and ammonium (K_N) – both acting merely as switch function – were set to 0.2 Cmmol·L^{-1} and 0.0001 mmol·L^{-1}, respectively. When modeling the batch/cycle experiments, the PHB inhibition factor (Marang et al., 2015) was removed from the kinetic expression for acetate uptake as the PHB content remained well below its maximum.

6.2.4. MICROBIAL COMMUNITY ANALYSIS

In order to analyze the microbial community structure, biomass samples were collected from the SFBR for PCR-DGGE and fluorescence *in situ* hybridization (FISH). The used primers and probes are listed in Table 6.1.

Table 6.1: Primers for PCR-DGGE analysis and oligonucleotide probes for FISH analysis used in this study.

Code	Function	Sequence (5'-3')	Specificity	Reference
341F-GC	Primer	cct acg gga ggc agc ag*	Bacteria	Schäfer and Muyzer (2001)
907R	Primer	ccg tca att cmt ttg agt tt	Bacteria	Schäfer and Muyzer (2001)
EUB338 I	Probe	gct gcc tcc cgt agg agt	Bacteria	Amann et al. (1990)
EUB338 II	Probe	gca gcc acc cgt agg tgt	Bacteria	Daims et al. (1999)
EUB338 III	Probe	gct gcc acc cgt agg tgt	Bacteria	Daims et al. (1999)
BET42a	Probe	gcc ttc cca ctt cgt tt	Betaproteobacteria	Manz et al. (1992)
GAM42a	Probe	gcc ttc cca cat cgt tt	Gammaproteobacteria	Manz et al. (1992)
UCB823	Probe	cct ccc cac cgt cca gtt	*P. acidivorans*	Johnson et al. (2009a)

* Contains GC-clamp (5'-cgcccgccgcgccccgcgcccgtcccgccgcccccgcccg-3') at the 5' end of the primer.

For the PCR-DGGE analysis, 16S rRNA gene fragments of the different community constituents were obtained as described by Marang et al. (2016). The PCR products were sequenced by a commercial company (BaseClear, Netherlands) and the sequences have been stored in GenBank under accession numbers: KX424708-KX424710.

FISH was used to verify the results of the PCR-DGGE analysis. A detailed description of the procedure can be found in Johnson et al. (2009a). The general probe mixture EUB338I-III was used to visualize all bacteria in the sample, the probe BET42a to indicate the presence of Betaproteobacteria, and the specific probe UCB823 to indicate the presence of *P. acidivorans*. In order to minimize erroneous hybridizations the unlabeled probe GAM42a was used to compete with the BET42a probe.

6.3. RESULTS AND DISCUSSION

6.3.1. CULTURE ENRICHMENT UNDER CONTINUOUS FEEDING

The first reactor operated in this study (SFBR100) was a sequencing fed-batch reactor where all substrate (acetate) was supplied via the continuous feed stream. Due to the continuous feeding, feast-famine conditions were not established. Throughout the cycle the acetate concentration was below the detection limit of the HPLC (<0.5 Cmmol·L^{-1}) and the PHB content of the enrichment culture was low (≤1 wt.%). To monitor the enrichment process, biomass samples were regularly observed under the microscope. This showed that after the inoculation with activated sludge the microbial diversity decreased steadily. Within two weeks, the culture was dominated by a rod-shaped and a filamentous bacterium (not shown). The latter eventually washed out.

After 3.6 months of operation (cycle #217), the microbial community structure was analyzed in detail by PCR-DGGE (Figure 6.1a). The dominant bands (B1 and B2) were excised, re-amplified, sequenced, and compared to the sequences stored in GenBank (NCBI). The first band (B1) showed more than 99% similarity to an unknown bacterium from the *Rhodocyclaceae* family. Using the ARB software (Ludwig et al., 2004) it was determined that it belongs to an uncultured cluster at the root of the *Thauera*, *Azoarcus*,

and *Zoogloea* lineages. The second and most pronounced band (B2) showed 100% similarity to *Zoogloea oryzae*. FISH confirmed the predominance of Betaproteobacteria. The general probe for this class, BET42a, hybridized with the vast majority (≥95%) of the cells in the sample (Figure 6.1b, cycle #227). The general probe for Betaproteobacteria does, however, not differentiate between *Zoogloea* and other bacteria from the *Rhodocyclaceae* family. Based on cell morphology the culture seemed to consist of predominantly one species: a significant second population could not be distinguished.

In activated sludge systems, continuous feeding and limiting substrate concentrations have frequently been linked to sludge bulking and the enrichment of filamentous biomass (Chudoba et al., 1973a; Martins et al., 2003; van Niekerk et al., 1987; Verachtert et al., 1980). The filamentous bacteria have been assumed to have lower half-saturation constants for substrate (K_S) than floc-forming bacteria (Chudoba et al., 1973b) and/or win the competition by protruding into the bulk liquid (Martins et al., 2003). Other than, for example, Verachtert et al. (1980) observed for a continuously-fed reactor on acetate, filamentous bacteria washed out from the system described here. The predominance of *Zoogloea* sp. rather than filamentous bacteria may be explained by the relatively short SRT applied in this study (1 day). van Niekerk et al. (1987) showed with defined co-culture experiments that at higher dilution rates (≥1 d^{-1}) *Zoogloea ramigera* outcompetes the filamentous organism Type 021N. Another possible explanation is the operation at a relatively high temperature (30°C). Krishna and van Loosdrecht (1999) studied the impact of temperature (15-35°C) on substrate storage and sludge settleability in an SBR with slow acetate feeding – like in this study the acetate concentration was always below the detection limit. At temperatures above 25°C, they found that *Zoogloea* species dominated the enrichment culture. More recently, also Cavaillé et al. (2016) reported the enrichment of *Zoogloea* sp. in a carbon- and phosphorus-limited CSTR on acetate, operated at 25°C and a dilution rate of 3 d^{-1}.

6.3.2. KINETIC PROPERTIES OF THE CONTINUOUSLY-FED CULTURE

To determine kinetic properties like the maximum biomass-specific substrate uptake rate ($q_{S,max}$) and maximum biomass-specific growth rate (μ_{max}) of the enrichment culture (SFBR100), batch experiments were conducted where the acetate was dosed at once. These experiments were conducted in a separate bioreactor operated at the same aeration rate, pH, and temperature as the SFBR. At the beginning of each experiment the reactor was filled with 1 L effluent from the SFBR and 1 L fresh medium comprising 36 mM sodium acetate in addition to the nutrients specified in section 6.2.1.

Table 6.2 gives an overview of the main parameters that were identified. The bacteria – cultivated under limiting substrate concentrations – responded to the presence of excess substrate with the storage of PHB (Figure 6.2). The maximum biomass-specific substrate uptake rate ($q_{S,max}$) of the culture was 0.61±0.07 Cmol·$Cmol^{-1}$·h^{-1} and the dosed

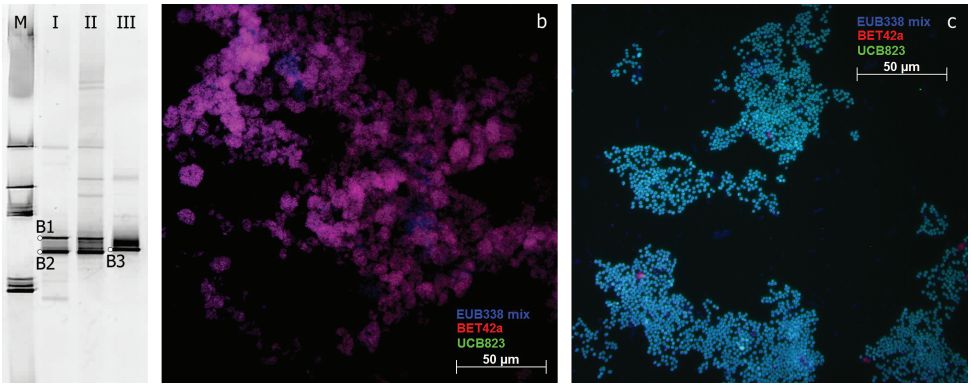

Figure 6.1: DGGE gel and FISH microscopic photographs. (a) DGGE gel of PCR-amplified 16S rRNA gene fragments from the cultures enriched under continuous feeding (SFBR100, lane I) and semi-continuous feeding (SFBR50, lane II-III). The samples loaded in lane II and III were collected, respectively, before (cycle #39) and after (cycle #77) the feast phase length shortened to less than half an hour. SmartLadder SF (Eurogentec) was loaded in lane M. The bands labeled B1-3 were excised and re-amplified for microbial identification. (b, c) Fluorescence microscopy images of the final cultures enriched in SFBR100 and SFBR50, respectively (40× magnification). The biomass was stained with a Cy5-labeled probe for Eubacteria (EUB338I-III, blue), Cy3-labeled probe for Betaproteobacteria (BET42a, red), and FLUOS-labeled probe for *P. acidivorans* (UCB823, green).

6

acetate (72 Cmmol) was taken up in around 200 minutes. A major fraction of the consumed acetate was stored as PHB ($Y_{PHB,S}$ = 0.53 Cmol·Cmol^{-1}) and at the end of the feast phase the PHB content reached 44±1 wt.%. Besides the storage, almost 10% of the acetate was found back as active biomass ($Y_{X,S}$ = 0.09 Cmol·Cmol^{-1}). This is significantly more than previously observed for enrichment cultures in a standard, pulse-fed SBR (Jiang et al., 2011c,a) (Table 6.2).

After acetate depletion, the accumulated PHB was degraded and used for biomass synthesis. The biomass-specific growth rate increased from 0.05±0.01 Cmol·Cmol^{-1}·h^{-1} on acetate ($\mu_{Ac,max}$) to, initially, 0.15±0.02 Cmol·Cmol^{-1}·h^{-1} on PHB. After 12 h, the experiment was stopped. The active biomass had almost doubled and the intracellular PHB content had decreased to less than 3 wt.% of the TSS. The average biomass-specific growth rate during the famine phase was 0.05 Cmol·Cmol^{-1}·h^{-1} (Table 6.2).

6.3.3. CULTURE ENRICHMENT UNDER SEMI-CONTINUOUS FEEDING

The second reactor operated in this study (SFBR50) was a sequencing fed-batch reactor where half of the substrate was supplied via the continuous feed stream and the other half dosed during the influent phase at the beginning of the cycle. As a result of the continuous feed stream, a strict famine phase was absent. Nevertheless, the typical dissolved oxygen pattern observed for pulse-fed SBRs (Jiang et al., 2011c) established only a few cycles after inoculation with activated sludge. The intermittent periods with

Table 6.2: Overview of observed variables, and model-derived yields and biomass-specific rates during normal reactor operation and (fed-)batch experiments. The presented average values and standard deviations are based on duplicate experiments (n=2) performed after obtaining a stable operational performance. The average feast phase length (SFBR50) is based on the final 30 cycles of operation (n=30, Figure 6.3). The yields for the accumulation experiments were determined over the first 4 h of the experiment. As the metabolic model did not properly fit the experimental data for SFBR50 (Figure 6.4) values with lower reliability have been italicized.

		SFBR 100 *This study*	**SFBR 50** *This study*	**Standard SBR** *Jiang et al. (2011c)*
Normal reactor operation				
Observed				
Length feast phase	[min]	-	27 ± 1	38
PHB min. cycle	[wt.%]	1 ± 0	1 ± 0	4
PHB max. cycle	[wt.%]	1 ± 0	37 ± 1	52
PHB max. cycle	[Cmol·Cmol^{-1}]	0.01 ± 0.00	0.68 ± 0.01	1.3
Batch/Cycle experiments				
Model-derived				
$Y_{PHB,S}^{feast}$	[Cmol·Cmol^{-1}]	0.53 ± 0.02	0.58 ± 0.00	0.67
$Y_{X,S}^{feast}$	[Cmol·Cmol^{-1}]	0.09 ± 0.01	0.06 ± 0.00	0.00
$Y_{CO2,S}^{feast}$	[Cmol·Cmol^{-1}]	0.37 ± 0.00	0.36 ± 0.00	0.33
$q_{S,max}$	[Cmol·Cmol^{-1}·h^{-1}]	0.61 ± 0.07	2.84 ± 0.11	4.38
$\mu_{Ac,max}$	[Cmol·Cmol^{-1}·h^{-1}]	0.05 ± 0.01	*0.16 ± 0.01*	0.00
m_{ATP}	[mol·Cmol^{-1}·h^{-1}]	0.01 ± 0.01	*0.01 ± 0.01*	0.00
k	[Cmol$^{1/3}$·Cmol$^{-1/3}$·h^{-1}]	-0.23 ± 0.02	*-0.33 ± 0.01*	-0.16
μ^{famine}, max.	[Cmol·Cmol^{-1}·h^{-1}]	0.15 ± 0.02	*0.18 ± 0.00*	0.14
μ^{famine}, average	[Cmol·Cmol^{-1}·h^{-1}]	0.05 ± 0.00	*0.05 ± 0.00*	0.06
Accumulation experiments				
Observed				
PHB max. acc	[wt.%]	53 ± 1	85 ±0	88
PHB max. acc	[Cmol·Cmol^{-1}]	1.3 ± 0.0	6.6 ± 0.2	8.3
Model-derived				
$Y_{PHB,S}^{acc}$	[Cmol·Cmol^{-1}]	0.50 ± 0.03	0.61 ± 0.01	0.61
$Y_{X,S}^{acc}$	[Cmol·Cmol^{-1}]	0.10 ± 0.01	0.04 ± 0.01	0.04
$Y_{CO2,S}^{acc}$	[Cmol·Cmol^{-1}]	0.41 ± 0.01	0.35 ± 0.00	0.35
$q_{PHB,max}$	[Cmol·Cmol^{-1}·h^{-1}]	0.28 ± 0.04	1.44 ± 0.09	1.74

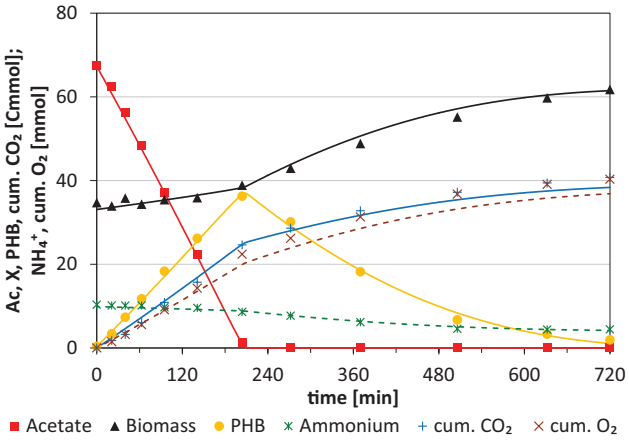

Figure 6.2: Results of a representative batch experiment with biomass from the continuously-fed reactor (SFBR100). The symbols represent measured data, the lines modeled data.

excess and limited carbon availability will be referred to as, respectively, the feast and 'famine' phase.

6

The length of the feast phase – as derived from the dissolved oxygen pattern – rapidly decreased to about one hour and seemed to stabilize around this value (Figure 6.3). PCR-DGGE analysis of a biomass sample collected during this period (Figure 6.1a, cycle #39) revealed that the microbial community structure was similar to that in the continuously-fed reactor (SFBR100). Afterwards – over the course of more than twenty cycles – the feast phase shortened further (Figure 6.3). Once the length of the feast phase had reduced to less than half an hour, analysis of the microbial community structure by PCR-DGGE was repeated (Figure 6.1a, cycle #77). The sequence derived from the dominant band (B3) showed 99.8% similarity to that of *P. acidivorans*, and previous analyses had shown that the band just above B3 also belongs to this organism (Jiang et al., 2011a). FISH microscopy later confirmed the predominance of *P. acidivorans* (Figure 6.1c, cycle #150). A vast majority (≥95%) of the cells hybridized with the specific probe for *P. acidivorans* (UCB823), while almost no Betaproteobacteria were found. At stable operational conditions, the length of the feast phase was 27±1 min. During the feast phase the PHB content of the cells increased from about 1 to 37±1 wt.% (Table 6.2 and Figure 6.3).

These enrichment results show that the absence of a strict famine phase does not impede the enrichment of *P. acidivorans*. Although half of the dosed substrate was taken up under substrate limited conditions, the enrichment was as effective as when all substrate was dosed in the feast phase (Jiang et al., 2011c; Johnson et al., 2009a). *P. acidivorans* degraded its stored PHB and used it for biomass synthesis, concomitant with the consumption of acetate. The fact that *P. acidivorans* was the sole dominant organism, shows that it was able to successfully compete for the acetate at low concentrations.

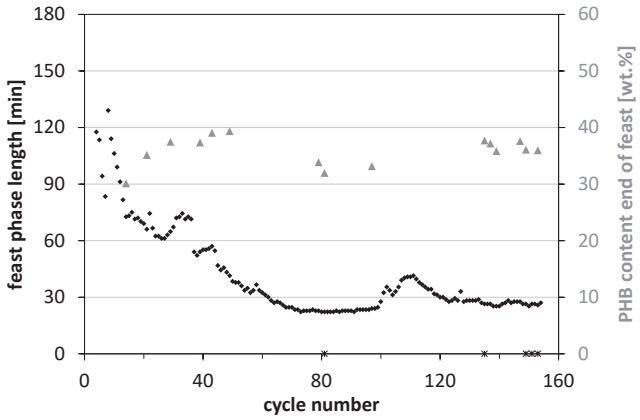

Figure 6.3: Performance of SFBR50 over the full operational period (3 months). The black diamonds indicate the length of the feast phase (min), the grey triangles the PHB content obtained at the end of the feast phase (wt.% of TSS). The asterisks on the x-axis indicate when cycle and/or accumulation experiments were performed.

These observations are different from those of Martins et al. (2003), who also studied the impact of acetate leaching in open systems and already observed a change in the microbial community structure (i.e., the growth of filamentous biomass) when just 20% of the acetate was leached to the 'famine'. A major difference between the two studies is the applied SRT: 1 versus 10 days. Also in our study the competitive advantage of *P. acidivorans* was reduced, though. The reduction of the feast phase length (Figure 6.3) was more gradual than observed in previous, pulse-fed SBRs (Jiang et al., 2011c,a). Moreover, when all substrate had to be taken up under substrate limited conditions – i.e. in SFBR100 – *Zoogloea* sp. was enriched (Figure 6.1). The enrichment of *Zoogloea* sp. rather than *P. acidivorans* under continuous feeding may be explained by the considerably smaller cell size of the first (Jiang et al., 2011a) (Figure 6.1). The larger specific surface area of *Zoogloea* sp. may well account for a lower half-saturation constant for substrate (K_S).

6.3.4. KINETIC PROPERTIES OF THE SEMI-CONTINUOUSLY-FED CULTURE

Cycle experiments were conducted to evaluate the performance and determine the biomass-specific conversion rates of the semi-continuously-fed enrichment culture (SFBR50). During these experiments the SFBR was closely monitored by online (e.g. off-gas O_2 and CO_2) and offline (acetate, ammonium, TSS, and PHB) measurements. The results of the experiments and consecutive modeling are shown in Table 6.2 and Figure 6.4.

The maximum biomass-specific substrate uptake rate ($q_{S,max}$) of the culture was 2.84 ±0.11 Cmol·Cmol^{-1}·h^{-1}. The majority of the pulse-fed acetate was stored as PHB ($Y_{PHB,S}$ = 0.58 Cmol·Cmol^{-1}) and at the end of the feast phase, after 27±1 min, the PHB con-

tent reached 37±1 wt.% (Figure 6.4). Besides the conversion to PHB, six percent of the pulse-fed acetate was converted to biomass ($Y_{X,S}$ = 0.06 Cmol·Cmol^{-1}) and the remaining 36% respired to carbon dioxide (Table 6.2). Overall, the culture's response to excess substrate availability lay in between that observed for the culture enriched under fully continuous feeding (SFBR100) and that observed for previous cultures enriched in a standard, pulse-fed SBR (Jiang et al., 2011c). The biomass-specific substrate uptake rate in SFBR50 was almost five times as high as the uptake rate in SFBR100, but still lower than in the standard, pulse-fed SBR (Table 6.2). Similarly, the PHB yield – the fraction of substrate stored as PHB during the feast phase – was higher than in the continuously-fed reactor, but lower than in the standard SBR. Although the PHB yield was slightly reduced, the lower PHB content found at the end of the feast phase in SFBR50 (37 wt.% vs. 52 wt.% in the SBR) is primarily explained by the fact that at that point only half of the total substrate has been dosed. When the intracellular PHB content is expressed in Cmoles PHB per Cmol active biomass, it shows very clear that the PHB content in SFBR50 is roughly half that observed for the pulse-fed SBR: 0.68 vs. 1.3 Cmol·Cmol^{-1} (Table 6.2). The fact that only half the substrate has been dosed also causes the reduced feast phase length, in spite of the lower biomass-specific substrate uptake rate in SFBR50.

The applied metabolic model (Marang et al., 2015) could well describe the feast phase and uptake of the first 36 Cmmol acetate. However, it did not completely fit the experimental data for the 'famine' phase (Figure 6.4). Initially, the PHB degradation rate and resulting biomass growth rate are overestimated, while later during the 'famine' phase the PHB degradation and biomass growth rate are underestimated (Figure 6.4). Under strict famine conditions, the degradation of PHB is generally considered to be the rate-limiting step. The biomass-specific PHB degradation rate (q_{PHB}) has been shown to depend solely on the PHB content of the cell (f_{PHB}) (Beun et al., 2002) and is therefore defined as $q_{PHB} = k \cdot f_{PHB}^{2/3}$ in both the model applied in this study (Marang et al., 2015) and other models (Johnson et al., 2009b; Reis et al., 2003). Using this kinetic description, the PHB degradation will be fastest right at the start of the famine phase, when the PHB content is the highest. Over the course of the famine phase, the specific PHB degradation and biomass growth rate will decrease due to the reducing PHB content of the cells. The PHB degradation in SFBR50 would be better described by a sigmoid curve, though (Figure 6.4). Likely, the degradation of PHB is no longer the true rate-determining step. At the start of the 'famine' phase, when there is a relatively large amount of both acetate and PHB available for growth, the bacteria may reach their maximum biomass-specific growth rate (μ_{max}). For a correct description of the simultaneous uptake of acetate and degradation of PHB, additional experiments and a revision of the kinetic model will be required.

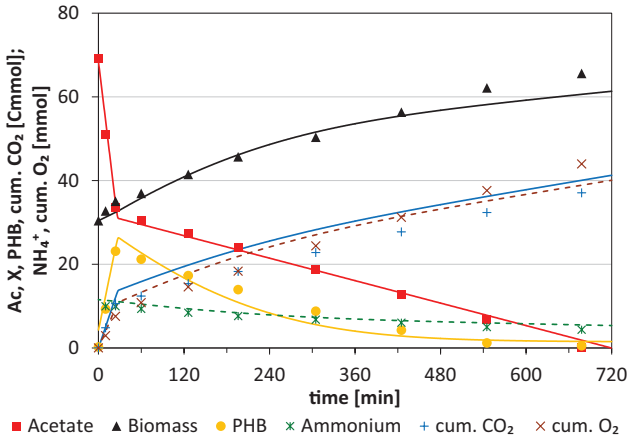

Figure 6.4: Results of a representative cycle experiment during normal operation of the semi-continuously-fed reactor (SFBR50). The symbols represent measured data, the lines modeled data.

6.3.5. MAXIMAL PHB CONTENT

To evaluate the PHB production rate and maximum storage capacity of the two enrichment cultures, fed-batch accumulation experiments were conducted. During these experiments the availability of ammonium was limited to that remaining from the previous SFBR cycle (±2 mmol) and the ammonium got depleted in 2-4 h (Figure 6.5). Carbon (acetate), on the other hand, was available in excess and additional carbon continuously supplied to the reactor via pH control (Johnson et al., 2009a).

The culture enriched under semi-continuous feeding and dominated by *P. acidivorans* (SFBR50) accumulated large amounts of PHB (Figure 6.6). The PHB content of this culture reached more than 80 wt.% in just 4 h, which is similar to what has been reported for *P. acidivorans* when it was enriched in a standard SBR (Jiang et al., 2011c). The maximum PHB content – 85±0 wt.% – was obtained after 12 h. This is slightly lower than the maximum storage capacity reported for *P. acidivorans* (89 wt.%) (Johnson et al., 2009a). The difference could be due to the presence of a flanking population or change in the kinetic properties of *P. acidivorans* itself. Both would be in agreement with the slightly reduced biomass-specific substrate uptake and PHB production rate observed for SFBR50 (Table 6.2).

It had already been observed during batch experiments (Figure 6.2) that the culture enriched under continuous feeding (SFBR100) produces PHB when it is exposed to excess carbon. The culture – enriched in *Zoogloea* sp. – accumulated 50 wt.% PHB in 12 h (Figure 6.6). Thereafter the PHB content increased little further: the next morning PHB contents of 53±1 wt.% were found (Table 6.2). Also other researchers have reported the accumulation of PHB during batch experiments with bacteria that have been cultivated or enriched under carbon-limited conditions (Dionisi et al., 2006; Martins et al., 2003;

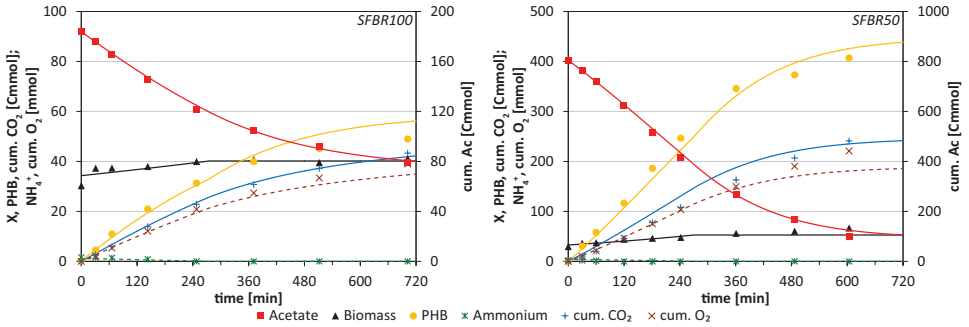

Figure 6.5: Results of a representative accumulation experiment with biomass from the continuously-fed reactor (SFBR100) and semi-continuously-fed reactor (SFBR50), respectively. The symbols represent measured data, the lines modeled data.

van Niekerk et al., 1987). As PHB storage is a common bacterial trait (Steinbüchel, 1991), it is not surprising that the absence of a selective pressure for PHB production does not result in the absence of a storage response. However, it did result in a dramatically lowered PHB production rate and storage capacity: both were only one-fifth of that observed for SFBR50 (Table 6.2 and Figure 6.5). The biomass-specific PHB production rate in SFBR100 was 0.28±0.04 Cmol·Cmol^{-1}·h^{-1}, versus 1.44±0.09 Cmol·Cmol^{-1}·h^{-1} in SBFR50. And the final amount of stored PHB was only 1.3 Cmol per Cmol active biomass, instead of the 6.6 Cmol·Cmol^{-1} accumulated in SFBR50.

6.3.6. IMPLICATIONS FOR INDUSTRIAL IMPLEMENTATION

The results of this study clearly show that the absence of a true famine phase does not impede the enrichment of bacteria with a superior PHA-producing capacity. Despite the continuous supply of acetate, the enrichment culture in SFBR50 was dominated by *P. acidivorans* and accumulated up to 85 wt.% PHB. This suggests that the SBR-based cultivation, as normally applied for the enrichment of PHA-producing bacteria, can readily be converted to a 2-stage CSTR system – where true famine conditions will be absent as well (Albuquerque et al., 2010a; Marang et al., 2015). The possibility to apply less strict famine conditions also has strong advantages for scale-up of the SBR process itself. Feeding substrate throughout the cycle reduces the need for buffer volume and alkalinity, as the dosage of the acidic substrate no longer outruns the consumption.

6.4. CONCLUSION

For the enrichment of bacteria with a superior PHA-producing capacity, periodic substrate absence – a true famine phase – is not strictly necessary. This offers important operational flexibility compared to when a strict, pulse-fed SBR system would have been required, and enables an economic scale-up of the non-axenic PHA production process.

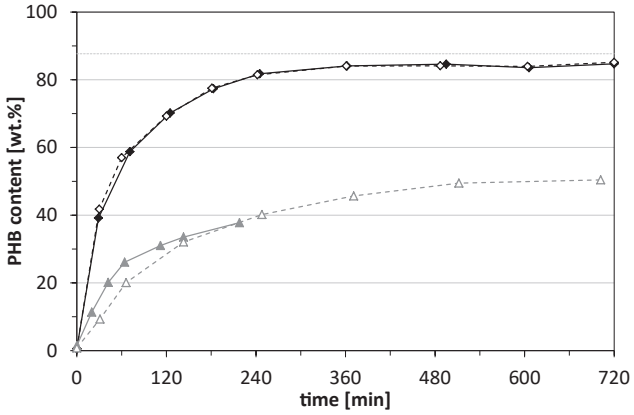

Figure 6.6: Production of PHB (wt.% of TSS) during accumulation experiments with biomass enriched in SFBR50 (black diamonds) and SFBR100 (grey triangles). The filled and open symbols represent results obtained during duplicate experiments. The horizontal grey, dotted line indicates the PHB content obtained with *P. acidivorans* dominated biomass enriched in a pulse-fed SBR (Jiang et al., 2011c).

To assure a high PHA production rate and high PHA storage capacity, periodic substrate excess – a true feast phase – remains essential.

NOMENCLATURE

k	rate constant for PHB degradation	[Cmol$^{1/3}$·Cmol$^{-1/3}$·h^{-1}]
K_S	half-saturation constant for substrate	[Cmmol·L^{-1}]
$\mu_{Ac,max}$	maximum biomass-specific growth rate on acetate	[Cmol·Cmol^{-1}·h^{-1}]
μ^{famine}	biomass-specific growth rate during the famine phase	[Cmol·Cmol^{-1}·h^{-1}]
m_{ATP}	biomass-specific ATP requirement for maintenance	[mol·Cmol^{-1}·h^{-1}]
$q_{PHB,max}$	maximum biomass-specific PHB production rate	[Cmol·Cmol^{-1}·h^{-1}]
$q_{S,max}$	maximum biomass-specific substrate uptake rate	[Cmol·Cmol^{-1}·h^{-1}]
$Y_{i,j}$	modeled actual yield of compound i on j	[Cmol·Cmol^{-1}]

7

Conclusions and Outlook

7.1. WASTEWATER COMPOSITION

The aim of this thesis was to investigate scale-up aspects of the PHA production from agro-industrial waste streams by microbial enrichment cultures. The intended use of an (acidified) waste stream as substrate requires knowledge on the fate of the different constituents in order to allow the selection of suitable waste streams and optimization of the process, in particular the pre-fermentation of the organic waste. Three biologically important groups of compounds were investigated: carbon sources that are – to different extends – suitable for PHA production, carbon sources that do not give rise to PHA production, and nutrients (specifically nitrogen).

7.1.1. THE IDEAL SUBSTRATE

The ideal substrate for PHA production yields a microbial enrichment culture with a high maximum PHA content, a high biomass-specific PHA production rate, and a high product yield. The enrichment cultures on butyrate (Chapter 2) showed the best performance on these criteria. The cultures were dominated by *P. acidivorans* – an organism that can accumulate up to 9 Cmol PHB per Cmol active biomass (Johnson et al., 2009a) and was also enriched on other VFAs, like acetate (Johnson et al., 2009a) and propionate (Jiang et al., 2011b). Its ability to convert different VFAs enables the production of the copolymer poly(3-hydroxybutyrate-co-3-hydroxyvalerate) (PHBV), which is important when aiming at the use of PHA as a bioplastic. The biomass-specific uptake rate of *P. acidivorans* for butyrate was 50% higher than for acetate: 6.7 vs. 4.4 $Cmol \cdot Cmol^{-1} \cdot h^{-1}$ (Table 2.4). Furthermore, only a minor fraction of the substrate was used for growth or respired to carbon dioxide. The high observed product yield (0.93 Cmol PHB/Cmol butyrate) resulted from a minimal ATP requirement to convert butyrate to PHB. The generation of NADH during PHB synthesis from butyrate (Figure 1.5) is almost sufficient to generate the required ATP and reduces the respiration requirements for butyrate as compared to acetate. Together, the high substrate uptake rate and high product yield caused a doubling of the biomass-specific PHB production rate. During accumulation experiments the PHB content of the culture reached already 83 wt.% (5.8 $Cmol_{PHB} \cdot Cmol_X^{-1}$) in 3.4 h (Chapter 2).

Based on the stoichiometric product yield and oxygen requirement for PHB production from lactate (Table 7.1), lactate is in theory also a highly suitable substrate for PHB production – ranking somewhere in between acetate and butyrate. A study by Jiang et al. (2011c) showed that *Plasticicumulans lactativorans* (Jiang et al., 2014) was enriched when using sole lactate as substrate. This organism has an extraordinary PHB storage capacity (92 wt.%, 13.5 $Cmol_{PHB} \cdot Cmol_X^{-1}$) and a high biomass-specific PHB production rate. However, when using a mixture of acetate and lactate, a co-culture of *P. acidivorans* – taking up the acetate – and *Thauera* sp. – taking up the lactate – was enriched. *Thauera* sp. has a significantly lower biomass-specific PHB production rate (0.96

Table 7.1: Overview of the stoichiometric yields and experimentally determined rates and yields for PHB production from acetic, butyric, and lactic acid.

		Acetic acid	**Butyric acid**	**Lactic acid**	
		Jiang et al. (2011c)	*Chapter 2*	*Jiang et al. (2011c)*	
Stoichiometric yields					
$Y_{PHB,S}$	[Cmol·Cmol^{-1}]	0.67	0.94	0.74	
$Y_{O2,PHB}$	[mol·Cmol^{-1}]	0.38	0.20	0.23	
$Y_{CO2,PHB}$	[Cmol·Cmol^{-1}]	0.50	0.06	0.35	
Observed					
Dominant species		*P. acidivorans*	*P. acidivorans*	*P. lactativorans*	*Thauera* sp.
PHB max. feast	[wt.%]	52	57	53	48
PHB max. acc	[wt.%]	88	88	92	81
PHB max. feast	[Cmol·Cmol^{-1}]	1.3	1.6	1.3	1.1
PHB max. acc	[Cmol·Cmol^{-1}]	8.3	8.3	13.5	5.1
Model-derived					
Accumulation step					
$q_{PHB,max}$	[Cmol·Cmol^{-1}·h^{-1}]	1.74	3.64	2.07	0.96
$Y_{PHB,S}$	[Cmol·Cmol^{-1}]	0.61	0.89	0.63	0.64

Cmol·Cmol^{-1}·h^{-1}) and PHB storage capacity (81 wt.%, 5.1 $Cmol_{PHB}$·$Cmol_X^{-1}$) (Jiang et al., 2011c). This result illustrates the importance of these experiments and suggests that within a complex substrate mixture, such as an acidified agro-industrial waste stream, lactate will not be the best substrate.

Overall, to optimize the PHA production process, the acidogenic pre-fermentation step should be directed towards the production of butyrate rather than acetate or lactate. When aiming at the use of PHA as a bioplastic – i.e. the production of PHBV – the synthesis of a certain, constant fraction of VFAs with an odd number of carbon atoms (propionate and/or valerate) should also be ensured. The production of alcohols should be avoided. Although ethanol gives rise to the accumulation of PHB, the product yields ($Y_{PHB,S}$) reported for batch experiments with ethanol are low (Beccari et al., 2002; Tamis et al., 2014a). Moreover, Tamis et al. (2014a) reported the accumulation of a significant amount of non-PHA storage compounds.

7.1.2. NON-PHA SUBSTRATES

Besides the organic acids suitable for PHA production, (fermented) organic waste streams will also contain compounds that are more slowly degraded and do not contribute to the accumulation of PHA. Although the pre-fermentation step aims to convert as much of the organic carbon as possible to organic acids, it will rarely be possible to achieve a full conversion to VFAs. The impact of these more slowly degradable, non-PHA substrates was investigated in Chapter 3, using methanol as a model-substrate. Feeding the SBR with acetate and methanol in a ratio of 1:1 Cmol led to the co-enrichment of a non-PHA-storing population, growing on methanol, that reduced the maximum PHA

content of the culture from more than 80 to 66 wt.% (>5 to 2.3 $Cmol_{PHB} \cdot Cmol_X^{-1}$) (Figure 3.5). When ammonium was present during the accumulation step, unrestricted growth of the non-storing, methylotrophic population further reduced the maximum overall PHA content (52 wt.%, 1.3 $Cmol_{PHB} \cdot Cmol_X^{-1}$).

Other than optimizing the pre-fermentation step and restricting growth during the accumulation step, additional strategies to reduce the size and impact of the non-PHA-storing population may be required. The experiments in Chapter 3 showed that upon acetate depletion (after 36 min), 80% of the initially dosed methanol still remained in the reactor liquid. The depletion of methanol followed roughly 1.5 h later (after 125 min). The inclusion of a concentration step directly after depletion of the compounds suitable for PHA production (VFAs, lactate, etc.) would allow the removal of a large part of the remaining external substrate. The selective removal of substrates unsuitable for PHA production from the enrichment reactor will reduce the availability for and thereby the size of the non-PHA-storing population.

The strategy was successfully further investigated by Korkakaki et al. (2016b), who showed that, depending on the timing and discharge volume, 60% of the methanol could be removed from the system. This increased the fraction of *P. acidivorans* in the enrichment culture from 40 to 63%.

7.1.3. THE ROLE OF NUTRIENT LIMITATION

The prevention of growth by limiting the availability of an essential nutrient (e.g. nitrogen or phosphorus) is often presented as a prerequisite to obtain high PHA contents (Bengtsson et al., 2008b; Johnson et al., 2010; Serafim et al., 2004). However, when butyrate (Chapter 2) or lactate (Jiang et al., 2011c) was used as substrate, the cultures accumulated 83-85 wt.% PHB (6 $Cmol_{PHB} \cdot Cmol_X^{-1}$) before the ammonium got depleted. Accumulation experiments with the enrichment culture on acetate and methanol under nitrogen-limited and nitrogen-excess conditions (Chapter 3) also indicated that *P. acidivorans* accumulated large amounts of PHB (>5 $Cmol_{PHB} \cdot Cmol_X^{-1}$) despite the presence of ammonium. The reduced PHB content could be ascribed to unrestricted growth of the non-PHA-storing population. Under nitrogen-excess conditions, the maximum PHB content (52 wt.%, 1.3 $Cmol_{PHB} \cdot Cmol_X^{-1}$) was reached after 4 h. Afterwards, the amount of PHB in the reactor kept increasing, but the overall PHB content started to decline (Figure 3.4 and 3.5).

Nutrient limitation is therefore not a strict prerequisite to obtain a high PHA content, but merely a strategy to restrict the impact of growth by the non-PHA-storing population. If the PHA production rate is high enough and the accumulation step can be ended in time, the presence of ammonium does not impede obtaining a high PHA content. This broadens the range of organic waste streams suitable for PHA production by microbial enrichment cultures, and specifically by *P. acidivorans*. In the case of a nitrogen-rich

waste stream, alternative strategies – such as discussed in section 7.1.2 – could be applied to reduce the size and impact of the non-PHA-storing population. Further research on the impact of ammonium on PHA accumulation and the use of nitrogen-rich waste streams is required and has been performed by, e.g., Korkakaki et al. (2016a).

7.2. PROCESS DESIGN

The common, batch-wise operation of lab and pilot reactors (Albuquerque et al., 2010b; Anterrieu et al., 2014; Jiang et al., 2012; Morgan-Sagastume et al., 2014; Tamis et al., 2014a) creates a highly dynamic process with a distinct feast and famine phase. These two periods have highly different oxygen requirements, and the uncoupling of dosage and uptake of substrate causes a high usage of chemicals for pH control. Moreover, the periodic feed and discharge will require relatively large storage volumes and pumping capacity to treat a continuous wastewater stream. Alternative process configurations were investigated where, e.g., the number of process steps was reduced (Chapter 4) or the feast-famine conditions were established in a continuous system (Chapter 5).

7.2.1. COMBINING THE ENRICHMENT AND ACCUMULATION STEP

The process for non-axenic PHA production generally comprises four steps (Figure 1.7). To reduce capital cost, the feasibility of combining the enrichment and accumulation step in a single reactor was assessed in Chapter 4. Operating the SBR at a high volume exchange ratio (0.75, i.e. 18 h cycles and 1 d SRT) allowed the production of biomass with 70 wt.% PHB (2.8 $Cmol_{PHB} \cdot Cmol_X^{-1}$) in a single-step process from acetate. It does not seem feasible to obtain much higher PHB contents when omitting the accumulation step. By increasing the exchange ratio to 0.83 (20 h cycles), the PHB content of the harvested biomass increased up to 75 wt.% (3.6 $Cmol_{PHB} \cdot Cmol_X^{-1}$), but the operational stability decreased (Figure 4.4). And the intended use of an acidified organic waste stream as substrate will result in the co-enrichment of non-PHA-storing bacteria and thereby a reduction of the culture's PHA content.

Maximizing the volume exchange ratio is a suitable strategy for the production of PHA-rich biomass in the SBR, but does not ensure the enrichment of a microbial culture with a superior PHA productivity. When operating the SBR at these high exchange ratios, bacteria have to increase their growth rate and external substrate will be available for relatively long periods (Section 4.4.2). This allows the establishment of larger flanking populations and negatively affected the kinetic properties of *P. acidivorans*. The PHA storage rate, yield, and capacity of the enrichment culture were severely compromised (Table 4.2).

Rather than reducing capital cost by combining the full enrichment and accumulation step, the feast and accumulation step could be combined in a single reactor, while the growth on stored PHA is facilitated in a separate famine reactor. The steps requir-

ing a high oxygen transfer rate are thus combined in one reactor. The famine phase, which has much lower oxygen requirements, could be performed at a higher biomass concentration in a small, second reactor. The inclusion of a solid-liquid separation step between the feast and famine reactor simultaneously allows the independent design of both reactors and the selective removal of substrates unsuitable for PHA production as proposed in section 7.1.2.

7.2.2. A STAGED CSTR SYSTEM

The use of a staged CSTR system for the enrichment of PHA-producing bacteria addresses several scale-up issues: the in- and effluent stream will be continuous, the substrate dosage will be in balance with the uptake, and the feast and famine phase – with their different oxygen requirements – will be physically separated. The separation between feast and famine conditions will become less strict, though – especially in a 2-stage CSTR system. Simulations of the growth of *P. acidivorans* in competition with a non-storing heterotroph (Chapter 5) confirmed that in the 2-stage CSTR system the selective pressure for PHA-producing bacteria is significantly lower than in the SBR, and strongly dependent on the chosen feast-famine ratio (Figure 5.1 and 5.2). To increase the selective pressure, a third reactor could be added that ensures excess substrate conditions in the feast reactor and prevents leaching of substrate to the famine reactor. The importance of minimizing the substrate leaching to the famine reactor depends on the (relative) substrate affinities of *P. acidivorans* and its competitors (Figure 5.6). These values are, however, not known. The impact of continuous substrate availability on the enrichment of PHA-producing bacteria was, therefore, investigated in Chapter 6.

When the substrate (acetate) was dosed continuously, substrate had to be taken up under limited conditions and the competition was based on substrate affinities. This removed the selective pressure for PHA-producing bacteria. The enrichment culture became dominated by *Zoogloea* sp. (Figure 6.1), which indicates that *P. acidivorans* has a lower substrate affinity than its competitors, as was assumed in the model (Chapter 5). When half of the substrate was dosed continuously and the other half at once, feast conditions were established but strict famine conditions remained absent. This mimicked the leaching of substrate as it will occur in a 2-stage CSTR system. Even though half of the dosed substrate had to be taken up under substrate-limited conditions, *P. acidivorans* dominated the enrichment culture (Figure 6.1). The absence of a significant second population indicated that *P. acidivorans* was able to successfully compete for the acetate at low concentrations. It degraded its stored PHA and used it for biomass synthesis concomitant with the consumption of acetate. These results suggest that the current SBR-based cultivation can be readily converted to a 2-stage CSTR system.

A second factor that affects the selective pressure for PHA-producing bacteria in a staged CSTR system is the distribution of the residence times, and consequently the dis-

tribution of bacterial states. The developed agent-based model (Chapter 5 and Appendix A) showed that cells in the feast reactor contain a wide range of intracellular PHA contents, but only a minor fraction contains extremely low or high amounts of PHA. In the famine reactor, a major fraction of *P. acidivorans* (46%) contained virtually no PHA and does, therefore, not contribute to the overall PHA degradation rate (Figure 5.4). Again, increasing the number of CSTRs in series could strengthen the competitive advantage of PHA-producing bacteria, as it would narrow the residence time distribution.

Both the modeling results (Chapter 5) and the experimental data obtained from the SBRs with a continuous substrate supply (Chapter 6) indicated that the competitive advantage of *P. acidivorans* in a 2-stage CSTR system will be reduced, but remains present. The use of an acidified organic waste stream, comprising multiple compounds in varying concentrations, will, however, complicate setting the optimal feast-famine ratio. For a robust PHA production process by microbial enrichment cultures a (dispersed) plug flow system will be preferable. Rather than the temporal plug flow in an SBR, this could be a spatial plug flow reactor with partial biomass recirculation. Such a plug flow reactor would just like the 2-stage CSTR system, allow a truly continuous process and the separation of periods with highly distinct oxygen requirements over different reactors.

7.2.3. OXYGEN

As the PHA is produced aerobically, the maximum volumetric productivity of the reactor will be determined by the oxygen transfer rate (OTR) that can be achieved. The high biomass and product concentrations reported for pure culture processes (Chen, 2009) are a result of the relatively low biomass-specific rates. In our microbial enrichment cultures the biomass-specific rates are much higher. Consequently, the maximal allowed biomass concentration during the feast or accumulation step will be lower. There is no intrinsic difference between the oxygen requirements of a pure and an enrichment culture, so the maximum volumetric productivities will be similar. The capital cost per cubic meter of reactor will be much higher for pure cultures (stainless steel reactors) than for microbial enrichment cultures (open tanks), though.

Being a determining factor, oxygen is a recurring subject throughout this thesis – although none of the experiments were optimized for their volumetric productivity. The oxygen needed to produce a gram of PHA can be reduced by properly selecting your substrate. PHB synthesis from butyric acid was shown to require almost 50% less oxygen than from acetic acid, for example (Chapter 2 and Table 7.1). Moreover, the oxygen consumption for non-PHA processes should be reduced by eliminating non-storing populations and removing substrates unsuitable for PHA production from the enrichment reactor before they are taken up (Chapter 3). The reactor's oxygen transfer capacity may also be used more optimally. For example, by feeding part of the substrate continuously (Chapter 6) or by combining the steps with a high oxygen demand – the feast and ac-

cumulation – rather than the feast and the famine in a single reactor (Chapter 4). In the current SBR process, the high oxygen requirements during the feast phase determine the reactor design, while during the significantly longer famine phase the requirements are much lower. The physical separation of the feast and famine phase can also be achieved with the use of a staged CSTR system (Chapter 5).

7.3. TOWARDS INDUSTRIAL IMPLEMENTATION

The research presented in this thesis was part of a larger STW project aimed at developing the overall production chain for waste-based PHA from microbial enrichment cultures. Within this project also the acidogenic fermentation step (Tamis et al., 2015), the downstream process (Jiang et al., 2015), the use of PHA as bioplastic, and the use as chemical building block (Spekreijse et al., 2015, 2016) were investigated. Moreover, life cycle and techno-economic analyses (Fernández-Dacosta et al., 2015, 2016) and a first pilot study (Tamis et al., 2014a) were performed. The pilot plant comprised two anaerobic reactors to acidify effluent from the Mars candy bar factory, a 200 L SBR for the culture enrichment, and a 200 L fed-batch reactor for the PHA production step. After anaerobic fermentation, the VFA fraction of the wastewater was on average 0.64 gCOD/gCOD. The enriched PHA-producing microbial culture was dominated by *P. acidivorans* and accumulated 70 wt.% PHBV (of VSS) in the production step (Tamis et al., 2014a). Although further optimization and fine-tuning of the process will be required, especially for the acidogenic fermentation step, these are promising results.

The major obstacle for successful industrial implementation is, currently, the application development. When aiming at the use of PHA as bioplastic, the focus is often on replacing polypropylene (PP). PHA shares properties with PP, but is a different polymer. Especially at the early stage of large-scale, waste-based PHA production by microbial enrichment cultures, one should aim at simple applications, where one can truly exploit properties that make PHA different. The amount of PHA produced when treating agro-industrial waste streams will also be of a different scale than PP production. When developing applications one should, therefore, look for on-site or close-by applications in particular. The application of PHA as platform chemical is still at the research stage. Such non-plastic applications definitely deserve attention, though.

7.4. SUGGESTIONS FOR FUTURE RESEARCH

Over the past two decades, the enrichment and accumulation step of non-axenic PHA production have been extensively studied by various research groups. With the first pilot studies published (Anterrieu et al., 2014; Morgan-Sagastume et al., 2014; Tamis et al., 2014a), the scale-up aspects investigated in this thesis, and the recent work by Korkakaki (2017) on nitrogen-rich waste streams, many important topics have been covered.

Regarding the optimization of the PHA production process by directing the pre-fermentation step towards specific fermentation products, it might still be worth to determine the impact of ethanol and valerate – alone and in a mixture with acetate – on the enrichment of PHA-producing bacteria. Ethanol is a common fermentation product and known to give rise to PHB production. It should likely be avoided as substrate, though, as simultaneously other (storage) compounds are produced (Tamis et al., 2014a). Valerate is usually a minor fermentation product. However, it might be preferred over propionate for the synthesis of HV monomers, like butyrate is preferred over acetate for the synthesis of HB (Chapter 2). In that case, the synthesis of valerate should be optimized, for example by adjusting the pH (Albuquerque et al., 2007; Reis et al., 1991).

The developed model for staged CSTR systems (Chapter 5) should still be validated with (lab-scale) experiments. The experiments with continuous carbon supply in Chapter 6 already revealed that the equation used for PHB degradation ($q_{PHB} = k \cdot f_{PHB}{}^{2/3}$) does not properly describe the degradation of PHB in presence of external substrate (Figure 6.4). Likely, the bacteria reached their maximum biomass-specific growth rate and PHB degradation was no longer the rate-determining step. A new kinetic description should be developed. Also, because the current expression is based on the assumption that during an SBR cycle the biomass concentration is constant (Tamis et al., 2014b). When the SBR is operated at 12 h cycles and 1 d SRT, this is not a valid assumption – the biomass will double each cycle. Nevertheless, the formula generally fitted the PHB degradation.

Besides for the validation of the model, in general, more experiments with the staged CSTR system will be required. A CSTR system with just two stages is most practical to investigate at lab-scale and would scientifically be interesting to study. The investigation of a (dispersed) plug flow system, with more reactors in series, will be more relevant in view of industrial implementation and should be realized in an industrial setting, at pilot-scale, rather than in the lab.

Not related to the development of the non-axenic PHA production process, but at a more fundamental level, it may be interesting to analyze the genome and/or gene expression of *P. acidivorans* in biomass samples collected during the enrichment period. The timescale of the enrichment period in Chapter 4 (2 years), together with the continued predominance of *P. acidivorans* and significant reduction of the feast phase length, suggests that the enrichment process involved more than just the wash-out of flanking populations. The kinetic properties of *P. acidivorans* itself – especially its maximum biomass-specific acetate uptake rate – will likely have changed as well. Similarly, Johnson et al. (2009a) reported the gradual increase of the biomass-specific PHB production rate and PHB storage capacity over the course of many months. Analysis of the genome and/or gene expression of *P. acidivorans* over time may reveal what changed and provide more insight into possible cellular adaptation alongside the microbial selection.

Finally, the main character of this thesis, *Plasticicumulans acidivorans*, is not only a

highly interesting organism for the production of PHA by microbial enrichment cultures, but could also be interesting for pure culture processes or the genetic modification of others. Studying its genome, gene expression, or metabolome could reveal what makes that *P. acidivorans* has such a high specific substrate uptake rate and stores such large amounts of PHA, or how its dynamic metabolism is regulated, for example.

ABBREVIATIONS

AcCoA	acetyl coenzyme A
ATP	adenosine triphosphate
C:N ratio	carbon-to-nitrogen ratio
CL	cycle length
Cmol	carbon-mole
CSTR	continuous stirred-tank reactor
DGGE	denaturing gradient gel electrophoresis
DO	dissolved oxygen
F/M ratio	food-to-microorganism ratio
FISH	fluorescent in situ hybridization
GAO	glycogen-accumulating organism
HB	3-hydroxybutyrate
HPLC	high-performance liquid chromatography
HRT	hydraulic retention time
HV	3-hydroxyvalerate
NADH	nicotinamide adenine dinucleotide
OLR	organic loading rate
OTR	oxygen transfer rate
PAO	phosphate-accumulating organism
PCR	polymerase chain reaction
PHA	polyhydroxyalkanoate

PHB	poly(3-hydroxybutyrate)
PHBV	poly(3-hydroxybutyrate-co-3-hydroxyvalerate)
PP	polypropylene
qPCR	quantitative real-time PCR
RuMP	ribulose monophosphate
SBR	sequencing batch reactor
SFBR	sequencing fed-batch reactor
SRT	solids retention time
SSqRE	sum of the squared relative error
TSS	total suspended solids
VFA	volatile fatty acid

REFERENCES

Agler, M.T., Wrenn, B.A., Zinder, S.H., and Angenent, L.T., 2011. Waste to bioproduct conversion with undefined mixed cultures: The carboxylate platform. Trends Biotechnol 29 (2), 70–78.

Albuquerque, M.G.E., Eiroa, M., Torres, C., Nunes, B.R., and Reis, M.A.M., 2007. Strategies for the development of a side stream process for polyhydroxyalkanoate (PHA) production from sugar cane molasses. J Biotechnol 130 (4), 411–421.

Albuquerque, M.G.E., Concas, S., Bengtsson, S., and Reis, M.A.M., 2010a. Mixed culture polyhydroxyalkanoates production from sugar molasses: The use of a 2-stage CSTR system for culture selection. Bioresour Technol 101 (18), 7112–7122.

Albuquerque, M.G.E., Torres, C.A.V., and Reis, M.A.M., 2010b. Polyhydroxyalkanoate (PHA) production by a mixed microbial culture using sugar molasses: Effect of the influent substrate concentration on culture selection. Water Res 44 (11), 3419–3433.

Albuquerque, M.G.E., Carvalho, G., Kragelund, C., Silva, A.F., Barreto Crespo, M.T., Reis, M.A.M., and Nielsen, P.H., 2013. Link between microbial composition and carbon substrate-uptake preferences in a PHA-storing community. ISME J 7 (1), 1–12.

Amann, R.I., Binder, B.J., Olson, R.J., Chisholm, S.W., Devereux, R., and Stahl, D.A., 1990. Combination of 16S rRNA-targeted oligonucleotide probes with flow cytometry for analyzing mixed microbial populations. Appl Environ Microbiol 56 (6), 1919–1925.

Anderson, A.J. and Dawes, E.A., 1990. Occurrence, metabolism, metabolic role, and industrial uses of bacterial polyhydroxyalkanoates. Microbiol Rev 54 (4), 450–472.

Anterrieu, S., Quadri, L., Geurkink, B., Dinkla, I., Bengtsson, S., Arcos-Hernandez, M., Alexandersson, T., Morgan-Sagastume, F., Karlsson, A., Hjort, M., Karabegovic, L., Magnusson, P., Johansson, P., Christensson, M., and Werker, A., 2014. Integration of biopolymer production with process water treatment at a sugar factory. New Biotechnol 31 (4), 308–323.

Anthony, C., 1978. The prediction of growth yields in methylotrophs. J Gen Microbiol 104 (1), 91–104.

Baev, M.V., Schklyar, N.L., Chistoserdova, L.V., Chistoserdov, A.Y., Polanuer, B.M., Tsygankov, Y.D., and Sterkin, V.E., 1992. Growth of the obligate methylotroph *Methylobacillus flagellatum* under stationary and nonstationary conditions during continuous cultivation. Biotechnol Bioeng 39 (6), 688–695.

Beccari, M., Dionisi, D., Giuliani, A., Majone, M., and Ramadori, R., 2002. Effect of different carbon sources on aerobic storage by activated sludge. Water Sci Technol 45 (6), 157–168.

Beccari, M., Bertin, L., Dionisi, D., Fava, F., Lampis, S., Majone, M., Valentino, F., Vallini, G., and Villano, M., 2009. Exploiting olive oil mill effluents as a renewable resource for production of biodegradable polymers through a combined anaerobic-aerobic process. J Chem Technol Biotechnol 84 (6), 901–908.

Bengtsson, S., Hallquist, J., Werker, A., and Welander, T., 2008a. Acidogenic fermentation of industrial wastewaters: Effects of chemostat retention time and pH on volatile fatty acids production. Biochem Eng J 40 (3), 492–499.

Bengtsson, S., Werker, A., Christensson, M., and Welander, T., 2008b. Production of polyhydroxyalkanoates by activated sludge treating a paper mill wastewater. Bioresour Technol 99 (3), 509–516.

Bengtsson, S., 2009. The utilization of glycogen accumulating organisms for mixed culture production of polyhydroxyalkanoates. Biotechnol Bioeng 104 (4), 698–708.

Bengtsson, S., Pisco, A.R., Reis, M.A.M., and Lemos, P.C., 2010. Production of polyhydroxyalkanoates from fermented sugar cane molasses by a mixed culture enriched in glycogen accumulating organisms. J Biotechnol 145 (3), 253–263.

Beun, J.J., Dircks, K., van Loosdrecht, M.C.M., and Heijnen, J.J., 2002. Poly-β-hydroxybutyrate metabolism in dynamically fed mixed microbial cultures. Water Res 36 (5), 1167–1180.

Bourque, D., Ouellette, B., André, G., and Groleau, D., 1992. Production of poly-β-hydroxybutyrate from methanol: characterization of a new isolate of *Methylobacterium extorquens*. Appl Microbiol Biotechnol 37 (1), 7–12.

Bourque, D., Pomerleau, Y., and Groleau, D., 1995. High-cell-density production of poly-β-hydroxybutyrate (PHB) from methanol by *Methylobacterium extorquens*: production of high-molecular-mass PHB. Appl Microbiol Biotechnol 44 (3-4), 367–376.

Cavaillé, L., Albuquerque, M., Grousseau, E., Lepeuple, A.S., Uribelarrea, J.L., Hernandez-Raquet, G., and Paul, E., 2016. Understanding of polyhydroxybutyrate

production under carbon and phosphorus-limited growth conditions in non-axenic continuous culture. Bioresour Technol 201, 65–73.

Chanprateep, S., 2010. Current trends in biodegradable polyhydroxyalkanoates. J Biosci Bioeng 110 (6), 621–632.

Chen, G.Q., 2009. A microbial polyhydroxyalkanoates (PHA) based bio- and materials industry. Chem Soc Rev 38 (8), 2434–2446.

Chistoserdova, L., Lapidus, A., Han, C., Goodwin, L., Saunders, L., Brettin, T., Tapia, R., Gilna, P., Lucas, S., Richardson, P.M., and Lidstrom, M.E., 2007. Genome of *Methylobacillus flagellatus*, molecular basis for obligate methylotrophy, and polyphyletic origin of methylotrophy. J Bacteriol 189 (11), 4020–4027.

Chistoserdova, L. and Lidstrom, M.E., 2013. Aerobic methylotrophic prokaryotes, Springer, Berlin Heidelberg, *The prokaryotes: Prokaryotic physiology and biochemistry*, chapter 7, pp. 267–285.

Choi, J. and Lee, Y.S., 1999. Factors affecting the economics of polyhydroxyalkanoate production by bacterial fermentation. Appl Microbiol Biotechnol 51 (1), 13–21.

Chudoba, J., Ottová, V., and Maděra, V., 1973a. Control of activated sludge filamentous bulking - I. effect of the hydraulic regime or degree of mixing in an aeration tank. Water Res 7 (8), 1163–1182.

Chudoba, J., Grau, P., and Ottová, V., 1973b. Control of activated-sludge filamentous bulking - II. selection of microorganisms by means of a selector. Water Res 7 (10), 1389–1406.

Coats, E.R., Loge, F.J., Smith, W.A., Thompson, D.N., and Wolcott, M.P., 2007. Functional stability of a mixed microbial consortium producing PHA from waste carbon sources. Appl Biochem Biotechnol 137-140, 909–925.

Daims, H., Brühl, A., Amann, R., Schleifer, K.H., and Wagner, M., 1999. The domain-specific probe EUB338 is insufficient for the detection of all bacteria: Development and evaluation of a more comprehensive probe set. Syst Appl Microbiol 22 (3), 434–444.

Danckwerts, P.V., 1953. Continuous flow systems: Distribution of residence times. Chem Eng Sci 2 (1), 1–13.

Defoirdt, T., Boon, N., Sorgeloos, P., Verstraete, W., and Bossier, P., 2009. Short-chain fatty acids and poly-β-hydroxyalkanoates: (New) Biocontrol agents for a sustainable animal production. Biotechnol Adv 27 (6), 680–685.

Dias, J.M.L., Serafim, L.S., Lemos, P.C., Reis, M.A.M., and Oliveira, R., 2005. Mathematical modelling of a mixed culture cultivation process for the production of polyhydroxybutyrate. Biotechnol Bioeng 92 (2), 209–222.

van Dien, S.J. and Lidstrom, M.E., 2002. Stoichiometric model for evaluating the metabolic capabilities of the facultative methylotroph *Methylobacterium extorquens* AM1, with application to reconstruction of C3 and C4 metabolism. Biotechnol Bioeng 78 (3), 296–312.

Dionisi, D., Majone, M., Papa, V., and Beccari, M., 2004. Biodegradable polymers from organic acids by using activated sludge enriched by aerobic periodic feeding. Biotechnol Bioeng 85 (6), 569–579.

Dionisi, D., Carucci, G., Papini, M.P., Riccardi, C., Majone, M., and Carrasco, F., 2005a. Olive oil mill effluents as a feedstock for production of biodegradable polymers. Water Res 39 (10), 2076–2084.

Dionisi, D., Beccari, M., Di Gregorio, S., Majone, M., Papini, M.P., and Vallini, G., 2005b. Storage of biodegradable polymers by an enriched microbial community in a sequencing batch reactor operated at high organic load rate. J Chem Technol Biotechnol 80 (11), 1306–1318.

Dionisi, D., Majone, M., Levantesi, C., Bellani, A., and Fuoco, A., 2006. Effect of feed length on settleability, substrate uptake and storage in a sequencing batch reactor treating an industrial wastewater. Environ Technol 27 (8), 901–908.

Dionisi, D., Majone, M., Vallini, G., Di Gregorio, S., and Beccari, M., 2007. Effect of the length of the cycle on biodegradable polymer production and microbial community selection in a sequencing batch reactor. Biotechnol Prog 23 (5), 1064–1073.

Dobroth, Z.T., Hu, S., Coats, E.R., and McDonald, A.G., 2011. Polyhydroxybutyrate synthesis on biodiesel wastewater using mixed microbial consortia. Bioresour Technol 102 (3), 3352–3359.

Fernández-Dacosta, C., Posada, J.A., Kleerebezem, R., Cuellar, M.C., and Ramirez, A., 2015. Microbial community-based polyhydroxyalkanoates (PHAs) production from wastewater: Techno-economic analysis and ex-ante environmental assessment. Bioresour Technol 185, 368–377.

Fernández-Dacosta, C., Posada, J.A., and Ramirez, A., 2016. Techno-economic and carbon footprint assessment of methyl crotonate and methyl acrylate production from wastewater-based polyhydroxybutyrate (PHB). J Clean Prod 137, 942–952.

Föllner, C., Babel, W., Valentin, H., and Steinbüchel, A., 1993. Expression of polyhydroxyalkanoic-acid-biosynthesis genes in methylotrophic bacteria relying on the ribulose monophosphate pathway. Appl Microbiol Biotechnol 40, 284–291.

Gujer, W., Henze, M., Mino, T., and van Loosdrecht, M.C.M., 1999. Activated sludge model No. 3. Water Sci Technol 39 (1), 183–193.

Gujer, W., 2002. Microscopic versus macroscopic biomass models in activated sludge systems. Water Sci Technol 45 (6), 1–11.

Hao, O.J. and Chang, C.H., 1987. Kinetics of growth and phosphate uptake in pure culture studies of *Acinetobacter* species. Biotechnol Bioeng 29 (7), 819–831.

Jacquel, N., Lo, C.W., Wei, Y.H., Wu, H.S., and Wang, S.S., 2008. Isolation and purification of bacterial poly(3-hydroxyalkanoates). Biochem Eng J 39 (1), 15 – 27.

Jiang, Y., Marang, L., Kleerebezem, R., Muyzer, G., and van Loosdrecht, M.C.M., 2011a. Effect of temperature and cycle length on microbial competition in PHB-producing sequencing batch reactor. ISME J 5 (5), 896–907.

Jiang, Y., Hebly, M., Kleerebezem, R., Muyzer, G., and van Loosdrecht, M.C.M., 2011b. Metabolic modeling of mixed substrate uptake for polyhydroxyalkanoate (PHA) production. Water Res 45 (3), 1309–1321.

Jiang, Y., 2011. Polyhydroxyalkanoates production by bacterial enrichments. Ph.D. thesis, Delft University of Technology.

Jiang, Y., Marang, L., Kleerebezem, R., Muyzer, G., and van Loosdrecht, M.C.M., 2011c. Polyhydroxybutyrate production from lactate using a mixed microbial culture. Biotechnol Bioeng 108 (9), 2022–2035.

Jiang, Y., Sorokin, D.Y., Kleerebezem, R., Muyzer, G., and van Loosdrecht, M.C., 2011d. *Plasticicumulans acidivorans* gen. nov., sp. nov., a polyhydroxyalkanoate-accumulating gammaproteobacterium from a sequencing-batch bioreactor. Int J Syst Evol Microbiol 61 (9), 2314–2319.

Jiang, Y., Marang, L., Tamis, J., van Loosdrecht, M.C.M., Dijkman, H., and Kleerebezem, R., 2012. Waste to resource: Converting paper mill wastewater to bioplastic. Water Res 46 (17), 5517–5530.

Jiang, Y., Sorokin, D.Y., Junicke, H., Kleerebezem, R., and van Loosdrecht, M.C.M., 2014. *Plasticicumulans lactativorans* sp. nov., a polyhydroxybutyrate-accumulating gammaproteobacterium from a sequencing-batch bioreactor fed with lactate. Int J Syst Evol Microbiol 64 (1), 33–38.

Jiang, Y., Mikova, G., Kleerebezem, R., van der Wielen, L.A., and Cuellar, M.C., 2015. Feasibility study of an alkaline-based chemical treatment for the purification of polyhydroxybutyrate produced by a mixed enriched culture. AMB Express 5 (5).

Johnson, K., Jiang, Y., Kleerebezem, R., Muyzer, G., and van Loosdrecht, M.C.M., 2009a. Enrichment of a mixed bacterial culture with a high polyhydroxyalkanoate storage capacity. Biomacromolecules 10 (4), 670–676.

Johnson, K., Kleerebezem, R., and van Loosdrecht, M.C.M., 2009b. Model-based data evaluation of polyhydroxybutyrate producing mixed microbial cultures in aerobic sequencing batch and fed-batch reactors. Biotechnol Bioeng 104 (1), 50–67.

Johnson, K., Kleerebezem, R., and van Loosdrecht, M.C.M., 2010. Influence of ammonium on the accumulation of polyhydroxybutyrate (PHB) in aerobic open mixed cultures. J Biotechnol 147 (2), 73–79.

Johnson, K., 2010. PHA Production in Aerobic Mixed Microbial Cultures. Ph.D. thesis, Delft University of Technology.

Khosravi-Darani, K., Mokhtari, Z.B., Amai, T., and Tanaka, K., 2013. Microbial production of poly(hydroxybutyrate) from C1 carbon sources. Appl Microbiol Biotechnol 97 (4), 1407–1424.

Kim, S.W., Kim, P., Lee, H.S., and Kim, J.H., 1996. High production of poly-β-hydroxybutyrate (PHB) from *Methylobacterium organophilum* under potassium limitation. Biotechnol Lett 18 (1), 25–30.

Kleerebezem, R., Joosse, B., Rozendal, R., and van Loosdrecht, M.C.M., 2015. Anaerobic digestion without biogas? Rev Environ Sci Biotechnol 14 (4), 787–801.

Koller, M., Atlíc, A., Dias, M., Reiterer, A., and Braunegg, G., 2010. Microbial PHA production from waste raw materials, Springer, Berlin Heidelberg, *Microbiology Monographs*, volume 14, pp. 85–119.

Koller, M., Niebelschütz, H., and Braunegg, G., 2013. Strategies for recovery and purification of poly[(R)-3-hydroxyalkanoates] (PHA) biopolyesters from surrounding biomass. Eng Life Sci 13 (6), 549–562.

Korkakaki, E., Mulders, M., Veeken, A., Rozendal, R., van Loosdrecht, M.C., and Kleerebezem, R., 2016a. PHA production from the organic fraction of municipal solid waste (OFMSW): Overcoming the inhibitory matrix. Water Res 96, 74–83.

Korkakaki, E., van Loosdrecht, M.C., and Kleerebezem, R., 2016b. Survival of the fastest: Selective removal of the side population for enhanced PHA production in a mixed substrate enrichment. Bioresour Technol 216, 1022–1029.

Korkakaki, E., 2017. Process optimization for polyhydroxyalkanoate (PHA) production from waste via enrichment cultures. Ph.D. thesis, Delft University of Technology.

Krishna, C. and van Loosdrecht, M.C.M., 1999. Effect of temperature on storage polymers and settleability of activated sludge. Water Res 33 (10), 2374–2382.

Lee, S.Y., 1996. Bacterial polyhydroxyalkanoates. Biotechnol Bioeng 49 (1), 1–14.

Lemoigne, M., 1926. Produits de dehydration et de polymerisation de l'acide β-oxobutyrique. Bull Soc Chim Biol 8, 770–782.

Lemos, P.C., Serafim, L.S., and Reis, M.A.M., 2006. Synthesis of polyhydroxyalkanoates from different short-chain fatty acids by mixed cultures submitted to aerobic dynamic feeding. J Biotechnol 122 (2), 226–238.

van Loosdrecht, M., Pot, M., and Heijnen, J., 1997. Importance of bacterial storage polymers in bioprocesses. Water Sci Technol 35 (1), 41–47.

Ludwig, W., Strunk, O., Westram, R., Richter, L., Meier, H., Yadhukumar, Buchner, A., Lai, T., Steppi, S., Jobb, G., Förster, W., Brettske, I., Gerber, S., Ginhart, A.W., Gross, O., Grumann, S., Hermann, S., Jost, R., König, A., Liss, T., Lüßmann, R., May, M., Nonhoff, B., Reichel, B., Strehlow, R., Stamatakis, A., Stuckmann, N., Vilbig, A., Lenke, M., Ludwig, T., Bode, A., and Schleifer, K.H., 2004. ARB: a software environment for sequence data. Nucleic Acids Res 32 (4), 1363–1371.

Luef, K.P., Stelzer, F., and Wiesbrock, F., 2015. Poly(hydroxy alkanoate)s in medical applications. Chem Biochem Eng 29 (2), 287–297.

Manz, W., Amann, R., Ludwig, W., Wagner, M., and Schleifer, K.H., 1992. Phylogenetic oligodeoxynucleotide probes for the major subclasses of proteobacteria: Problems and solutions. Syst Appl Microbiol 15 (4), 593–600.

Marang, L., Jiang, Y., van Loosdrecht, M.C.M., and Kleerebezem, R., 2013. Butyrate as preferred substrate for polyhydroxybutyrate production. Bioresour Technol 142, 232–239.

Marang, L., Jiang, Y., van Loosdrecht, M.C.M., and Kleerebezem, R., 2014. Impact of non-storing biomass on PHA production: An enrichment culture on acetate and methanol. Int J Biol Macromol 71, 74–80.

Marang, L., van Loosdrecht, M.C.M., and Kleerebezem, R., 2015. Modeling the competition between PHA-producing and non-PHA-producing bacteria in feast-famine SBR and staged CSTR systems. Biotechnol Bioeng 112 (12), 2475–2484.

Marang, L., van Loosdrecht, M.C.M., and Kleerebezem, R., 2016. Combining the enrichment and accumulation step in non-axenic PHA production: Cultivation of *Plasticicumulans acidivorans* at high volume exchange ratios. J Biotechnol 231, 260–267.

Martins, A.M.P., Heijnen, J.J., and van Loosdrecht, M.C.M., 2003. Effect of feeding pattern and storage on the sludge settleability under aerobic conditions. Water Res 37 (11), 2555–2570.

Mockos, G.R., Smith, W.A., Loge, F.J., and Thompson, D.N., 2008. Selective enrichment of a methanol-utilizing consortium using pulp and paper mill waste streams. Appl Biochem Biotechnol 148 (1-3), 211–226.

Morgan-Sagastume, F., Karlsson, A., Johansson, P., Pratt, S., Boon, N., Lant, P., and Werker, A., 2010. Production of polyhydroxyalkanoates in open, mixed cultures from a waste sludge stream containing high levels of soluble organics, nitrogen and phosphorus. Water Res 44 (18), 5196–5211.

Morgan-Sagastume, F., Valentino, F., Hjort, M., Cirne, D., Karabegovic, L., Gerardin, F., Johansson, P., Karlsson, A., Magnusson, P., Alexandersson, T., Bengtsson, S., Majone, M., and Werker, A., 2014. Polyhydroxyalkanoate (PHA) production from sludge and municipal wastewater treatment. Water Sci Technol 69 (1), 177–184.

Muyzer, G., de Waal, E., and Uitterlinden, A., 1993. Profiling of complex microbial populations by denaturing gradient gel electrophoresis analysis of polymerase chain reaction-amplified genes coding for 16S rRNA. Appl Environ Microbiol 59 (3), 695–700.

van Niekerk, A.M., Jenkins, D., and Richard, M.G., 1987. The competitive growth of *Zoogloea ramigera* and Type 021N in activated sludge and pure culture: A model for low F:M bulking. J Water Pollut Control Fed 59 (5), 262–273.

Pedrós-Alió, C., Mas, J., and Guerrero, R., 1985. The influence of poly-β-hydroxybutyrate accumulation on cell volume and buoyant density in *Alcaligenes eutrophus*. Arch Microbiol 143 (2), 178–184.

Peyraud, R., Schneider, K., Kiefer, P., Massou, S., Vorholt, J., and Portais, J.C., 2011. Genome-scale reconstruction and system level investigation of the metabolic network of *Methylobacterium extorquens* AM1. BMC Syst Biol 5 (1), 189.

Pfluger, A.R., Wu, W.M., Pieja, A.J., Wan, J., Rostkowski, K.H., and Criddle, C.S., 2011. Selection of type I and type II methanotrophic proteobacteria in a fluidized bed reactor under non-sterile conditions. Bioresour Technol 102 (21), 9919–9926.

Pham, T.P.T., Kaushik, R., Parshetti, G.K., Mahmood, R., and Balasubramanian, R., 2015. Food waste-to-energy conversion technologies: Current status and future directions. Waste Manage 38, 399–408.

Pieja, A.J., Rostkowski, K.H., and Criddle, C.S., 2011. Distribution and selection of poly-3-hydroxybutyrate production capacity in methanotrophic proteobacteria. Microb Ecol 62 (3), 564–573.

Reis, M.A.M., Lemos, P.C., Martins, M.J., Costa, P.C., Gonçalves, L.M.D., and Carrondo, M.J.T., 1991. Influence of sulfates and operational parameters on volatile fatty acids concentration profile in acidogenic phase. Bioprocess Biosyst Eng 6 (4), 145–151.

Reis, M.A.M., Serafim, L.S., Lemos, P.C., Ramos, A.M., Aguiar, F.R., and van Loosdrecht, M.C.M., 2003. Production of polyhydroxyalkanoates by mixed microbial cultures. Bioprocess Biosyst Eng 25 (6), 377–385.

Rhu, D.H., Lee, W.H., Kim, J.Y., and Choi, E., 2003. Polyhydroxyalkanoate (PHA) production from waste. Water Sci Technol 48 (8), 221–228.

Satoh, H., Iwamoto, Y., Mino, T., and Matsuo, T., 1998. Activated sludge as a possible source of biodegradable plastic. Water Sci Technol 38 (2), 103–109.

Schäfer, H. and Muyzer, G., 2001. Denaturing gradient gel electrophoresis in marine microbial ecology, Academic Press, *Methods in Microbiology*, volume 30, pp. 425–468.

Schrader, J., Schilling, M., Holtmann, D., Sell, D., Filho, M.V., Marx, A., and Vorholt, J.A., 2009. Methanol-based industrial biotechnology: Current status and future perspectives of methylotrophic bacteria. Trends Biotechnol 27 (2), 107–115.

Schuler, A.J., 2005. Diversity matters: Dynamic simulation of distributed bacterial states in suspended growth biological wastewater treatment systems. Biotechnol Bioeng 91 (1), 62–74.

Schuler, A.J., 2006. Process hydraulics, distributed bacterial states, and biological phosphorus removal from wastewater. Biotechnol Bioeng 94 (5), 909–920.

Schweitzer, D., Mullen, C.A., Boateng, A.A., and Snell, K.D., 2015. Biobased *n*-butanol prepared from poly-3-hydroxybutyrate: Optimization of the reduction of *n*-butyl crotonate to *n*-butanol. Org Process Res Dev 19 (7), 710–714.

Serafim, L.S., Lemos, P.C., Oliveira, R., and Reis, M.A.M., 2004. Optimization of polyhydroxybutyrate production by mixed cultures submitted to aerobic dynamic feeding conditions. Biotechnol Bioeng 87 (2), 145–160.

Serafim, L.S., Lemos, P.C., Albuquerque, M.G.E., and Reis, M.A.M., 2008. Strategies for PHA production by mixed cultures and renewable waste materials. Appl Microbiol Biotechnol 81, 615–628.

Shi, H., Shiraishi, M., and Shimizu, K., 1997. Metabolic flux analysis for biosynthesis of poly(β-hydroxybutyric acid) in *Alcaligenes eutrophus* from various carbon sources. J Ferm Bioeng 84 (6), 579–587.

Šmejkalová, H., Erb, T.J., and Fuchs, G., 2010. Methanol assimilation in *Methylobacterium extorquens* AM1: demonstration of all enzymes and their regulation. PLoS ONE 5 (10), e13001.

Spekreijse, J., Le Nôtre, J., Sanders, J.P.M., and Scott, E.L., 2015. Conversion of polyhydroxybutyrate (PHB) to methyl crotonate for the production of biobased monomers. J Appl Polym Sci 132 (35), 42462.

Spekreijse, J., Ortega, J.H., Sanders, J., Bitter, J., and Scott, E., 2016. Conversion of polyhydroxyalkanoates to methyl crotonate using whole cells. Bioresour Technol 211, 267–272.

Steinbüchel, A., 1991. Polyhydroxyalkanoic acids, Stockton Press, New York, *Biomaterials: Novel Materials from Biological Sources*, chapter 3, pp. 123–213.

Steinbüchel, A. and Valentin, H.E., 1995. Diversity of bacterial polyhydroxyalkanoic acids. FEMS Microbiol Lett 128 (3), 219–228.

Tamis, J., Lužkov, K., Jiang, Y., van Loosdrecht, M.C.M., and Kleerebezem, R., 2014a. Enrichment of *Plasticicumulans acidivorans* at pilot-scale for PHA production on industrial wastewater. J Biotechnol 192 (A), 161–169.

Tamis, J., Marang, L., Jiang, Y., van Loosdrecht, M.C.M., and Kleerebezem, R., 2014b. Modeling PHA-producing microbial enrichment cultures - towards a generalized model with predictive power. New Biotechnol 31 (4), 324–334.

Tamis, J., Joosse, B.M., van Loosdrecht, M.C.M., and Kleerebezem, R., 2015. High-rate volatile fatty acid (VFA) production by a granular sludge process at low pH. Biotechnol Bioeng 112 (11), 2248–2255.

Tan, G.Y.A., Chen, C.L., Li, L., Ge, L., Wang, L., Razaad, I.M.N., Li, Y., Zhao, L., Mo, Y., and Wang, J.Y., 2014. Start a research on biopolymer polyhydroxyalkanoate (PHA): A review. Polymers 6 (3), 706–754.

Temudo, M.F., Kleerebezem, R., and van Loosdrecht, M.C.M., 2007. Influence of the pH on (open) mixed culture fermentation of glucose: A chemostat study. Biotechnol Bioeng 98 (1), 69–79.

Towner, K., 2006. The Genus *Acinetobacter*, Springer, New York, *The Prokaryotes*, volume 6, chapter 25, pp. 746–758.

Valentino, F., Beccari, M., Fraraccio, S., Zanaroli, G., and Majone, M., 2014. Feed frequency in a sequencing batch reactor strongly affects the production of polyhydroxyalkanoates (PHAs) from volatile fatty acids. New Biotechnol 31 (4), 264–275.

Vandamme, P. and Coenye, T., 2004. Taxonomy of the genus *Cupriavidus*: A tale of lost and found. Int J Syst Evol Microbiol 54 (6), 2285–2289.

Verachtert, H., van den Eynden, E., Poffé, R., and Houtmeyers, J., 1980. Relations between substrate feeding pattern and development of filamentous bacteria in activated sludge processes: Part II. Influence of substrates present in the influent. Eur J Appl Microbiol Biotechnol 9 (2), 137–149.

Vishniac, W. and Santer, M., 1957. The Thiobacilli. Bacteriol Rev 21 (3), 195–213.

Wagner, M., Erhart, R., Manz, W., Amann, R., Lemmer, H., Wedi, D., and Schleifer, K.H., 1994. Development of an rRNA-targeted oligonucleotide probe specific for the genus *Acinetobacter* and its application for in situ monitoring in activated sludge. Appl Environ Microbiol 60 (3), 792–800.

Yezza, A., Fournier, D., Halasz, A., and Hawari, J., 2006. Production of polyhydroxyalkanoates from methanol by a new methylotrophic bacterium *Methylobacterium* sp. GW2. Appl Microbiol Biotechnol 73 (1), 211–218.

Zhang, X., Luo, R., Wang, Z., Deng, Y., and Chen, G.Q., 2009. Application of (R)-3-hydroxyalkanoate methyl esters derived from microbial polyhydroxyalkanoates as novel biofuels. Biomacromolecules 10 (4), 707–711.

Zoetemeyer, R.J., van den Heuvel, J.C., and Cohen, A., 1982. pH influence on acidogenic dissimilation of glucose in an anaerobic digestor. Water Res 16 (3), 303–311.

A

PROGRAM CODE AGENT-BASED MODEL 2-STAGE CSTR SYSTEM

```
%% AGENT BASED MODEL 2-CSTR SYSTEM (version 2014-11)

% Modeling substrate uptake, growth and PHB production in a 2-stage CSTR
% system with Plasticicumulans acidivorans and another, non-storing bacterium.
% The bacteria are grown on sodium acetate as sole carbon source.
%
%                               ^
%                            50%|        ____________
%                 _______       |   50% |            |
%                |       |- - - - - - - >|            |
%                | Feast |               |   Famine   |
%                |_______|< - - - - - - -|            |
%                             100%       |____________|
%

function ABModel_2CSTR_201411

clear
clc

global recycle_ratio RT_feast RT_famine ...
       Pa_qS_max Pa_qX_max Pa_mATP Pa_alfa Pa_k Pa_K_S Pa_K_N Pa_fPHB_max ...
       other_qX_max other_mATP other_K_S other_K_N ...
       Y_PHB_S Y_X_S Y_X_PHB Y_N_X Y_ATP_S Y_ATP_PHB


%% 1. INPUT: PROCESS PARAMETERS
   %SRT           =  24;    % Solid retention time (h)
    HRT           =  24;    % Hydraulic retention time (h)
    recycle_ratio =  0.5;   % Fraction of broth cycled between the reactors
    V_2           =  2;     % Working volume famine reactor (l)
    ff_ratio      =  0.065; % feast-to-famine ratio
    OLR           =  2.25;  % Organic loading rate (Cmmol/l/h)
    CN_ratio      =  8;     % C:N ratio


%% 2. INPUT: BIOMASS-SPECIFIC PARAMETERS (KINETICS)
    % Kinetic parameters of the PHB-producing bacterium, P. acidivorans
    Pa_qS_max     =  3.5;   % Max. specific substrate uptake rate (Cmol/Cmol/h)
    Pa_qX_max     =  0.1;   % Max. specific growth rate (Cmol/Cmol/h)
    Pa_mATP       =  0.001; % Specific ATP requirement for maintenance (mol/Cmol/h)
    Pa_alfa       =  3.0;   % Exponent of the PHB inhibition term (-)
    Pa_k          = -0.16;  % Rate constant for PHB degradation ((Cmol/Cmol)^(1/3)/h)
    Pa_K_S        =  0.3;   % Half-saturation constant substrate (Cmmol/l)
    Pa_K_N        =  0.001; % Half-saturation constant ammonium (mmol/l)
    Pa_fPHB_max   =  8.5;   % Max. fraction of PHB (Cmol/Cmol)

    % Kinetic parameters of the non-storing bacterium, i.e. 'Other'
    other_qX_max  =  0.47;  % Max. specific growth rate (Cmol/Cmol/h)
    other_mATP    =  0.001; % Specific ATP requirement for maintenance (mol/Cmol/h)
    other_K_S     =  0.1;   % Half-saturation constant substrate (Cmmol/l)
    other_K_N     =  0.001; % Half-saturation constant ammonium (mmol/l)


%% 3. INPUT: BIOMASS-SPECIFIC PARAMETERS (STOICHIOMETRIC YIELDS)
    % Overview of the considered reactions (on Cmol basis):
    % A  1 HAc + 1 ATP                         ->  1 AcCoA
    % 1  1 AcCoA                               ->  1 CO2 + 2 NADH
    % 2  1 AcCoA + 0.25 NADH                   ->  1 PHB
    % 3  1.267 AcCoA + 0.2 NH3 + 2.16 ATP      ->  1 X + 0.267 CO2 + 0.434 NADH
    % 4  1 PHB + 0.25 ATP                      ->  1 AcCoA + 0.25 NADH
    % O  1 NADH + 0.5 O2                       ->  delta ATP

    % Call functions calculating the yield with value for delta (P/O ratio)
    Y_PHB_S   = yield1(2.0); % PHB production from acetate (Cmol/Cmol)
    Y_X_S     = yield2(2.0); % Biomass growth on acetate (Cmol/Cmol)
    Y_X_PHB   = yield3(2.0); % Biomass growth on PHB (Cmol/Cmol)
    Y_N_X     = 0.20;        % Ammonium needed for growth (mol/Cmol)
    Y_ATP_S   = yield4(2.0); % Energy yield catabolism of acetate (mol/Cmol)
    Y_ATP_PHB = yield5(2.0); % Energy yield catabolism of PHB (mol/Cmol)
```

```
%% 4. CALCULATE FLOWS AND VOLUMES
    RT_feast  = ff_ratio/(1+ff_ratio) * recycle_ratio*HRT;
                                                % Average retention time feast (h)
    RT_famine = recycle_ratio*HRT - RT_feast;  % Average retention time famine (h)

    f_recycle = V_2/RT_famine;                  % Flow rate recycle stream (l/h)
    f_total   = 1/(1-recycle_ratio)*f_recycle; % Total flow leaving feast reactor (l/h)
    f_feed    = f_total - f_recycle;            % Flow rate influent (l/h)
    f_waste   = f_feed;                         % Flow rate waste stream (l/h)

    V_1       = RT_feast*(f_recycle+f_waste);  % Working volume feast reactor (l)

    cS_feed   = OLR * (V_1 + V_2/(1-recycle_ratio)) / f_feed;
                                                % Acetate conc. feed (Cmmol/l)
    cN_feed   = cS_feed / CN_ratio;             % Ammonium conc. feed (mmol/l)


%% 5. INITIAL CONDITIONS - CREATE INDIVIDUALS
    % Create an array with 5000 storers, 'P. acidivorans'
    % For all individuals: X = 0.001 Cmmol and PHB = 0.001 Cmmol
    storers             = zeros(5000,4);
    storers(1:5000,3:4) = 0.001;
    % Place 5% (250 indiv) in the feast, location = 1; and the rest in the
    % famine, location = 2
    storers(1:250,1)    = 1;
    storers(251:5000,1) = 2;
    % Randomly define the retention time of each individual
    parfor i = 1:5000
        if i <= 250
            storers(i,2) = random('exp',RT_feast);
        else
            storers(i,2) = random('exp',RT_famine);
        end
    end

    % Create an array with 5000 non-storers, 'Other'
    % For all individuals: X = 0.001 Cmmol and PHB = 0 Cmmol
    nonstorers             = zeros(5000,4);
    nonstorers(1:5000,3)   = 0.001;
    % Place 5% (250 indiv) in the feast, location = 1; and the rest in the
    % famine, location = 2
    nonstorers(1:250,1)    = 1;
    nonstorers(251:5000,1) = 2;
    % Randomly define the retention time of each individual
    parfor i = 1:5000
        if i <= 250
            nonstorers(i,2) = random('exp',RT_feast);
        else
            nonstorers(i,2) = random('exp',RT_famine);
        end
    end


%% 6. INITIAL CONDITIONS - OVERALL CONCENTRATIONS
    % Sum of X and P from 'P. acidivorans' in feast and famine:
    X_Pa1  = 0.25; % Cmmol P. acidivorans biomass in the feast reactor
    P1     = 0.25; % Cmmol PHB in the feast reactor
    X_Pa2  = 4.75; % Cmmol P. acidivorans biomass in the famine reactor
    P2     = 4.75; % Cmmol PHB in the famine reactor
    % Sum of X from 'Other' in feast and famine:
    X_oth1 = 0.25; % Cmmol other biomass in the feast reactor
    X_oth2 = 4.75; % Cmmol other biomass in the famine reactor

    % Set initial amounts of acetate and ammonium:
    S1     = 5.00; % Cmmol substrate (acetate) in the feast reactor
    N1     = 0.00; %  mmol NH4+ in the feast reactor
    S2     = 0.00; % Cmmol substrate (acetate) in the famine reactor
    N2     = 5.00; %  mmol NH4+ in the famine reactor


%% 7. RUN MODEL/SIMULATION
    % Time range, step, etc.
```

```
145     dt     = 0.005;       % length timestep (h)
146     T      = (0:dt:480)'; % time range simulation (h)
147     tpoint = 1;           % i.e. pointer for pre-allocated matrix 'Y'
148
149     % Pre-allocate storage for result matrix;
150     % total amounts of S, N, X_Pa, X_oth, and P (in (C)mmol) over time.
151     Y      = zeros(96001,10);
152     Y(1,:) = [S1 N1 X_Pa1 X_oth1 P1 S2 N2 X_Pa2 X_oth2 P2];
153
154     % Go!
155     for t = dt:dt:480
156
157         if t == round(t)
158             disp(t)       % To monitor the progress
159         end
160
161         % Reset values for change in total amount of S/N/X/P (in (C)mmol/h)
162         sum_dS1     = 0;        sum_dS2     = 0;
163         sum_dN1     = 0;        sum_dN2     = 0;
164         sum_dX_Pa1  = 0;        sum_dX_Pa2  = 0;
165         sum_dX_oth1 = 0;        sum_dX_oth2 = 0;
166         sum_dP1     = 0;        sum_dP2     = 0;
167
168         % Check if substrate and ammonium concentrations are non-negative
169         for k = [1,2,6,7]
170             if Y(tpoint,k) < 0
171                 fprintf('At t = %g h, compound %d got negative!\n', t,k);
172             end
173         end
174
175         % Update actual amounts and concentrations
176         nr_Pa    = length(storers);    % Actual number of P. acidivorans
177         nr_Other = length(nonstorers); % Actual number of other bacteria
178
179         cS1 = Y(tpoint,1)/V_1;  % Actual acetate conc. feast (Cmmol/l)
180         cN1 = Y(tpoint,2)/V_1;  % Actual ammonium conc. feast (mmol/l)
181         cS2 = Y(tpoint,6)/V_2;  % Actual acetate conc. famine (Cmmol/l)
182         cN2 = Y(tpoint,7)/V_2;  % Actual ammonium conc. famine (mmol/l)
183
184
185         for i = 1:nr_Pa
186         % For all individuals of 'P. acidivorans' (storers)...
187             % Run kinetic conversions:
188             if storers(i,1) == 1
189                 [X PHB dS1 dN1 dX_Pa1 dP1] = ...
190                             Pa_convert(storers(i,3),storers(i,4),dt,cS1,cN1);
191
192                 % Determine impact on overall S/N/X/P (in (C)mmol/h)
193                 sum_dS1      = sum_dS1     + dS1;
194                 sum_dN1      = sum_dN1     + dN1;
195                 sum_dX_Pa1   = sum_dX_Pa1  + dX_Pa1;
196                 sum_dP1      = sum_dP1     + dP1;
197
198                 % Update properties of individual
199                 storers(i,3) = X;
200                 storers(i,4) = PHB;
201
202             elseif storers(i,1) == 2
203                 [X PHB dS2 dN2 dX_Pa2 dP2] = ...
204                             Pa_convert(storers(i,3),storers(i,4),dt,cS2,cN2);
205
206                 % Determine impact on overall S/N/X/P (in (C)mmol/h)
207                 sum_dS2      = sum_dS2     + dS2;
208                 sum_dN2      = sum_dN2     + dN2;
209                 sum_dX_Pa2   = sum_dX_Pa2  + dX_Pa2;
210                 sum_dP2      = sum_dP2     + dP2;
211
212                 % Update properties of individual
213                 storers(i,3) = X;
214                 storers(i,4) = PHB;
215             end
216
```

```
            % Split/move/discard bacteria once their residence time in the
            % reactor has passed:
            if t > storers(i,2)
                [new indiv dX_Pa1 dP1 dX_Pa2 dP2] = Pa_move(storers(i,:),dt);

                % Determine impact on overall X/P (in Cmmol/h)
                sum_dX_Pa1   = sum_dX_Pa1  + dX_Pa1;
                sum_dP1      = sum_dP1     + dP1;
                sum_dX_Pa2   = sum_dX_Pa2  + dX_Pa2;
                sum_dP2      = sum_dP2     + dP2;

                % Update properties of individual
                storers(i,:) = indiv(1:4);

                % Add new individuals to 'storers'
                storers = [storers; new];
            end
        end

        for i = 1:nr_Other
        % For all individuals of 'Other' (non-storers)...
            % Run kinetic conversions:
            if nonstorers(i,1) == 1
                [X dS1 dN1 dX_oth1] = Other_convert(nonstorers(i,3),dt,cS1,cN1);

                % Determine impact on overall S/N/X (in (C)mmol/h)
                sum_dS1         = sum_dS1     + dS1;
                sum_dN1         = sum_dN1     + dN1;
                sum_dX_oth1     = sum_dX_oth1 + dX_oth1;

                % Update properties of individual
                nonstorers(i,3) = X;

            elseif nonstorers(i,1) == 2
                [X dS2 dN2 dX_oth2] = Other_convert(nonstorers(i,3),dt,cS2,cN2);

                % Determine impact on global S/N/X (in (C)mmol/h)
                sum_dS2         = sum_dS2     + dS2;
                sum_dN2         = sum_dN2     + dN2;
                sum_dX_oth2     = sum_dX_oth2 + dX_oth2;

                % Update properties of individual
                nonstorers(i,3) = X;
            end

            % Split/move/discard bacteria once their residence time in the
            % reactor has passed:
            if t > nonstorers(i,2)
                [new indiv dX_oth1 dX_oth2] = Other_move(nonstorers(i,:),dt);

                % Determine impact on overall X (in Cmmol/h)
                sum_dX_oth1     = sum_dX_oth1 + dX_oth1;
                sum_dX_oth2     = sum_dX_oth2 + dX_oth2;

                % Update properties of individual
                nonstorers(i,:) = indiv(1:4);

                % Add new individuals to 'nonstorers'
                nonstorers = [nonstorers; new];
            end

        end

        % Prepare data for a new round...
        % Save total amounts of S, N, X and PHB for next time point:
        % Feast reactor
        Y(tpoint+1, 1) = Y(tpoint, 1) + (f_feed*cS_feed + f_recycle*cS2 ...
                         - (f_recycle+f_waste)*cS1 + sum_dS1)*dt; % S1
        Y(tpoint+1, 2) = Y(tpoint, 2) + (f_feed*cN_feed + f_recycle*cN2 ...
                         - (f_recycle+f_waste)*cN1 + sum_dN1)*dt; % N1
        Y(tpoint+1, 3) = Y(tpoint, 3) +  sum_dX_Pa1 *dt; % X_Pa1
        Y(tpoint+1, 4) = Y(tpoint, 4) +  sum_dX_oth1*dt; % X_oth1
```

A

```
289         Y(tpoint+1, 5) = Y(tpoint, 5) +  sum_dP1    *dt; % P1
290         % Famine reactor
291         Y(tpoint+1, 6) = Y(tpoint, 6) + (f_recycle*(cS1-cS2) + sum_dS2)*dt; % S2
292         Y(tpoint+1, 7) = Y(tpoint, 7) + (f_recycle*(cN1-cN2) + sum_dN2)*dt; % N2
293         Y(tpoint+1, 8) = Y(tpoint, 8) +  sum_dX_Pa2 *dt; % X_Pa2
294         Y(tpoint+1, 9) = Y(tpoint, 9) +  sum_dX_oth2*dt; % X_oth2
295         Y(tpoint+1,10) = Y(tpoint,10) +  sum_dP2    *dt; % P2
296
297         % Update time point:
298         tpoint = tpoint + 1;
299
300         % Remove discarded individuals from the list:
301         % Go backwards through list of 'P. acidivorans' (storers)
302         for i = nr_Pa:-1:1
303             if storers(i,1) == 0
304                 storers(i,:)=[];
305             end
306         end
307         % Go backwards through list of 'Other' (non-storers)
308         for i = nr_Other:-1:1
309             if nonstorers(i,1) == 0
310                 nonstorers(i,:)=[];
311             end
312         end
313
314     end
315
316
317 %% 8. RESULT/OUTPUT
318     % Save workspace variables to MAT-file
319     save('preliminaryresult.mat')
320
321     % Calculate concentrations of S, N, X_Pa, X_oth and P over time and at
322     % the end of the simulation from the total amounts saved in 'Y':
323     Y_conc_feast  = Y(:,1: 5)./V_1;
324     Y_conc_famine = Y(:,6:10)./V_2;
325
326     conc_feast_end  = Y_conc_feast(end,:);
327     conc_famine_end = Y_conc_famine(end,:);
328
329     % Print flow rates, reactor volumes, and final concentrations:
330     disp('Determined flow rates, reactor volumes, and concentrations:');
331     fprintf('\n  HRT           = %#6.3g h',       HRT);
332     fprintf('\n  recycle ratio = %#6.3g h',       recycle_ratio);
333     fprintf('\n  rt_feast      = %#6.3g h',       RT_feast);
334     fprintf('\n  rt_famine     = %#6.3g h',       RT_famine);
335     fprintf('\n\n  V_feast       = %#6.3g l',     V_1);
336     fprintf('\n  V_famine      = %#6.3g l',       V_2);
337     fprintf('\n\n  f_feed        = %#6.3g l/h',   f_feed);
338     fprintf('\n  f_recycle     = %#6.3g l/h',     f_recycle);
339     fprintf('\n  f_waste       = %#6.3g l/h\n\n', f_waste);
340     disp('Composition feed:');
341     fprintf('  cS_feed    = %#6.3g Cmmol/l',      cS_feed);
342     fprintf('\n  cN_feed    = %#6.3g mmol/l\n\n', cN_feed);
343     disp('Final concentrations feast reactor:');
344     fprintf('  cS_1       = %#6.3g Cmmol/l',      conc_feast_end(1));
345     fprintf('\n  cN_1       = %#6.3g mmol/l',     conc_feast_end(2));
346     fprintf('\n  cX_Pa_1    = %#6.3g Cmmol/l',     conc_feast_end(3));
347     fprintf('\n  cX_other_1 = %#6.3g Cmmol/l',    conc_feast_end(4));
348     fprintf('\n  cPHB_1     = %#6.3g Cmmol/l\n\n',conc_feast_end(5));
349     disp('Final concentrations famine reactor:');
350     fprintf('  cS_2       = %#6.3g Cmmol/l',      conc_famine_end(1));
351     fprintf('\n  cN_2       = %#6.3g mmol/l',     conc_famine_end(2));
352     fprintf('\n  cX_Pa_2    = %#6.3g Cmmol/l',     conc_famine_end(3));
353     fprintf('\n  cX_other_2 = %#6.3g Cmmol/l',    conc_famine_end(4));
354     fprintf('\n  cPHB_2     = %#6.3g Cmmol/l\n',  conc_famine_end(5));
355
356     % Create graph with the overall concentrations over time:
357     figure
358     set(0,'DefaultAxesColorOrder',[1 0 0; 0 1 1; 0 0 0; 0 1 0; 1 1 0],...
359           'DefaultAxesLineStyleOrder','-|-.')
360     plot(T,Y_conc_feast, T,Y_conc_famine)
```

```
set(gca,'XTick',0:48:480)
set(gca,'XTickLabel',{'0','','96','','192','','288','','384','','480'})
set(gca,'YTick',0:5:30)
set(gca,'YTickLabel',{'0','5','10','15','20','25','30'})
xlabel('\bfTime (h)')
ylabel('\bf(Cmmol/l)')
legend('cS feast', 'cN feast', 'cX_{Pa} feast', 'cX_{other} feast', ...
       'cPHB feast', 'cS famine', 'cN famine', 'cX_{Pa} famine', ...
       'cX_{other} famine', 'cPHB famine', 'Location', 'NorthEastOutside')
pbaspect([3 2 2])
saveas(gcf,'Reactor_Development.pdf')

% Calculate the PHB content (fPHB, in Cmol/Cmol) of all individuals of
% P. acidivorans at the end of the simulation:
fPHB_feast  = [];
fPHB_famine = [];

for i = 1:length(storers)
    if storers(i,1) == 1
        fPHB_feast(end+1)  = storers(i,4)/storers(i,3);
    elseif storers(i,1) == 2
        fPHB_famine(end+1) = storers(i,4)/storers(i,3);
    end
end

% Plot final distribution of fPHB in the feast and famine reactor:
x_hist = 0.05:0.1:7.95;

hist_feast   = hist(fPHB_feast,x_hist);
hist_famine  = hist(fPHB_famine,x_hist);
nr_feast     = length(fPHB_feast);
nr_famine    = length(fPHB_famine);

histt_feast  = hist_feast./nr_feast .*100;
histt_famine = hist_famine./nr_famine .*100;

figure
bar(x_hist,histt_feast, 'barwidth',1)
set(gca,'XLim',[0 8])
set(gca,'YLim',[0 10])
set(gca,'YTick',0:1:10)
set(gca,'YTickLabel',{'0','','2','','4','','6','','8','','10'})
xlabel('PHB content feast reactor (Cmol_{PHB}/Cmol_{X})', 'FontWeight','bold')
ylabel('# individuals of \it{P. acidivorans} (%)', 'FontWeight','bold')
pbaspect([3 2 2])
saveas(gcf,'PHB_Distribution_Feast.pdf')

figure
bar(x_hist,histt_famine, 'barwidth',1)
set(gca,'XLim',[0 8])
set(gca,'YLim',[0 50])
set(gca,'YTick',0:5:50)
set(gca,'YTickLabel',{'0','','10','','20','','30','','40','','50'})
xlabel('PHB content famine reactor (Cmol_{PHB}/Cmol_{X})', 'FontWeight','bold')
ylabel('# individuals of \it{P. acidivorans} (%)', 'FontWeight','bold')
pbaspect([3 2 2])
saveas(gcf,'PHB_Distribution_Famine.pdf')

% Export results to MS Excel...
% Overview process parameters/flows/volumes:
descr = {'HRT (h)';           'recycle ratio';      'rt_feast (h)';
         'rt_famine (h)';     'V_feast (l)';        'V_famine (l)';
         'f_feed (l/h)';      'f_recycle (l/h)';    'f_waste (l/h)';
         'cS_feed (Cmmol/l)'; 'cN_feed (mmol/l)';   'cS_1 (Cmmol/l)';
         'cN_1 (mmol/l)';     'cX_Pa_1 (Cmmol/l)';  'cX_oth_1 (Cmmol/l)';
         'cPHB_1 (Cmmol/l)';  'cS_2 (Cmmol/l)';     'cN_2 (mmol/l)';
         'cX_Pa_2 (Cmmol/l)'; 'cX_oth_2 (Cmmol/l)'; 'cPHB_2 (Cmmol/l)'};

xlswrite('Results.xlsx', descr,            'Overview', 'A1:A21');
xlswrite('Results.xlsx', HRT,              'Overview', 'B1');
xlswrite('Results.xlsx', recycle_ratio,    'Overview', 'B2');
xlswrite('Results.xlsx', RT_feast,         'Overview', 'B3');
```

A

```
    xlswrite('Results.xlsx', RT_famine,        'Overview', 'B4');
    xlswrite('Results.xlsx', V_1,              'Overview', 'B5');
    xlswrite('Results.xlsx', V_2,              'Overview', 'B6');
    xlswrite('Results.xlsx', f_feed,           'Overview', 'B7');
    xlswrite('Results.xlsx', f_recycle,        'Overview', 'B8');
    xlswrite('Results.xlsx', f_waste,          'Overview', 'B9');
    xlswrite('Results.xlsx', cS_feed,          'Overview', 'B10');
    xlswrite('Results.xlsx', cN_feed,          'Overview', 'B11');
    xlswrite('Results.xlsx', conc_feast_end',  'Overview', 'B12:B16');
    xlswrite('Results.xlsx', conc_famine_end', 'Overview', 'B17:B21');

    % Total amounts of S, N, X, and PHB over time:
    head1 = {'time' 'S1'    'N1'   'X_Pa1' 'X_oth1' 'P1' ...
                    'S2'    'N2'   'X_Pa2' 'X_oth2' 'P2';
             'h'    'Cmmol' 'mmol' 'Cmmol' 'Cmmol'  'Cmmol' ...
                    'Cmmol' 'mmol' 'Cmmol' 'Cmmol'  'Cmmol'};

    xlswrite('Results.xlsx', head1, 'Total amounts1', 'A1:K2')
    xlswrite('Results.xlsx', T,     'Total amounts1', 'A3:A65003')
    xlswrite('Results.xlsx', Y,     'Total amounts1', 'B3:K65003')

    xlswrite('Results.xlsx', head1,          'Total amounts2', 'A1:K2')
    xlswrite('Results.xlsx', T(65001:end),   'Total amounts2', 'A3:A35003')
    xlswrite('Results.xlsx', Y(65001:end,:), 'Total amounts2', 'B3:K35003')

    % Final composition of the individual storers (loc, RT, X, P):
    head2 = {'#' 'location' 'RT' 'X' 'PHB'; ''  '' 'h' 'Cmmol' 'Cmmol'};
    nr_storers = 1:length(storers);

    xlswrite('Results.xlsx', head2,      'Storers end', 'A1:E2')
    xlswrite('Results.xlsx', nr_storers','Storers end', 'A3:A20003')
    xlswrite('Results.xlsx', storers,    'Storers end', 'B3:E20003')

    % Final composition of the individual non-storers (loc, RT, X):
    nr_nonstorers = 1:length(nonstorers);

    xlswrite('Results.xlsx', head2,         'NonStorers end', 'A1:D2')
    xlswrite('Results.xlsx', nr_nonstorers','NonStorers end', 'A3:A20003')
    xlswrite('Results.xlsx', nonstorers,    'NonStorers end', 'B3:D20003')

    % Save workspace variables to MAT-file
    save('result.mat')

end


function Y_PHB_S = yield1(delta)
    % Calculate stoichiometric yield for PHB production from acetate
    % Reactions involved: RA, R1, R2, RO
    A1 = [-1   0   0       delta;...    % ATP balance
           0   2  -0.25   -1;...        % NADH balance
           1  -1  -1       0;...        % AcCoA balance
           1   0   0       0];          % bootstrap (RA = 1)

    b1 = [0; 0; 0; 1];
    x1 = A1\b1;                         % Vector containing RA, R1, R2, RO

   %Y1_CO2_PHB = x1(2) / x1(3);
   %Y1_O2_PHB  = 0.5*x1(4) / x1(3);
    Y_PHB_S    = x1(3) / x1(1);
end

function Y_X_S = yield2(delta)
    % Calculate stoichiometric yield for growth on acetate
    % Reactions involved: RA, R1, R3, RO
    A2 = [-1   0  -2.16    delta;...    % ATP balance
           0   2   0.434  -1;...        % NADH balance
           1  -1  -1.267   0;...        % AcCoA balance
           1   0   0       0];          % bootstrap (RA = 1)

    b2 = [0; 0; 0; 1];
    x2 = A2\b2;                         % Vector containing RA, R1, R3, RO
```

```
505
506     %Y1_CO2_X = (x2(2) + 0.267*x2(3)) / x2(3);
507     %Y1_O2_X  = 0.5*x2(4) / x2(3);
508      Y_X_S    = x2(3) / x2(1);
509  end
510
511  function Y_X_PHB = yield3(delta)
512      % Calculate stoichiometric yield for growth on PHB
513      % Reactions involved: R1, R3, R4, R0
514      A3 = [ 0  -2.16   -0.25   delta;... % ATP balance
515             2   0.434   0.25  -1;...     % NADH balance
516            -1  -1.267   1      0;...     % AcCoA balance
517             0   0       1      0];       % bootstrap (R4 = 1)
518
519      b3 = [0; 0; 0; 1];
520      x3 = A3\b3;                         % Vector containing R1, R3, R4, R0
521
522     %Y2_CO2_X = (x3(1) + 0.267*x3(2)) / x3(2);
523     %Y2_O2_X  = 0.5*x3(4) / x3(2);
524      Y_X_PHB  = x3(2) / x3(3);
525  end
526
527  function Y_ATP_S = yield4(delta)
528      % Calculate stoichiometric energy yield for catabolism on acetate
529      % Reactions involved: RA, R1, R0
530      A4 = [ 0   2  -1;...                % NADH balance
531             1  -1   0;...                % AcCoA balance
532             1   0   0];                  % bootstrap (RA = 1)
533
534      b4 = [0; 0; 1];
535      x4 = A4\b4;                         % Vector containing RA, R1, R0
536
537     %Y_CO2_S = x4(2) / x4(1);
538     %Y_O2_S  = -0.5*x4(3) / -x4(1);
539      Y_ATP_S = (delta*x4(3) - x4(1)) / x4(1);
540  end
541
542  function Y_ATP_PHB = yield5(delta)
543      % Calculate stoichiometric energy yield for catabolism on PHB
544      % reactions involved: R1, R4, R0
545      A5 = [  2  0.25  -1;...             % NADH balance
546             -1  1      0;...             % AcCoA balance
547              0  1      0];               % bootstrap (R4 = 1)
548
549      b5 = [0; 0; 1];
550      x5 = A5\b5;                         % Vector containing R1, R4, R0
551
552     %Y2_CO2_PHB = x5(1) / x5(2);
553     %Y2_O2_PHB  = -0.5*x5(3) / -x5(2);
554      Y_ATP_PHB  = (delta*x5(3) - 0.25*x5(2)) / x5(2);
555  end
556
557
558  function [X PHB dS dN dX_Pa dP] = Pa_convert(X,PHB,dt,cS,cN)
559      % Growth, maintenance, and PHB production/consumption by P. acidivorans
560
561      global Pa_qS_max Pa_qX_max Pa_mATP Pa_alfa Pa_k Pa_K_S Pa_K_N Pa_fPHB_max ...
562             Y_PHB_S Y_X_S Y_X_PHB Y_N_X Y_ATP_S Y_ATP_PHB
563
564      qS      = Pa_qS_max * cS/(Pa_K_S+cS) * (1 - ((PHB/X)/Pa_fPHB_max)^Pa_alfa);
565                                                  % Substrate uptake
566      m_S     = Pa_mATP/Y_ATP_S * cS/(Pa_K_S+cS);       % Maintenance on substrate
567      m_PHB   = Pa_mATP/Y_ATP_PHB * (1 - cS/(Pa_K_S+cS));    % Maintenance on PHB
568      qX_S    = Pa_qX_max * cN/(Pa_K_N+cN) * cS/(Pa_K_S+cS); % Growth on substrate
569      qP_prod = Y_PHB_S * (qS - qX_S/Y_X_S - m_S);          % PHB production
570      qP_cons = Pa_k * (PHB/X)^(2/3) * cN/(Pa_K_N+cN) * (1 - cS/(Pa_K_S+cS));
571                                                           % PHB consumption
572      qX_PHB  = Y_X_PHB * (-qP_cons - m_PHB);              % Growth on PHB
573
574      % Impact on the overall amounts of S, N, X and P (in (C)mmol/h)
575      dS      = - qS                    * X;
576      dN      = -(qX_S + qX_PHB)*Y_N_X * X;
```

```
577     dX_Pa   =  (qX_S + qX_PHB)       * X;
578     dP      =  (qP_prod + qP_cons)   * X;
579
580     % Update properties of the individual itself
581     X       = X   + dX_Pa*dt;
582     PHB     = PHB + dP   *dt;
583
584 end
585
586 function [X dS dN dX_oth] = Other_convert(X,dt,cS,cN)
587     % Growth and maintenance by 'Other'
588
589     global other_qX_max other_mATP other_K_S other_K_N ...
590            Y_X_S Y_N_X Y_ATP_S
591
592     qX_S    = other_qX_max * cN/(other_K_N+cN) * cS/(other_K_S+cS); % Growth
593     m_S     = other_mATP/Y_ATP_S * cS/(other_K_S+cS); % Maintenance on ext. substrate
594     m_X     = other_mATP/Y_ATP_S *(1 - cS/(other_K_S+cS)) * Y_X_S; % "Maintenance" on X
595     qS      = qX_S/Y_X_S + m_S; % Substrate uptake
596
597     % Impact on the overall amounts of S, N and X (in (C)mmol/h)
598     dS      = - qS                * X;
599     dN      = -(qX_S - m_X)*Y_N_X * X;
600     dX_oth  =  (qX_S - m_X)       * X;
601
602     % Update properties of the individual itself
603     X       = X + dX_oth*dt;
604
605 end
606
607
608 function [new indiv dX1 dP1 dX2 dP2] = Pa_move(indiv,dt)
609
610     global recycle_ratio RT_feast RT_famine
611
612     new     = [];
613     nr_new  = 1;
614     dX1_new = 0;   dP1_new = 0;   dX2_new = 0;   dP2_new = 0;
615     dX1     = 0;   dP1     = 0;   dX2     = 0;   dP2     = 0;
616
617     if indiv(3) > 0.002 % Need to split the cell before moving?
618     % Determine number of individuals after splitting & generate
619         nr_new   = floor(indiv(3)/0.001);
620         indiv(3) = indiv(3)/nr_new;
621         indiv(4) = indiv(4)/nr_new;
622
623         for i = 1:(nr_new-1)
624             new(i,1:4) = indiv(1:4);
625
626             % Move 'new' individuals
627             if new(i,1) == 1
628                 if random('unif',0,1) > (1-recycle_ratio)
629                 % The chance at being discarded equals 1 - recycle ratio
630                 % Move to famine reactor
631                     new(i,1) = 2;
632                     new(i,2) = new(i,2) + random('exp',RT_famine);
633
634                     dX1_new  = dX1_new - new(i,3)/dt;
635                     dP1_new  = dP1_new - new(i,4)/dt;
636                     dX2_new  = dX2_new + new(i,3)/dt;
637                     dP2_new  = dP2_new + new(i,4)/dt;
638                 else
639                 % Discard
640                     new(i,1) = 0; % Cleanup after for-loop...
641
642                     dX1_new  = dX1_new - new(i,3)/dt;
643                     dP1_new  = dP1_new - new(i,4)/dt;
644                 end
645
646             elseif new(i,1) == 2
647                 % Move to feast reactor
648                 new(i,1) = 1;
```

```
649                 new(i,2) = new(i,2) + random('exp',RT_feast);
650
651                 % Impact on overall X/P amounts accounted for by original
652             end
653         end
654
655         % Cleanup discarded 'new' individuals
656         for i = (nr_new-1):-1:1
657             if new(i,1) == 0
658                 new(i,:)=[];
659             end
660         end
661
662     end
663
664     % Move and discard original individuals
665     if indiv(1) == 1
666         if random('unif',0,1) > (1-recycle_ratio)
667         % The chance at being discarded equals 1 - recycle ratio
668         % Move to famine reactor
669             indiv(1) = 2;
670             indiv(2) = indiv(2) + random('exp',RT_famine);
671
672             dX1      = dX1_new - indiv(3)/dt;
673             dP1      = dP1_new - indiv(4)/dt;
674             dX2      = dX2_new + indiv(3)/dt;
675             dP2      = dP2_new + indiv(4)/dt;
676         else
677         % Discard
678             indiv(1) = 0;
679
680             dX1      = dX1_new - indiv(3)/dt;
681             dP1      = dP1_new - indiv(4)/dt;
682             dX2      = dX2_new;
683             dP2      = dP2_new;
684         end
685
686     elseif indiv(1) == 2
687         % Move to feast reactor
688         indiv(1) = 1;
689         indiv(2) = indiv(2) + random('exp',RT_feast);
690
691         dX1      =  indiv(3) *nr_new/dt;
692         dP1      =  indiv(4) *nr_new/dt;
693         dX2      = -indiv(3) *nr_new/dt;
694         dP2      = -indiv(4) *nr_new/dt;
695     end
696
697 end
698
699 function [new indiv dX1 dX2] = Other_move(indiv,dt)
700
701     global recycle_ratio RT_feast RT_famine
702
703     new     = [];
704     nr_new  = 1;
705     dX1_new = 0;  dX2_new = 0;
706     dX1     = 0;  dX2     = 0;
707
708     if indiv(3) > 0.002 % Need to split the cell before moving?
709         % Determine number of individuals after splitting & generate
710         nr_new   = floor(indiv(3)/0.001);
711         indiv(3) = indiv(3)/nr_new;
712         indiv(4) = indiv(4)/nr_new;
713
714         for i = 1:(nr_new-1)
715             new(i,1:4) = indiv(1:4);
716
717             % Move 'new' individuals
718             if new(i,1) == 1
719                 if random('unif',0,1) > (1-recycle_ratio)
720                 % The chance at being discarded equals 1 - recycle ratio
```

```
721                 % Move to famine reactor
722                     new(i,1) = 2;
723                     new(i,2) = new(i,2) + random('exp',RT_famine);
724
725                     dX1_new  = dX1_new - new(i,3)/dt;
726                     dX2_new  = dX2_new + new(i,3)/dt;
727                 else
728                 % Discard
729                     new(i,1) = 0; % Cleanup after for-loop...
730
731                     dX1_new  = dX1_new - new(i,3)/dt;
732                 end
733
734             elseif new(i,1) == 2
735                 % Move to feast reactor
736                 new(i,1) = 1;
737                 new(i,2) = new(i,2) + random('exp',RT_feast);
738
739                 % Impact on overall X/P amounts accounted for by original
740
741             end
742
743         end
744
745         % Cleanup discarded 'new' individuals
746         for i = (nr_new-1):-1:1
747             if new(i,1) == 0
748                 new(i,:)=[];
749             end
750         end
751
752     end
753
754     % Move and discard original individuals
755     if indiv(1) == 1
756         if random('unif',0,1) > (1-recycle_ratio)
757         % The chance at being discarded equals 1 - recycle ratio
758         % Move to famine reactor
759             indiv(1) = 2;
760             indiv(2) = indiv(2) + random('exp',RT_famine);
761
762             dX1      = dX1_new - indiv(3)/dt;
763             dX2      = dX2_new + indiv(3)/dt;
764
765         else
766         % Discard
767             indiv(1) = 0;
768
769             dX1  = dX1_new - indiv(3)/dt;
770             dX2  = dX2_new;
771
772         end
773
774     elseif indiv(1) == 2
775         % Move to feast reactor
776         indiv(1) = 1;
777         indiv(2) = indiv(2) + random('exp',RT_feast);
778
779         dX1      =  indiv(3) *nr_new/dt;
780         dX2      = -indiv(3) *nr_new/dt;
781
782     end
783
784 end
```

CURRICULUM VITAE

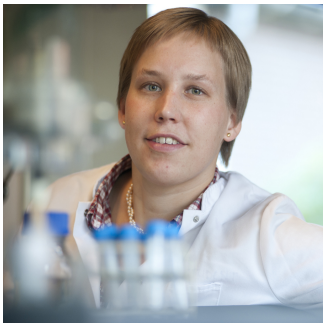

Leonie Marang was born on 16 May 1983 in Deventer, the Netherlands. After she finished her pre-university education (VWO) in 2001, she moved to Delft to study Architecture at Delft University of Technology. She obtained the propaedeutic diploma in one year, but later decided to switch studies.

In February 2005, she started her study Life Science & Technology at Leiden University and Delft University of Technology. For her BSc thesis she studied the pelleted growth of the fungus *Rhizopus oryzae*. She graduated for the MSc program with a thesis on the production of polyhydroxyalkanoates (PHA) from lactate, for which she received the Unilever research prize in 2011.

After a 6-month internship at DSM Food Specialties (Delft), where she investigated the effect of oxygen and hemin on the growth of *Lactococcus lactis*, she returned to Delft University of Technology as a PhD candidate. From May 2011, she continued her research on PHA production by microbial enrichment cultures under the supervision of prof.dr.ir. Mark van Loosdrecht and dr.ir. Robbert Kleerebezem (Environmental Biotechnology group). The aim of the research was to assess limiting steps in the scale-up of non-axenic PHA production. This thesis presents that research and its results.

LIST OF PUBLICATIONS

JOURNAL ARTICLES

10. **L. Marang**, M.C.M. van Loosdrecht, and R. Kleerebezem. 2017. Enrichment of PHA-producing bacteria under continuous substrate supply. Under review at New Biotechnology.

9. **L. Marang**, M.C.M. van Loosdrecht, and R. Kleerebezem. 2016. Combining the enrichment and accumulation step in non-axenic PHA production: Cultivation of *Plasticicumulans acidivorans* at high volume exchange ratios. Journal of Biotechnology 231, 260–267.

8. **L. Marang**, M.C.M. van Loosdrecht, and R. Kleerebezem. 2015. Modeling the competition between PHA-producing and non-PHA-producing bacteria in feast-famine SBR and staged CSTR systems. Biotechnology and Bioengineering 112 (12), 2475–2484.

7. **L. Marang**, Y. Jiang, M.C.M. van Loosdrecht, and R. Kleerebezem. 2014. Impact of non-storing biomass on PHA production: An enrichment culture on acetate and methanol. International Journal of Biological Macromolecules 71, 74–80.

6. J. Tamis, **L. Marang**, Y. Jiang, M.C.M. van Loosdrecht, and R. Kleerebezem. 2014. Modeling PHA-producing microbial enrichment cultures – towards a generalized model with predictive power. New Biotechnology 31 (4): 324–334.

5. **L. Marang**, Y. Jiang, M.C.M. van Loosdrecht, and R. Kleerebezem. 2013. Butyrate as preferred substrate for polyhydroxybutyrate production. Bioresource Technology 142, 232–239.

4. Y. Jiang, **L. Marang**, J. Tamis, M.C.M. van Loosdrecht, H. Dijkman, and R. Kleerebezem. 2012. Waste to resource: Converting paper mill wastewater to bioplastic. Water Research 46 (17), 5517–5530.

3. Y. Jiang*, **L. Marang***, R. Kleerebezem, G. Muyzer, and M.C.M. van Loosdrecht. 2011. Polyhydroxybutyrate production from lactate using a mixed microbial culture. Biotechnology and Bioengineering 108 (9), 2022–2035.
   * These authors contributed equally to this work.

2. Y. Jiang, **L. Marang**, R. Kleerebezem, G. Muyzer, and M.C.M. van Loosdrecht. 2011. Effect of temperature and cycle length on microbial competition in PHB-producing sequencing batch reactor. ISME Journal 5 (5), 896–907.

1. C.A. Roa Engel, W.M. van Gulik, **L. Marang**, L.A.M. van der Wielen, and A.J.J. Straathof. 2011. Development of a low pH fermentation strategy for fumaric acid production by *Rhizopus oryzae*. Enzyme and Microbial Technology 48: 39–47.

OTHER PUBLICATIONS

1. **L. Marang**, Y. Jiang, J. Tamis, H. Moralejo-Garate, M.C.M. van Loosdrecht, and R. Kleerebezem. 2012. Microbial community engineering: Producing bioplastic from waste. Bioplastics Magazine 7: 22–24.

CONFERENCE CONTRIBUTIONS

ORAL PRESENTATIONS

4. **L. Marang**, M.C.M. van Loosdrecht, and R. Kleerebezem. 9 January 2015. From waste to resource: Producing bioplastic from organic waste. 67^{e} Vakantiecursus Drinkwater en Afvalwater, Delft, Netherlands.

3. **L. Marang**, J. Tamis, Y. Jiang, H. Dijkman, M.C.M. van Loosdrecht, and R. Kleerebezem. 30 September 2014. *Plasticicumulans* and the chocolate factory: Non-axenic PHA production from organic waste. International Symposium on Biopolymers (ISBP), Santos, Brazil.

2. **L. Marang**, M.C.M. van Loosdrecht, and R. Kleerebezem. 11 September 2014. PHA production in SBR versus staged CSTR systems. 5th Workshop on PHA production by microbial consortia, Toulouse, France.

1. **L. Marang**, Y. Jiang, M.C.M. van Loosdrecht, and R. Kleerebezem. 20 September 2012. PHA production from substrate mixtures. 4th Workshop on PHA production by microbial consortia, Rome, Italy.

POSTER PRESENTATIONS

2. **L. Marang**, Y. Jiang, M.C.M. van Loosdrecht, and R. Kleerebezem. 7 October 2013. Impact of non-storing biomass on PHA production: An enrichment culture on acetate and methanol. European Symposium on Biopolymers (ESBP), Lisbon, Portugal.

1. **L. Marang**. 3 October 2013. From waste to resource: Producing polyhydroxyalkanoates from organic waste. STW Annual Congress, Nieuwegein, Netherlands.

AWARDS

Unilever Research Prize 2011

ACKNOWLEDGEMENTS

After 150 pages of big words, it is about time for some small talk. Without you – my colleagues, friends, and family – this thesis wouldn't have been what it is now... and the journey wouldn't have been as nice. Thank you!

First, I would like to thank my supervisors, Mark and Robbert, for giving me the opportunity to continue the work of my MSc thesis and the freedom to shape the research myself. Mark, thank you for the overwhelming amount of ideas generated each meeting. They left me both exhausted and full of energy to continue the work and investigate new things. Your dedication is inimitable. Your quick responses come at the strangest hours, from somewhere around the world. Robbert, thank you for our shared puzzling on the continuous setup, for your 'bottlenecks', and for the car rides (the talks, especially). I'm sorry for betraying your beloved Excel... Hopefully you have been convinced of my choice for Matlab.

Second, I would like to thank my fellow-members of the PHA team: Yang (my teacher, colleague, and friend), Helena, Jelmer (despite, or due to, our almost opposite characters we made a great team and I enjoyed our collaboration), Emma (bringing cheerfulness and drama to the lab), and Gerben. It was great to have you around, to teach and be taught. And to be able to share ideas, problems, frustrations, and successes with true 'experts in the field'. Thank you for babysitting my reactors, the dinners, the ice cream, and our trips to Rome and Toulouse.

I would also like to thank Lorena, my first MSc student, for mastering the enormous amount of tubes and fighting 'mister protozoa'. Your stories about your home-country put Costa Rica high on my bucket list.

My office mates: Mari, Shiva, Helena, Julian, Salah, Monica, Marissa, Simon, Jure, and Jules... thank you for the balance between nice and quiet, sharing the good and the bad, and the discussions about life at the end of a day.

And then, there are of course all those other EBTeans: Florence, Olga, Marco, Tommaso, Mario, Emanuelle, Matthijs, Simona, Andrea, Peter, Maaike, Eveline, Laurens, Bart, Danny, Laura, Michel, Yuemei, Cristian, Gijs, Julio, David, Geert-Jan, Miranda, Dimitry, Udo, Ben, Mitchell, and the many, many more that have visited or started since. I am glad to have met you. I truly miss our lunches in the botanical garden, that tended

to last when the weather was nice and nobody wanted to be the first to go back to work... Our homemade lunches, numerous farewell parties, the EBT retreat, Friday beers in the Keldertje, coffees at Architecture, and, above all, the frequent (homemade) cakes in the coffee corner. I expect little opposition to proposition number 11 from within the group.

More directly related to the work presented in this thesis, I would like to thank Udo, for his expertise in FISH, microscopy, and photography. Ben and Mitchell for their PCR and DGGE work. Rob, Dirk, and Song for their help with the reactor, recipes, and data logging, when Gollem refused service or relays got stuck. The workshop for fixing things that broke down. The analysts, Max, Johan, Cor, Patricia, and Mervin, for the nice chats and maintenance of the GC and HPLC. And Jannie, Apilena, and Astrid for autoclaving my impractical 5-liter bottles. You made life a lot easier.

I would also like to thank Ron Winkler, Henk Dijkman, Rene Rozendal, and the other members of the Users Committee for their interest in my work. And all BT members for the nice atmosphere in the lab. Sjaak and the feestcommissie played an important role in this by organizing the party's, labuitjes, visit of Sinterklaas, and Easter egg hunts in the botanical garden.

En dan was er gelukkig ook nog een leven buiten het lab... daarvoor wil ik graag mijn clubgenootjes bedanken: Arjan, Guus (en Eliana), Kees, Kirsten (en Sven), Kornelius (en Mirjam), Mark (en Lydia), Paul (en Aafke) en Petra (en Chiron). Onze herinneringen gaan inmiddels al weer 15 jaar terug! Bedankt voor alle gezelligheid en het samen genieten van het goede leven. En voor het stug blijven informeren naar mijn schimmels.

Bedankt ook, Sfinxjes. Marlous, Ingrid, Rianne, Afra, Ivonne, Koenie, Jessica, Danielle en Iris, bedankt voor de ontspannende bezoekjes aan de sauna, het wokken, de thee bij Kobus, de Vrimibo's... Ik zie sommigen van jullie vaker dan anderen, maar het is altijd weer gezellig om bij te kletsen.

Tot slot, lieve familie, pap, mam, Huub, Nicole en Mathijs, ik ben eindelijk klaar met 'studeren'! Bedankt voor jullie steun, gezelligheid en interesse. Pap en mam, bedankt voor jullie vertrouwen. Jullie staan altijd voor ons klaar en hebben altijd onze individuele kwaliteiten erkend en gevoed.

Hans en Marijke, jullie hoef ik werkelijk niets over 'feast phases' te leren.

Thomas, bedankt voor je onvoorwaardelijke steun. Je bent mijn grootste fan en criticus in één. Spoort me altijd aan om het nog beter te doen. Bedankt ook voor de taxiritjes naar het lab, wanneer er weer eens bij nacht en ontij een sample genomen moest worden. Ik hou van je.

En natuurlijk Marit... niemand heeft me beter af kunnen leiden van die laatste loodjes. Het is fantastisch om samen met jou de wereld opnieuw te mogen ontdekken.